ANNUAL PROGRAM REVIEW

CHEMICAL RECOVERY

March 23, 1995

ANNUAL PROGRAM REVIEW

CHEMICAL RECOVERY/CORROSION

March 23, 1995

Institute of Paper Science and Technology
500 10th Street, N.W.
Atlanta, GA 30318
(404) 853-9500

TABLE OF CONTENTS

INTRODUCTION

During the past year, work in the recovery area has undergone several changes. The major items are the following.

Work on the DOE-sponsored project on black liquor delivery systems has been completed and a final report written. Aside from several student efforts, no further immediate work is planned in the area of black liquor sprays.

The DOE-sponsored work on recovery boiler simulation has been extended for three years. This will continue as the joint program between IPST, UBC, and OSU with the addition of contributions from the University of Toronto and B&W. This program was under the direction of Dr. Robert Horton until his resignation in December, 1994. Fortunately, we were able to entice Dr. Tom Grace to reestablish his direct link with IPST as professor on our faculty. Tom has taken over direction of the modeling efforts including those funded by the state of Georgia. In addition, we are seeking a replacement for Dr. Wenrui Yang who was employed for three years as a post-doctoral fellow on the project. We have located a suitable replacement and expect him to be on board in April, 1995.

With the advice and council of the Recovery PAC, we have initiated several recovery oriented projects that are directed at the problems that occur as mills expand into low effluent technology. These include projects directed by Dr. Peter Pfromm using membrane separation and electrophoresis for purging inorganic salts of chloride or potassium and a fundamental study on the formation and separation of green liquor dregs directed by Dr. Jeff Empie. In addition, Dr. Terry Adams is continuing to expand on the series of direct visits to individual mills to discuss problems that are encountered as mills close up their effluent systems.

We continue to consider new technology such as black liquor gasification. Dr. Junyong Zhu has put together an initial report on problems with hot gas clean up and will have a proposal to discuss with the Recovery PAC in the near future.

Student efforts continue in a variety of areas such as NOx control, pulsed gasification, furnace simulation, dregs control, and effervescent spraying.

KRAFT RECOVERY FURNACE MODELING CAPABILITY PROJECT F016

ANNUAL PROGRAM REVIEW

March 23, 1995

Tom Grace
Steve Lien
Barry Hojattie

Institute of Paper Science and Technology
500 10th Street, N.W.
Atlanta, GA 30318
(404) 853-9500

ANNUAL PROGRAM REVIEW

Project Title:	KRAFT RECOVERY FURNACE MODELING CAPABILITY
Project Code:	MODEL
Project Number:	F016
PAC:	Chemical Recovery
Division:	Chemical and Biological Sciences
Project Staff:	Tom Grace, Steve Lien, Barry Hojattie, new post doc
FY 94-95 Budget:	$180,000

PROGRAM OBJECTIVE:

Upgrade the capability of kraft recovery boilers through the application of computer-based models of fireside processes. Specific objectives are as follows:

1. Support the development of computer-based models of fireside processes in kraft recovery furnaces.
2. Develop cost-effective techniques for using models to help solve problems on real recovery boilers.
3. Use recovery boiler model simulations to gain insight into fireside processes that affect recovery boiler operation.
4. Facilitate the tranfer of model technology to recovery boiler manufacturers and users.
5. Develop and implement strategies for validating models.

SUMMARY OF RESULTS:

Collaboration:

IPST's funding for work on recovery furnace models has come from three sources: the U.S.DOE, the State of Georgia, and the IPST funded research program. The DOE sponsored program was a collaborative effort with the University of British Columbia (UBC), Oregon State University (OSU), and T.M. Grace Company. The DOE project was recently extended for three years in order to complete and validate recovery furnace models and develop the capability to apply model simulation results to fouling of convective section heat transfer surfaces and boiler plugging. Two new collaborators

were formally brought into the project with the extension; Honghi Tran of the University of Toronto to provide expertise on recovery boiler fouling and plugging, and B&W to provide experimentally derived radiation heat transfer parameters. In addition, liaison is maintained with Abo Akademi in Finland and with the Advanced Combustion Engineering Research Center (ACERC) at Brigham Young University and the University of Utah.

Technical Results:

The majority of IPST's work on recovery boiler modeling in the past year was focused on two major areas: development of a complete recovery furnace model based on the FLUENT CFD code, and application of recovery boiler model simulations to recovery boilers in Georgia. A technical paper summarizing the results of the model applications is attached to this report.

Near the close of calendar 1994 the modeling program at IPST suffered a setback with the resignations of R. Horton and W. Yang. P. Siiskonen, a visiting scientist from Tampella Corporation, completed his tenure in February 1995. As a result it has become necessary to rebuild the recovery boiler modeling team at IPST. T. Grace has accepted a part time appointment at IPST and will head the effort. A new team is being assembled and should be operating by the end of March. As a result of the turnover, it has been necessary to devote some effort to examining and documenting the existing models to assess their reliability and need for upgrading.

Code transfer from UBC to IPST has been proceeding according to the agreed upon schedule. To date, no effort has been made to use the UBC codes that have been transferred. This will change. Comparative studies of different codes is planned for the near future as part of the overall model validation effort.

A comprehensive report on the first four years of the DOE project is in preparation and a draft of this report should be available in late March. This report will include an assessment of the current state of recovery boiler models and pinpoint what remains to be done to make the reliable and useful.

GOALS FOR FY 1995-1996: (Includes IPST funding from both DOE & IPST member dues)

1. Develop a second generation char burning model that can deal with subsurface reactions, bed structure, and smelt transfer as well as surface gasification and combustion reactions.

2. Upgrade FLUENT-based furnace model with updated black liquor burning models.

3. Develop and validate methodologies for using faster, simpler models to solve recovery boiler problems.

4. Establish a program for benchmarking different recovery boiler models by comparing model predictions on specific predefined cases.

5. Utilize model simulations to gain new insight into recovery boiler processes.

6. Develop an understanding of how to link recovery furnace model results to plugging/fouling in the convective sections of the boiler.

7. Develop increased confidence in the reliability of recovery furnace models.

Student Activities:

Ph.D. research is continuing on the relationship between liquor composition and the release of Nox precursors as black liquor burns. This information will be incorporated into Nox formation and destruction models that are being developed by others.

An MS student has started work on incorporating fume generation prediction capability into the models and using this model to examine the effects of firing conditions on fume production.

APPLICATIONS OF BOILER MODELS

A REVIEW OF RECOVERY BOILER MODEL APPLICATIONS

Steven J. Lien
Research Engineer
Institute of Paper Science and Technology
500 10th Street, NW
Atlanta, GA 30318

Robert R. Horton
Senior Engineer
Radian Corp.
P.O. Box 1300
Research Triangle Park, NC 27709

ABSTRACT

Recovery boiler computer models were used to study black liquor combustion. These simulations combine three-dimensional computational fluid dynamics (CFD) calculations, with single particle and char bed black liquor combustion models to simulate the furnace combustion zone. Several boilers were studied using these simulations and the results are reviewed in this paper.

RECOVERY BOILER MODEL

Three-dimensional recovery boiler simulations have been used at IPST since 1987. Details of IPST's recovery boiler model development and some applications have been reported in references (1-5). To improve our understanding of the furnace combustion processes, the computer model has been applied to a number of operating boilers over the past two years. This paper will review the results of these modeling studies to analyze the status, as well as the usefulness of the recovery boiler model.

The recovery boiler model consists of three main components:

1. A computational fluid dynamics (CFD) component describing gas flows and heat transfer
2. An in-flight black liquor combustion model describing the trajectories and combustion of droplets
3. A char bed model

The combustion models are at a stage of development where they can be used with a commercial CFD code in two different ways to predict recovery boiler behavior. In the first method, gas temperature is assumed to be constant (isothermal) and the gas flow patterns are solved based on the inlet gas velocities. The in-flight combustion model is solved by using the fixed gas flow field and assuming constant gas concentrations. The char bed model is not included in the isothermal model. In the second method, the three models are solved simultaneously (fully-coupled) and the temperature is computed.

The more sophisticated fully-coupled (non-isothermal) method takes considerably more computer time: 14 days versus 2 days for isothermal (on an IBM RISC 550). However, non-isothermal simulations provide more information, such as temperature and gas concentrations. In the application of the computer model, the isothermal approach has been used for the bulk of the simulations to minimize computational time. This simplified approach still provides much data on the boiler operation, including gas flow patterns and black liquor drop trajectories. In addition, a fully-coupled simulation has been carried out to verify results and to examine temperature and concentration fields.

Isothermal Gas Flow Model

Gas velocity patterns in the 3-D recovery boiler model were calculated using the commercial CFD program Fluent ver. 4.23. A Cartesian grid design was used for the isothermal models, which creates a stair-stepped char bed geometry (ref. 5). With this simple type of grid, the resulting velocity data can easily be imported into the in-flight black liquor combustion model for the simulation of particle trajectories and combustion behavior. The overall grid size used for these models ranged from 35,000 to 150,000 cells.

The In-flight Combustion Model

Velocity data, calculated from flow field model, are imported into the in-flight combustion model. Except for the velocity data, conditions in the furnace were assumed to be uniform. At each of the black liquor gun ports the boiler operating conditions are used to specify the initial liquor conditions (solids-% and temperature). A distribution of liquor drop sizes, initial directions and velocities are also specified.

The trajectory and combustion behavior of each drop are then calculated individually and sequentially. In this model the black liquor consists of four components, water, volatiles, char and smelt, which correspond to the processes of drying, pyrolysis and char burning (6). The black liquor combustion model determines the rate of drying, de-volatilization, and char burning, based on the heat and mass transfer rates for the individual drops. The

model provides information on the distribution of these mass transfer processes throughout the furnace. The fates of the combustible part of black liquor (volatiles and char) can be used to analyze boiler operation. For good reduction efficiency and bed control, the proper balance between suspension burning and bed burning needs to be maintained. The final fate of the drops can also be determined, i.e., whether it hit the wall, landed on the char bed, or was carried-over. One measure of boiler plugging tendency is the predicted carry-over (particles that are entrained with the gas stream at the outlet of the furnace).

Fully-coupled Model

The fully-coupled recovery boiler model has three major components: a CFD code for gas flow, heat transfer, and gas phase reactions; an in-flight particle model for particle trajectories and combustion in air; and a char bed model for combustion, sulfate reduction and temperature distribution in the char bed. The three components exchange information iteratively so that the results of one submodel will affect the others. A body-fitted coordinate (BFC) version of Fluent was used for CFD purposes and the black liquor combustion submodels were developed at IPST.

RECOVERY BOILER #1

Recovery Boiler #1 experienced plugging in the upper furnace heat transfer tubes, that caused frequent boiler shut-downs. Past efforts to reduce plugging had resulted in poor combustion efficiencies and high emission levels. The objective of this study was to use a recovery furnace computer model to gain a better understanding of key factors that affect physical carry-over of black liquor ash for this recovery boiler.

Isothermal CFD Model of Boiler Gas Flows

This is a small boiler with five secondary ports on each side wall and two secondary ports on the front and rear walls. The tertiary air system has 2 front ports and 3 rear ports (interlaced). The boiler is a B&W sloped bottom design and the char bed is a moderate sized mound-shaped bed that rises to about the secondary air port level. To simplify the CFD calculation, the lower furnace zone was simulated with a flat base and stair-stepped bed as a boundary for gas phase flows. A flat boundary condition at the top of the furnace was specified as the bullnose.

In order to maximize the resolution of the main combustion zone and air port specification, the furnace was specified with a vertical plane of symmetry running from the front to rear wall through the center of the boiler. The roughly 25 individual primary air ports on each wall were specified as a continuous slot with the appropriate width to conserve mass and momentum of the incoming primary air stream. Secondary and tertiary air ports were specified as individual air inlet streams. To maintain the correct momentum and mass flow into the furnace, the model air ports were enlarged to compensate for the lower density. The CFD specification of the boiler required 35,075 nodes.

Figure 1 shows an isometric view of the boiler boundary conditions. The boiler is oriented so that the front of the boiler (the outlet side) is on the left and the rear (bullnose) is on the right. This same isometric orientation is used in all of the subsequent flow figures. Because of the plane of symmetry only half of the boiler is shown. The CFD grid geometry is shown in Figure 2.

Contour plots characterizing the flow fields, as computed by the Fluent CFD program, are shown in Figure 3 for the base case (#1-A). The base case flow field used the standard operating conditions for the boiler with an air distribution of 60%:29%:11% (primary:secondary:tertiary). This figure displays the vertical velocity component for five horizontal slices. The most important feature discovered in the flow field results was that the two close secondary ports on the rear wall combined to form a single jet with a high degree of penetration. This combined with the three tertiary jets on the rear wall and tended to create a high velocity flow channel near the front wall, which could entrain droplets right around the bullnose.

It was hypothesized that the secondary air port arrangement might not be optimal due to the squeezing effect of the predominantly two side wall arrangement. This caused large upward flows at the front wall near the liquor gun. For this reason it was suggested that the secondary air distribution be reduced by 9% and distributed to the primary and tertiary level (where an oversized fan could handle the additional capacity). This was the basis for the second air distribution scheme of 65%:20%:15% (case #1-B - Figure 4). The chimney appears somewhat reduced in Figure 4, with a more uniform vertical velocity profile. Despite this apparent improvement in the flow field, combustion studies do not support a move to this air distribution because of higher carry-over predictions.

Black Liquor In-flight Combustion

This boiler has two liquor nozzles located on the front and rear walls of the boiler. The parameters investigated in this study were black liquor drop size (2.5mm vs.

1.5mm median drop diameter), and horizontal firing angle (-15°, -30°, -45°). Each of these six conditions was simulated in a factorial design with the two different air distributions described above.

The firing temperature of black liquor has only a small effect on droplet size until the flashing temperature is reached. At this point the drop size distribution in the spray becomes unstable as water in the black liquor evaporates and the median drop size decreases dramatically. The mill black liquor firing temperature of 245°F (67% solids) is near the flashing temperature, so that drop size may be very sensitive to liquor temperature.

The base case simulation for the #1 boiler was based on an assumed flashing condition with Dm=1.5mm. In order to simulate the effect of lowering black liquor firing temperature, a non-flashing spray was specified with a Dm of 2.5mm. It is the median droplet size that has the greatest effect on black liquor combustion and entrainment. The base case simulation was based on a firing angle -30° below horizontal. This is a relatively large downward angle compared to many boiler operations. A steeper downward firing angle and an angle closer to horizontal were also simulated in this study.

Gas phase temperature was specified as 1000°C throughout the combustion zone. Concentrations are typical of average conditions in the combustion zone (5% O2, 20% H2O, and 12% CO2). These conditions could be in error near air ports and near the surface of the bed, but these values are relatively good assumptions for bulk conditions.

Carry-over Results

One of the main predictions desired was that of carry-over. A listing of carry-over predictions for each combustion simulation is presented in Table 1. This table can be used to make some preliminary observations.

1) Although the flow field #1-B appeared slightly more uniform, carry-over was always higher for flow field #1-B than #1-A. The highest carry-over occurred when smaller droplets were injected at -15° horizontal angle (nearly 20% of ash is entrained).

2) Drop diameter was the firing variable with the most impact on carry-over. A reduction of firing temperature to non-flashing conditions (Dm=2.5mm) resulted in substantially reduced carry-over predictions. One of the biggest differences in combustion behavior between the flashing and non-flashing cases is that more black liquor mass reaches the bed un-combusted in the non-flashing case. Clearly the smaller drops burn in-flight to a larger degree, resulting in less char that goes directly to the bed.

3) Firing angle had a significant effect on combustion and carry-over and could potentially be used to optimize operation if black liquor temperature were reduced. A more thorough investigation of firing angle would be required to optimize this variable. It is interesting that the effect of firing angle differs between the two flow fields, and that the simulations with the highest and lowest levels of carry-over occurred with a -15° firing angle.

Spray Angle Theta	Carry-over (% of smelt) Dm= 2.5	Dm= 1.5
	Flow Field #1-A	
-15°	0.13%	1.28%
-30°	0.51%	2.18%
-45°	0.44%	1.24%
	Flow Field #1-B	
-15°	5.52%	19.59%
-30°	1.98%	8.59%
-45°	1.70%	7.37%

Table 1. Particle Carry-over - Recovery Boiler #1

RECOVERY BOILER #2

The main objectives of this study were to help determine the reason the boiler was plugging frequently and to explore improved air delivery and black liquor firing practices. Boiler #2 is a large, relatively new boiler.

Isothermal Gas Flow Calculation

Four different boiler operating conditions were simulated in this phase of the project. At the beginning of the study, the mill was operating with a high gas flow-rate to the tertiary jets (40% of the total flow). Later the mill returned to a more traditional gas flow arrangement with less tertiary air (20%). The mill was also interested in examining a "swirling" type of gas flow. In this design three secondary ports on the right side of each wall were closed up to impart a swirling motion to the air at the secondary level. For each of the two operating cases described above, a swirling air design was also tested, resulting in a total of four flow fields (listed in Table 2).

When this study began, the air distribution to boiler #2 was 30%:30%:40% (primary:secondary:tertiary) or about

twice the conventional tertiary air levels. Although reduction efficiency and emissions were not a concern, the boiler was plugging more frequently than normal.

If simulations of high tertiary (#2-A, Figure 5) are compared with conventional tertiary (#2-B, Figure 6) more uniform velocity profiles in the upper furnace are found for the high tertiary case. For low tertiary, the upward velocity is higher at the liquor gun level, because there is more total air introduced (80% vs. 60%) below the guns. In this case (#2-B), the high velocity region also extends into the upper furnace, since the tertiary air is not sufficient to break-up the high velocity core. In the upper part of the furnace before the superheater section, uniform velocity (and temperature) profiles are preferable for good boiler operation.

Air Level	Velocity (m/sec)	%Flow (%)
#2-A High Tertiary Non-Swirling		
Tertiary	40.9	40%
Secondary	34.0	30%
Primary	15.3	30%
#2-B Low Tertiary Non-Swirling		
Tertiary	34.2	20%
Secondary	50.7	45%
Primary	17.7	35%
#2-C High Tertiary Swirling		
Tertiary	40.9	40%
Secondary	43.8	30%
Primary	15.3	30%
#2-D Low Tertiary Swirling		
Tertiary	34.2	20%
Secondary	65.2	45%
Primary	17.7	35%

Table 2. Inlet Gas Flow - Recovery Boiler #2

Uniform velocity profiles also reduce physical carry-over so it follows that there should be less carry-over in the high tertiary case. This was what the isothermal simulations showed: very low carry-over for the high tertiary mode. This would suggest that the high plugging tendency reported by the mill was not caused by physical carry-over. Chemical analysis of deposit samples indicated that the plugging deposits were fume related.

Swirling air distributions and firing practices

Alternative air delivery and black liquor firing strategies, using a swirling air flow pattern, were investigated using computer simulations. Blocking secondary ports on the same side of each wall (right-hand corners) created significant rotation of flow (swirl) in the lower furnace. The simulations showed that swirl helps reduce carry-over since drops are pushed to the walls by centrifugal forces (Table 3).

However, the swirling action also changed the combustion behavior in the lower furnace by changing the distribution of black liquor. For example, much less char is burned in-flight and more char strikes the walls. This could have a dramatic effect on the overall boiler operation. Carry-over was highest for the low tertiary non-swirling air distribution (#2-B) and was also sensitive to drop size. Smaller drop sizes always led to increased physical carry-over, regardless of the air distribution.

Mass Distribution of Black Liquor Dm=2.5mm			
Case	Comb char	Hit Wall char	Char Bed char
Hi 3° Non-swirl	0.7807	0.1353	0.0841
Lo 3° Non-swirl	0.7955	0.1248	0.0797
Hi 3° Swirl	0.6824	0.2261	0.0916
Lo 3° Swirl	0.6168	0.3189	0.0639
	Hit Wall smelt	Char Bed smelt	Carry-over smelt
Hi 3° Non-swirl	0.3979	0.6017	0.0004
Lo 3° Non-swirl	0.5652	0.4294	0.0054
Hi 3° Swirl	0.7763	0.2225	0.0000
Lo 3° Swirl	0.8756	0.1219	0.0000

Table 3. Final Distribution of Black Liquor Components - Recovery Boiler #2

Conclusions

Computer simulations show that physical carry-over is unlikely for the high tertiary case (30:30:40). Physical carry-over is more likely to occur for a conventional air distribution (35:45:20). Carry-over is sensitive to drop size; small drops were carried out to a large degree, large drops were not carried out. Flashing of the liquor (high firing temperatures) will cause a high degree of carry-over which could lead to plugging in the superheater section.

Computer simulations show that "swirl" patterns reduce carry-over for both high tertiary and conventional air distributions but increase the amount of liquor striking the walls. This method should be tried cautiously since simulations show a drastic change in air flow patterns near the bed and lower walls.

RECOVERY BOILER #3

The main goal of this study has been to use a computer model to help determine optimal long-term operating strategies for this recovery boiler. A meeting was held at the mill to define specific objectives. The scope of work was limited to: 1) define a base case that is as close to the normal operating conditions as possible using recommendations from the boiler manufacturer, 2) look for potentially sensitive variables which could cause problems as boiler operation is adjusted, and 3) examine the issue of changing boiler load between 70% and 100% of design in terms of air delivery and the number of liquor guns and location.

Isothermal Flow Model

This is a very large recovery boiler with four separate air levels instead of the three levels used in traditional furnace designs. Inlet air port conditions were based on a design air flow-rate at 100% of the maximum continuous rating (MCR) and a constant gas density (0.267 kg/m3). Additional model simulations were performed based on 70% of MCR.

Results at 100% of Design Load

A "five finger" (three front, two rear) interlaced tertiary air port arrangement was used in all simulations. In the first flow field (Case #3-A) the air distribution was primary -35%, low secondary -40%, high secondary - 9.5% and tertiary -15.5%. All of the primary, low secondary and high secondary ports were used in this model.

Several variations on air delivery at 100% load were studied, but most of the changes to the base case conditions did not result in improved flow fields. The operating conditions that gave the best results are for case #3-B. Three changes were made to the base case to arrive at this improved flow field. First, the air flow at the low secondary level was reduced from 40% to 31% by closing two ports in each corner. Second, three start-up burners at the high secondary level were used to increase air flow at the high secondary level (from 9.5% to 17%). Finally, the air flow-rate (and the inlet velocity) at the tertiary level was increased from 15.5% to 17.0% of the total air.

Flow Fields at 100% of Design Load

The resulting flow fields for the base case (Case #3-A) are shown in Figure 7. The ports at all four air levels can be seen in this graph, along with the black liquor gun ports (3 per wall). A high velocity central-core region can be observed below the tertiary jets. The tertiary jets dissipate the high velocity core. A high velocity central core in the lower furnace is a common feature of recovery boilers, and can result in increased levels of physical carry-over if it extends into the upper regions of the furnace.

Case #3-B, also at 100% load, shows the effect of changing the port and air distribution, while maintaining the same total air flow-rate (see Figure 8). The core that forms above the secondary level is somewhat broader than in the base case. As in the previous case, the core is broken up by the tertiary jets. There are small remaining regions of higher velocity along both the front and back walls of the furnace. The velocity profile in the upper furnace is slightly more uniform for Case #3-B than for Case #3-A. This is due to a weaker core just above the secondary ports and higher tertiary velocities. Overall both of these cases resulted in what appear to be "good" flow patterns, with no obvious problems.

Combustion at 100% of Design Load

Three mass median drop sizes (2.0, 3.0 and 4.0mm) and three gun angles (0, 10 and 20 degrees below horizontal) were used for a total of nine in-flight combustion simulations with the base case flow field. At each of 12 nozzles, 30 drop diameters, and 17 individual angles were used, representing a total of over 6000 unique drops per simulation. The drop diameters are calculated from a square-root normal distribution based on the mass median diameter (7).

The fates of the combustible fractions of black liquor (volatiles and the char as shown in Figure 9) has been used to analyze predicted boiler operation. For good reduction efficiency and bed control, the proper balance between suspension burning and bed burning needs to be maintained. To minimize the boiler plugging tendency, predicted carry-over should be minimized.

The initial drop size had a strong influence on the amount of combustibles reaching the char bed. With a 2.0mm mass median drop size almost all the burning occurred in-flight and only about 1% of the combustible material reached the char bed. At 3.0mm about 11% of the combustibles and at 4.0mm about 30% of the combustibles reached the char bed. The variables that control the drop diameter (nozzle pressure and BL temperature) will have a significant impact on the char bed behavior.

The downward angle of the splash-plate nozzle had a weak effect on the fate of the black liquor components. As expected, increasing the downward spray angle resulted in slightly more combustible material reaching the char bed. At 3.0mm, changing the angle from 0 to

-20 degrees increased the amount reaching the bed from 11% to 18%.

The flow field simulations reveal a uniform vertical velocity in the upper furnace, indicating that physical carry-over should not be a problem in this boiler. The results from the in-flight model confirm this. In all of these simulations, only smelt was found to be carried over, with all the other liquor components being combusted. Figure 10 shows that the mass fraction of the smelt carry-over was 1% or less for both of the 100% load flow fields. Carry-over was sensitive to the flow patterns and was higher for the base case. The more uniform velocity profile resulting in Case #3-B helped reduce physical entrainment.

Results at 70% of Design Load

The computer model was used to study the effect of air distribution and black liquor firing practices at reduced loads. As the black liquor load to the boiler is reduced, it is necessary to reduce the total air flow. One option is to shut off the tertiary air when the load drops below 75% of MCR. An alternative approach is to maintain all four air levels while reducing the port area and flow-rate.

To compare the effect of these two options, additional testing was done at 70% of design load. In the first version (Case #3-C) tertiary air was not used so that more air was available at the three lower levels. All of the primary ports (90% open) were used. At the low secondary level, eight corner ports were closed completely and the remaining 32 ports were 75% open, and all eight high secondary ports were used. The second low load model (Case #3-D) used all primaries (80% open), 32 low secondary ports (75% open), 8 high secondary ports, and 5 tertiary ports (75% open).

Flow Fields at 70% of Design Load

The flow fields for Case #3-C, calculated at 70% of MCR without the tertiary air, are shown in Figure 11. The effect of not using tertiary jets can be seen in the persistence of the high velocity central core in the upper furnace. This caused higher carry-over. The upward velocity in the lower furnace was also somewhat higher since all the air was now injected at a lower level.

The use of tertiary air in Case #3-D significantly improved the air distribution and mixing in the upper furnace (see Figure 12). In the upper one third of the furnace the vertical velocity is quite uniform across the entire width of the furnace. Since this will increase the minimum retention time in the furnace, it should improve combustion efficiency.

Combustion Results at 70% of Design Load

Operation at low load means that either the size or number of nozzles has to be reduced to match the lower black liquor flow-rate. By maintaining the same liquor velocity (and temperature) through each nozzle, the initial drop size will remain constant. At 70% MCR, nozzle velocity is maintained by using either eight 24mm nozzles or twelve 20mm nozzles.

There are several ways to arrange these 8 black liquor guns, which affects the distribution of black liquor landing on the char bed. With three nozzles on the front and rear wall and a single nozzle on the side walls (3/3/1/1) the distribution of black liquor reaching the char bed is elongated in a direction parallel to the front wall. This suggests that the char bed would also have an elongated oval shape parallel to the front wall. The smelt ports for this boiler are located along the front wall, so this 3/3/1/1 layout should provide the most uniform delivery of smelt to the smelt spouts, and the best overall operation at 70% of design load.

The two flow field cases resulted in nearly identical distributions of combustible material. In general, the drops remain in the lower furnace and are not affected by the tertiary air. However, for black liquor particles that reach the upper furnace, the use of tertiary jets is important for minimizing carry-over. For the flow field where tertiary air was not used (and the high velocity core formed), the carry-over was twenty times higher for 2.0mm drops (see Figure 13). When tertiary air jets were used, the uniform velocity in the upper furnace almost eliminated carry-over.

Non-isothermal Model - Results and Discussion

A simulation (at 100% of the design load) was solved using the fully-coupled recovery boiler model. The fully-coupled recovery boiler model has three major components: a CFD code for gas flow; an in-flight model for particle trajectories and combustion; and a char bed model for combustion and sulfate reduction in the char bed. The three components exchange information iteratively so that the results of one submodel will affect the others. The results of this model provide a comparison with the isothermal flow field and in-flight model.

Case Setup

The geometry of the model was set up to match the actual boiler design and the isothermal model. The furnace is represented by a grid of $51 \times 51 \times 57$ ($=148257$) cells. The air flow-rates and inlet velocities match those used previously in the isothermal base case model (100% of

design load). A fixed smooth char bed shape was specified in the model. Figure 14 shows a detail of the bed surface grid which is the interface between gas cells and char bed cells.

Liquor spray conditions match those used in the previous isothermal case. Two mass median drop diameters (Dm) were used to test the effects of drop size on combustion and carry-over. Except where specified, the results presented are for Dm=3.0mm.

Flow Patterns Results

Figure 15 shows the vertical velocity contours at different elevations. Overall, there is good agreement with the isothermal flow field results (compare Figure 7) and the same main features can be seen in both versions. There is an upward central core above the secondary air level. This is expected from the symmetrical arrangement of the primary and secondary air ports. The channel is broken by the strong interlaced tertiary air jets, resulting in a uniform flow pattern in the upper furnace.

Temperature

Temperature distribution is closely related to the combustion of volatile and char components of the black liquor. The temperature distribution shown in Figure 16 has a hot region in the center of the lower furnace. This hot region results, in part, from the combustion of volatiles released from the bed. The hot gas stream follows a flow pattern that shifts slightly towards the front wall as it continues up the furnace. The tertiary air jets effectively break the hot channel, resulting in a fairly uniform temperature distribution at the bullnose level. The predicted exit gas temperatures range from 1180 to 1270 K (about 900 to 1000 °C), which agrees well with the design value (about 1000 °C).

It can be seen that the temperature profiles correspond with the velocity profiles shown previously, i.e., the regions of high temperature in the upper furnace coincide with regions of high velocity. Therefore, a uniform velocity contour from an isothermal model may be a good predictor of a uniform temperature profile.

Particle Trajectories and Mass Distribution

Table 4 shows the fractions of black liquor that was released in different zones. Most of the volatiles were released to the gas phase, with a small portion landing on the bed. Half of the carbon is burnt in air, a third lands on the bed, and the rest hits the walls. Smelt is nearly equally split between the walls and the bed. A very small fraction of smelt (0.14%) is carried out of the furnace. The values calculated in this model are in good agreement with the values calculated for the same conditions with the isothermal in-flight model.

Zone	CH_4	Char	Smelt	Total
In-flight	93%	47%	0%	52%
Walls	0.5%	18%	53%	21%
Bed	6.5%	35%	47%	27%
Carry-	0%	0%	.14%	.05%
Total	100%	100%	100%	100%

Table 4. Black Liquor Mass Release by Zone

Effect of Drop Size

In addition to the 3.0mm Dm simulation, a 2.0mm Dm was also tested to examine the effect of drop size on combustion. Table 5 compares results for the two drop sizes. Drop size did not have a large influence on the average gas temperature leaving the furnace (at the bullnose). The biggest difference in simulation results was that the char bed temperatures differ by more than 200 °C. Since less combustible material is reaching the char bed with the smaller drops, the higher temperature may be due to the increased in-flight combustion above the char bed. Carry-over was also sensitive to drop size. Smaller particles resulted in significantly more carry-over. This is intuitive and consistent with the isothermal results.

	2.0mm	3.0mm
Max Gas Temp (°C)	1600	1570
Avg Exit Temp (°C)	939	944
Avg Exit O_2 (%)	2.6	3.1
Carryover (% smelt)	0.97	0.14
Max Bed Temp (°C)	1039	831
Avg Bed Surf Temp	835	603

Table 5. Effects of Drop Size on Operation

Conclusions

The operation of recovery boiler # 3 has been simulated using both an isothermal method and a fully-coupled (non-isothermal) modeling technique. Results from the fully-coupled method agree with isothermal simulations and support the validity of the fixed-field modeling technique that was used for most of this work.

At 100% of design load, both the isothermal and the non-isothermal models produced "good" flow fields with uniform velocities in the upper furnace. The non-isothermal case simulation gave a uniform temperature profile in the exit flow at the bullnose level, which should result in good superheater performance. The exiting gas temperature and O_2 concentration agree well with the design.

The three-front ports, two-rear ports interlaced tertiary air system was effective in achieving a well distributed air flow pattern with good mixing.

In general it does not appear that carry-over of black liquor drops will be a significant problem with this boiler, unless the black liquor firing conditions are producing very small drops. Mass median drop diameter was a critical variable for black liquor particle behavior. Increasing the drop diameter resulted in increasing amounts of combustibles reaching the char bed and decreasing levels of carry-over. The average gas temperature leaving the furnace, however, was not affected significantly by drop size.

Under low load conditions the use of tertiary air is beneficial. At 70% of design load the elimination of tertiary air allows the formation of a high velocity central core which persists into the upper furnace. Simulations showed that the use of tertiary air breaks up the central core and creates a uniform vertical velocity in the upper furnace. As a result, the carry-over tendency was greatly reduced.

ACKNOWLEDGMENTS

Most of the work on specific recovery boiler simulations was funded by the Georgia Consortium for Technological Competitiveness in Pulp and Paper. Kraft recovery boiler model development research has been sponsored by the U.S. Department of Energy, program manager Stanley F. Sobczynski, and by the Institute of Paper Science and Technology. We would like to acknowledge assistance from James River Corp and Tampella Power.

REFERENCES

1. Horton, R.R., Grace, T.M., and Adams, T.N., "The Effects of Black Liquor Spray Parameters on Combustion Behavior in Recovery Furnace Simulations," 1992 International Recovery Conference Proceedings, pp. 85-99, June 1992.

2. Vakkilainen, E.K., Adams, T.N., and Horton, R.R., "The Effect of Recovery Furnace Bullnose Designs on Upper Furnace Flow and Temperature Profiles," 1992 International Recovery Conference Proceedings, pp. 101-112 , June, 1992.

3. Horton, R.R., Slayton, D.J., Grace, T.M., and Adams, T.N., "In-Flight Black Liquor Combustion Simulations Using a Three-Dimensional Computer Model: Sensitivity Studies," 1992 AIChE Forest Products Symposium Series, pp. 27-48, 1993.

4. Horton, R.R. and Vakkilainen, E.K., "Comparison of Simulation Results and Field Measurements of an Operating Recovery Boiler," TAPPI Engineering Conf. Proceedings, pp. 635-642, Orlando, Sept., 1993.

5. Yang, W., Horton, R.R., and Adams, T.N., "Effects of Boundary Geometries on CFD Simulations of Recovery Furnace Char Beds," TAPPI J. vol. 7, no. 8, pp. 189-199, Aug. 1994.

6. Frederick, J.W., "Combustion Processes in Black Liquor Recovery: Analysis and Interpretation of Combustion Rate Data and an Engineering design Model" US DOE Report DOE/CE/40637-T8(DE90012712), March 1990.

7. Empie, H.J., Lien, S.J., Yang, W.R., and Adams, T.N., "Spraying Characteristics of Commercial Black Liquor Nozzles," 1992 International Recovery Conference Proceedings, pp. 429-440, June 1992.

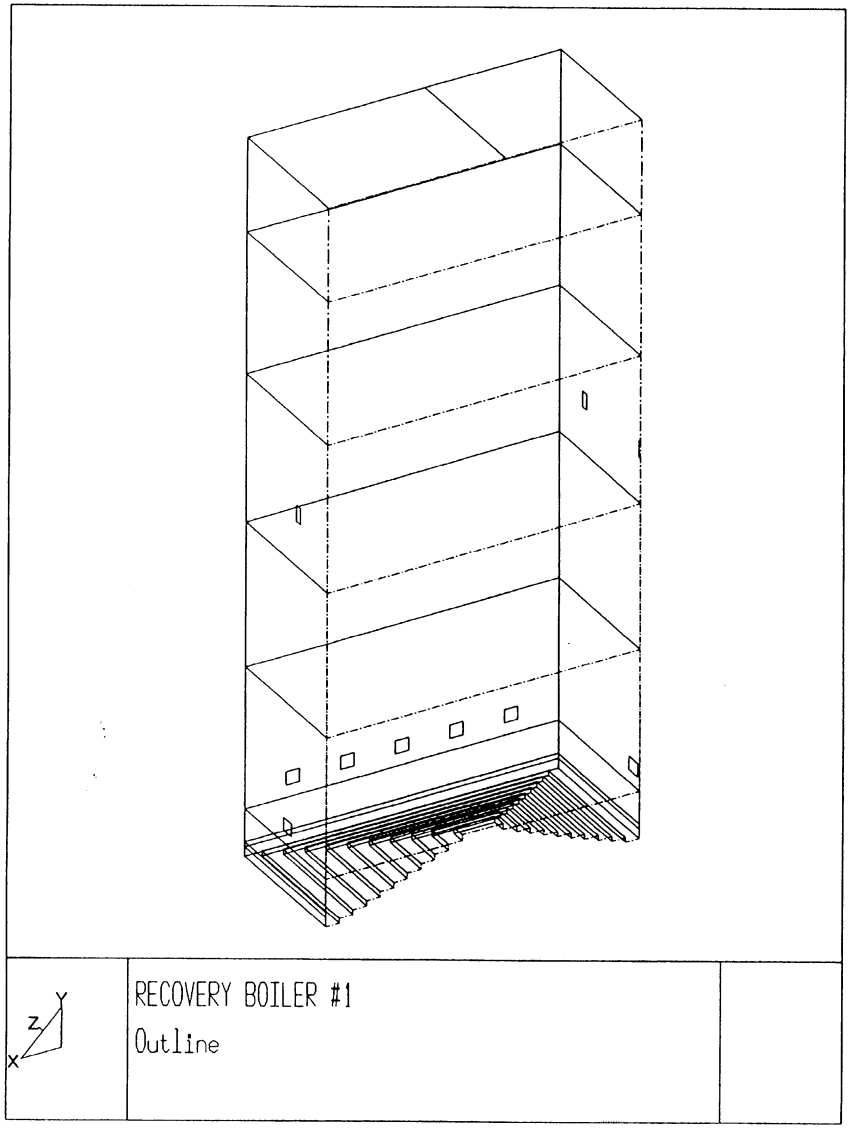

Figure 1 Recovery Boiler #1

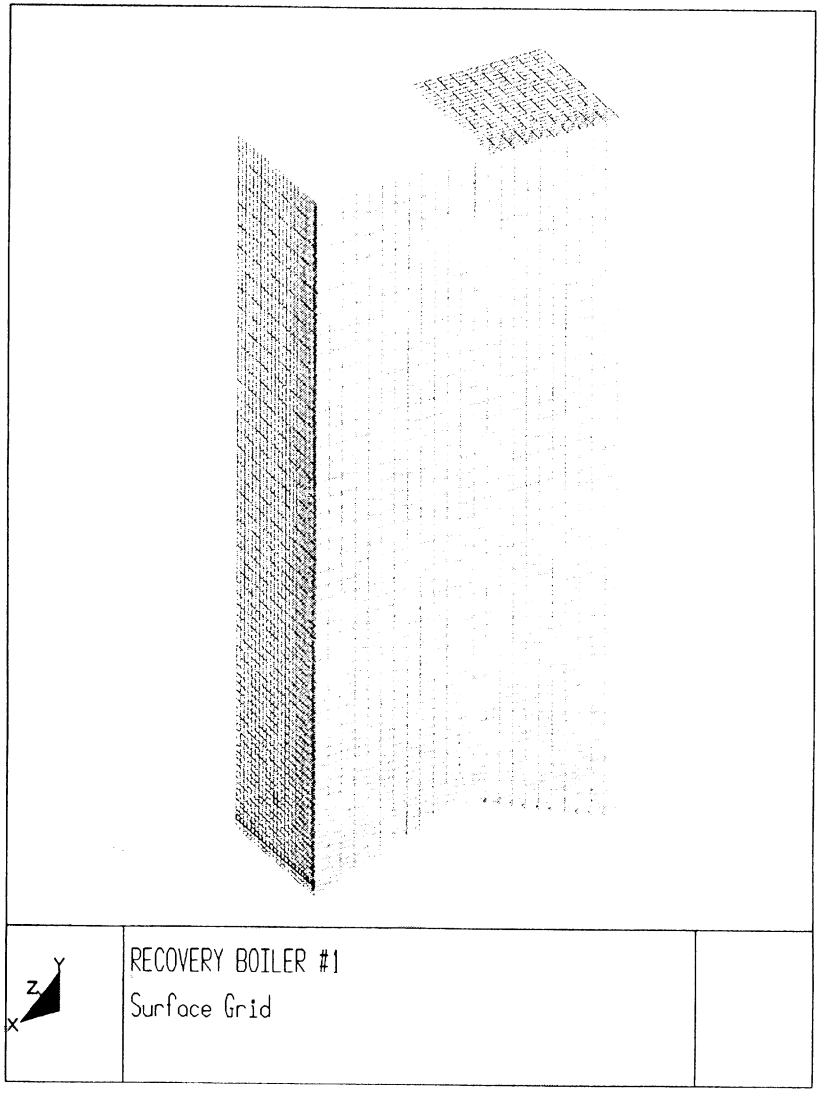

Figure 2 Recovery Boiler #1 - Grid

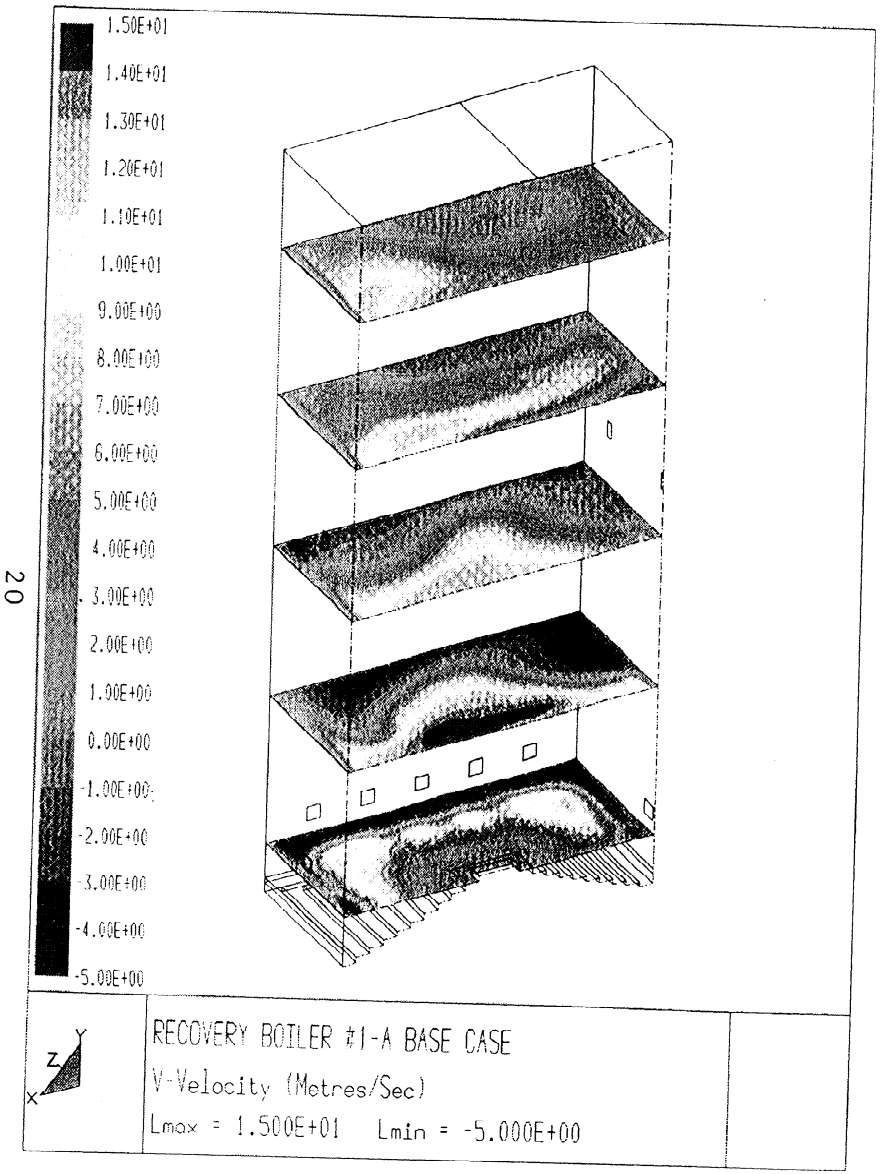

Figure 3 RB #1-A - Flow Field

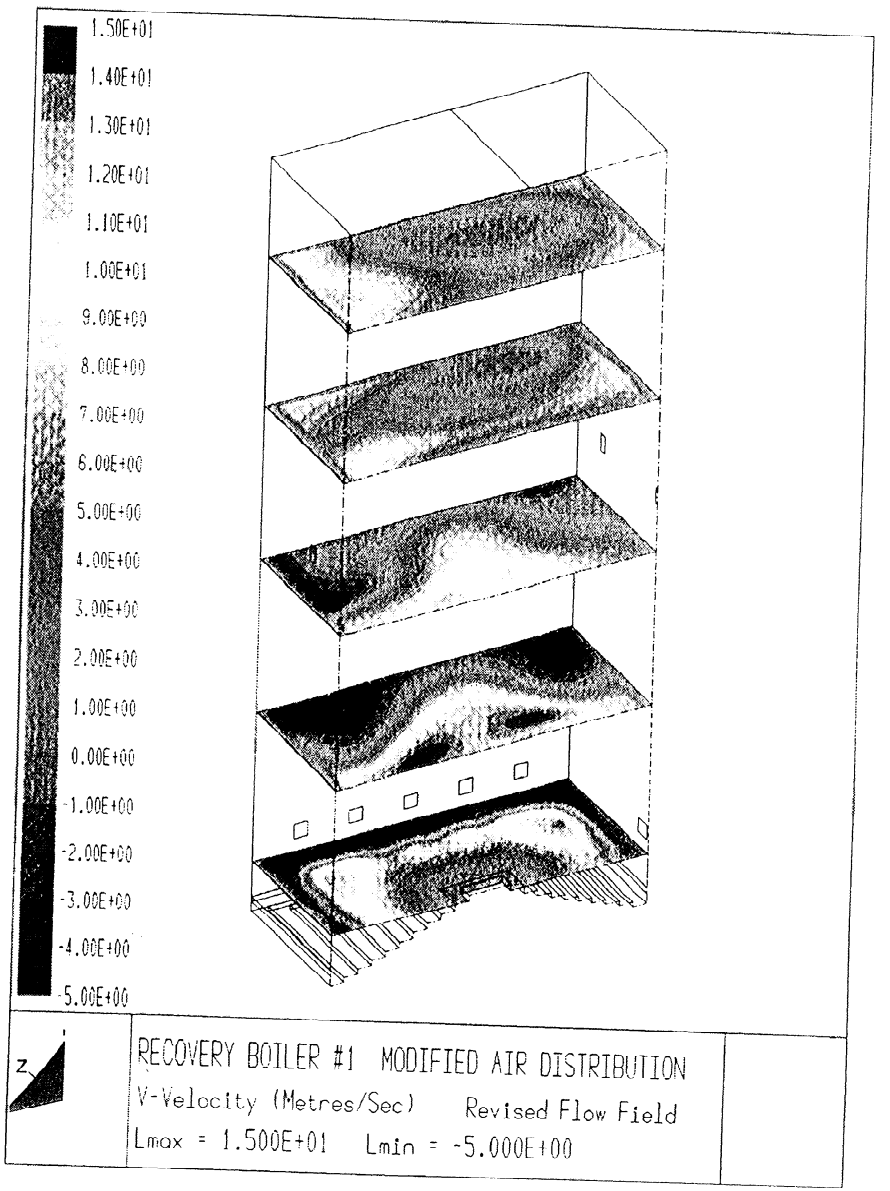

Figure 4 RB #1-B - FLow Field

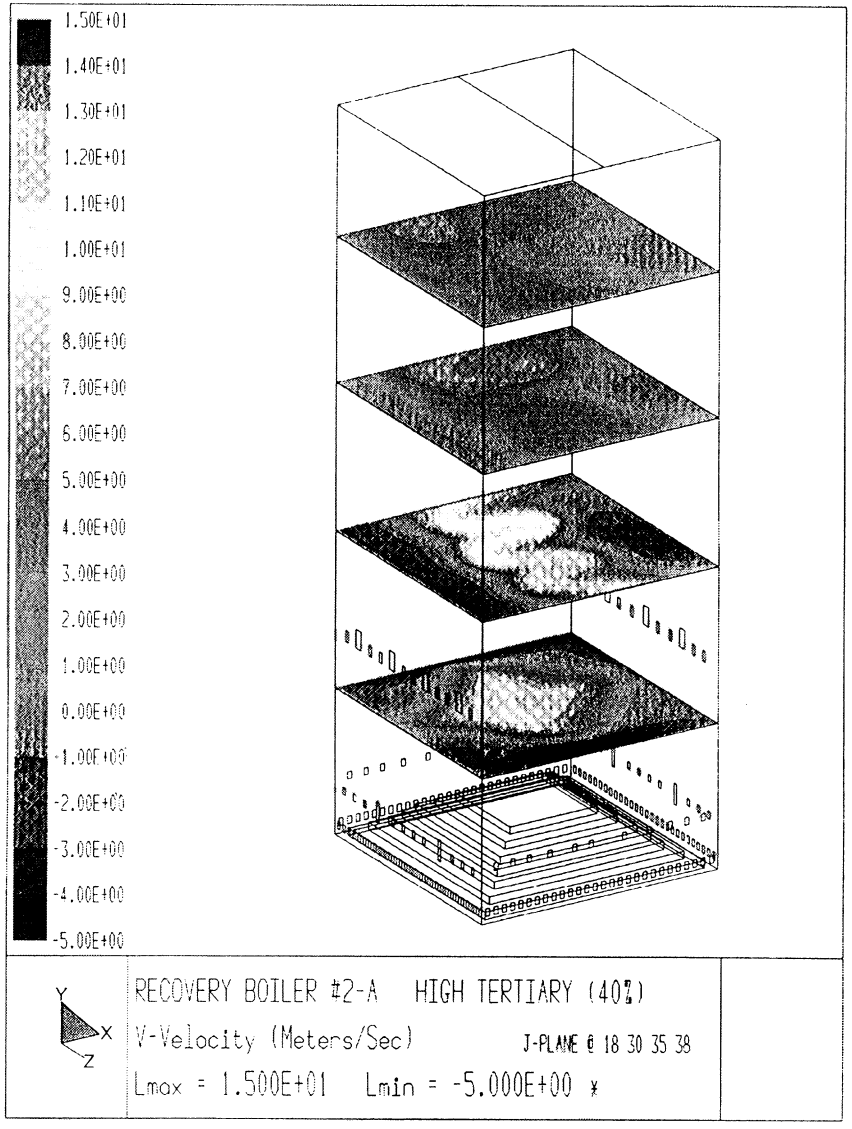

Figure 5 RB #2-A - Flow Field

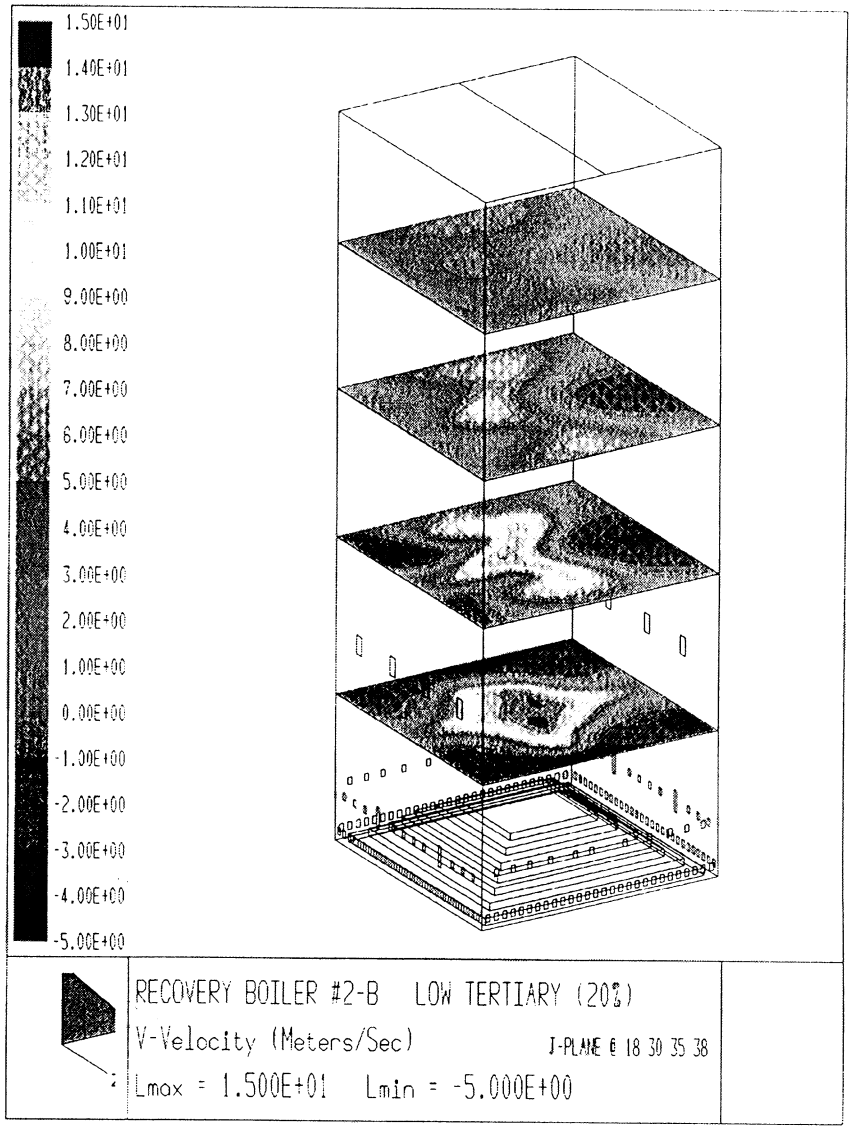

Figure 6 RB #2-B - Flow Field

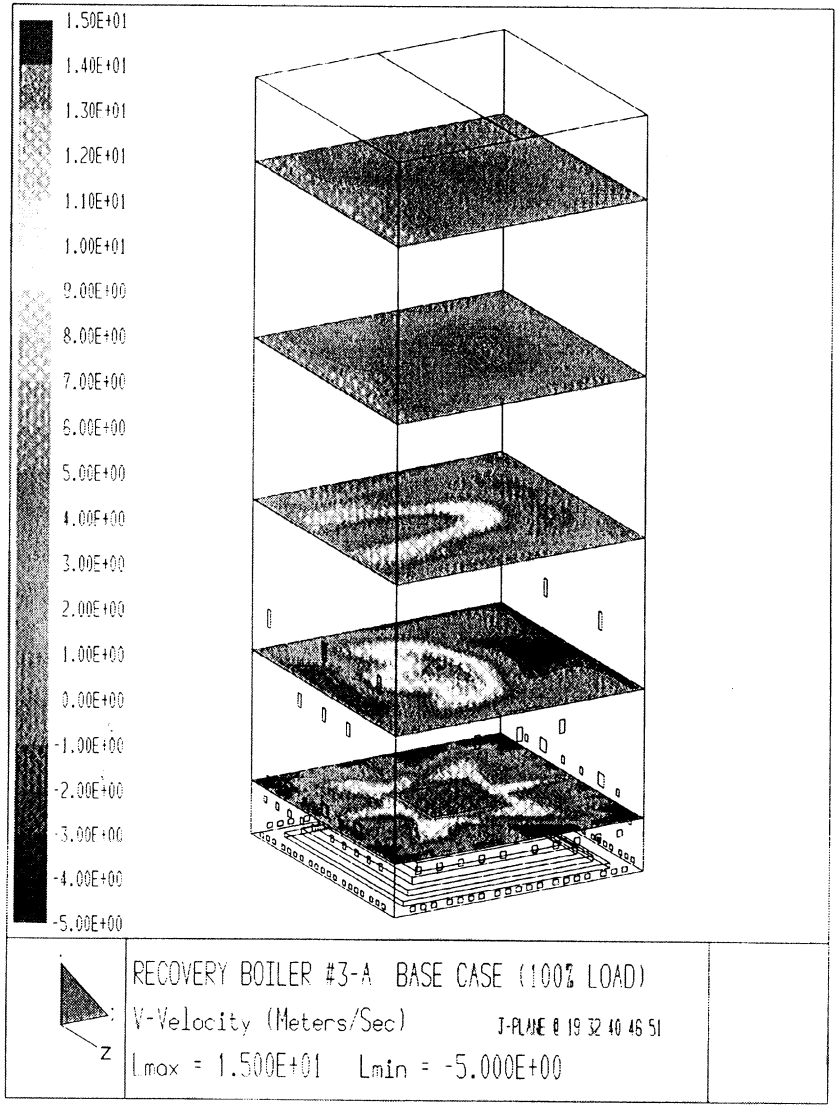

Figure 7 RB #3-A - Flow Field

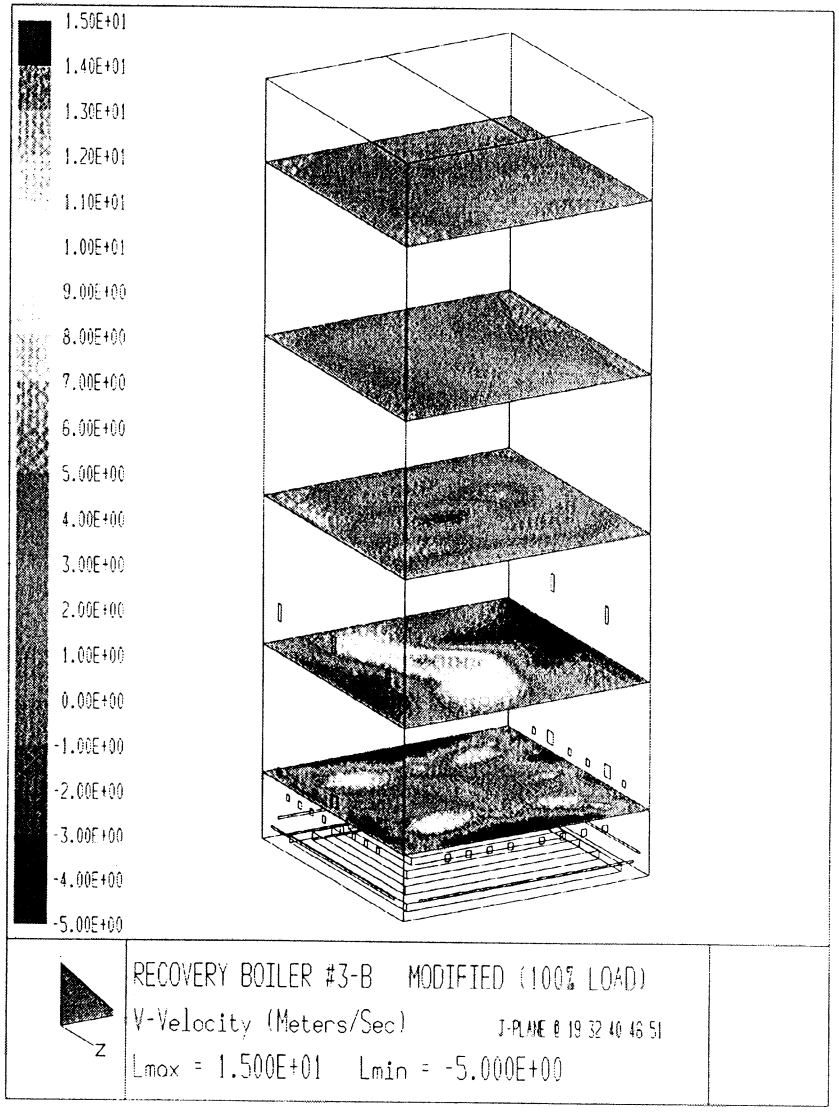

Figure 8 RB #3-B - Flow Field

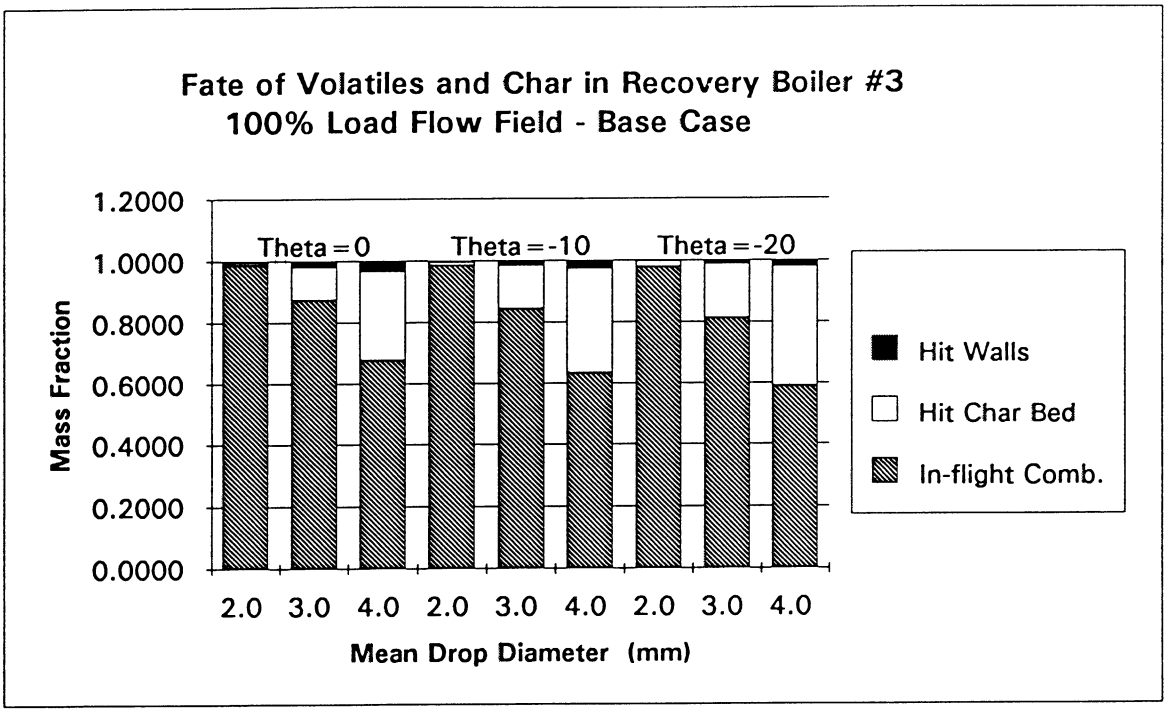

Figure 9 Distribution of Combustible Fraction of Black Liquor

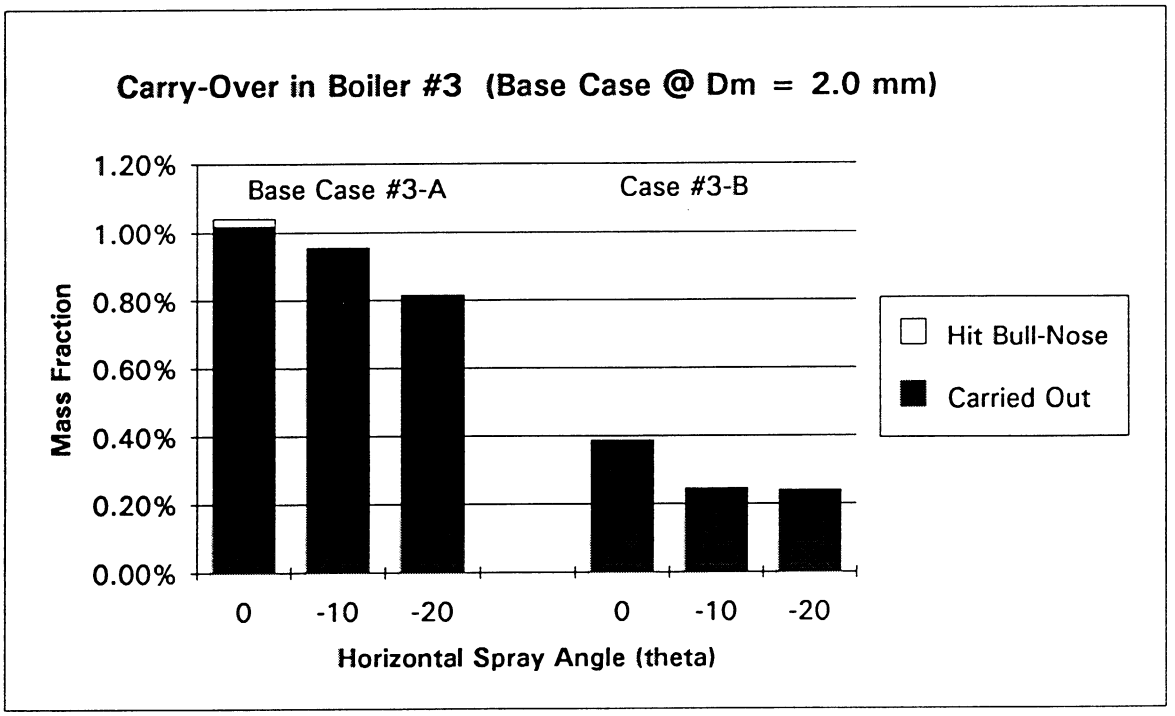

Figure 10 Carryover at 100% of Load (Dm = 2.0 mm)

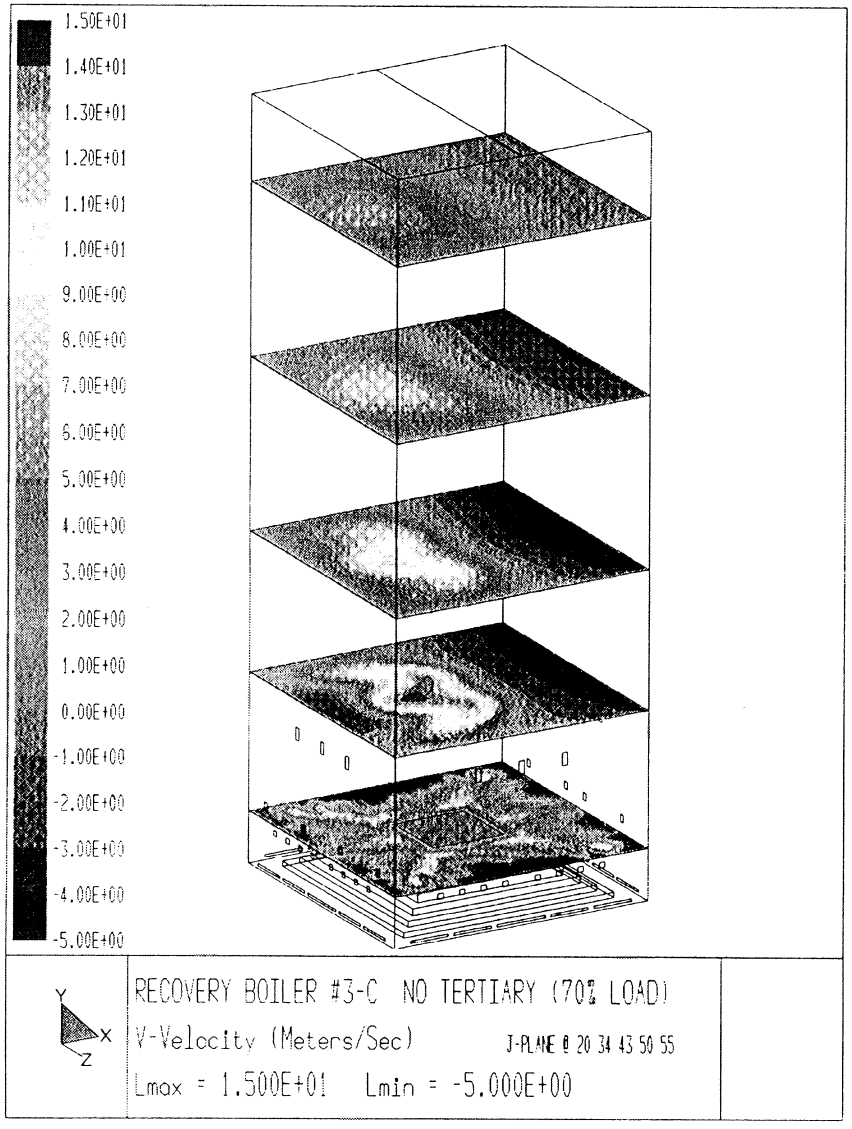

Figure 11 RB #3-C - Flow Field

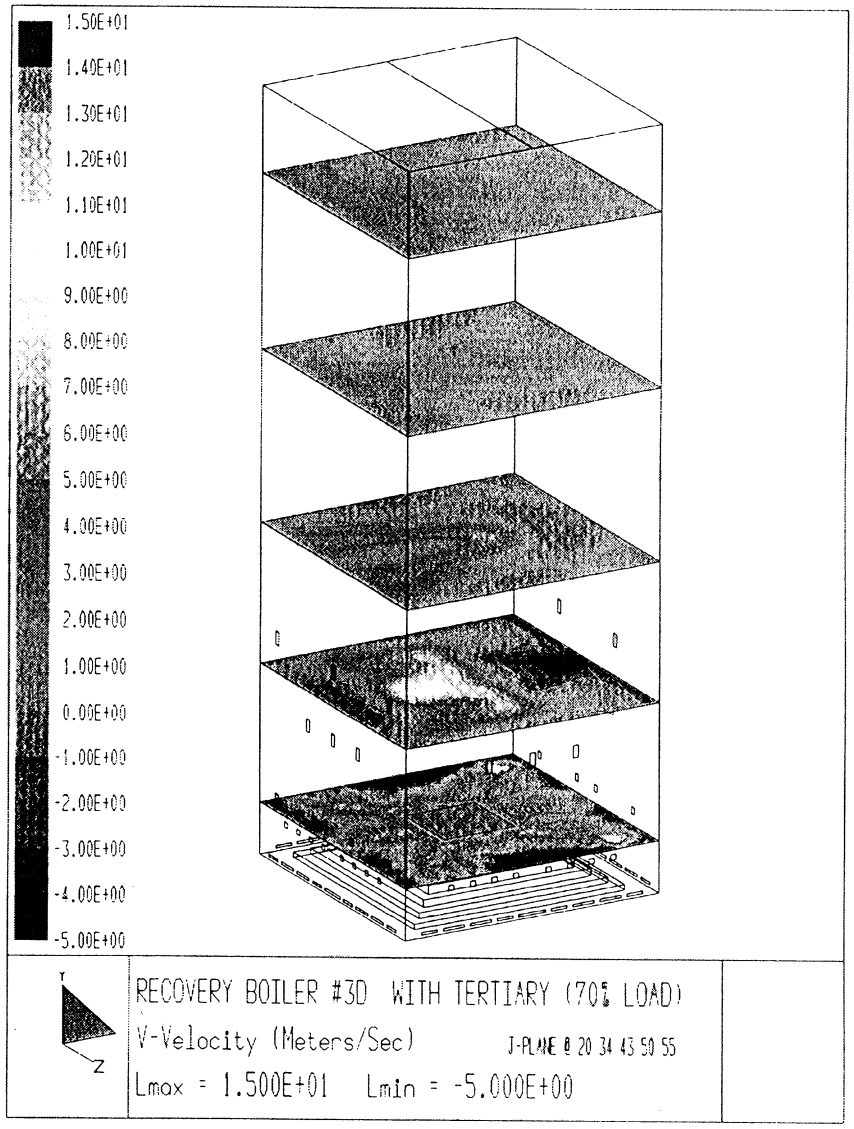

Figure 12 RB #3-D - Flow Field

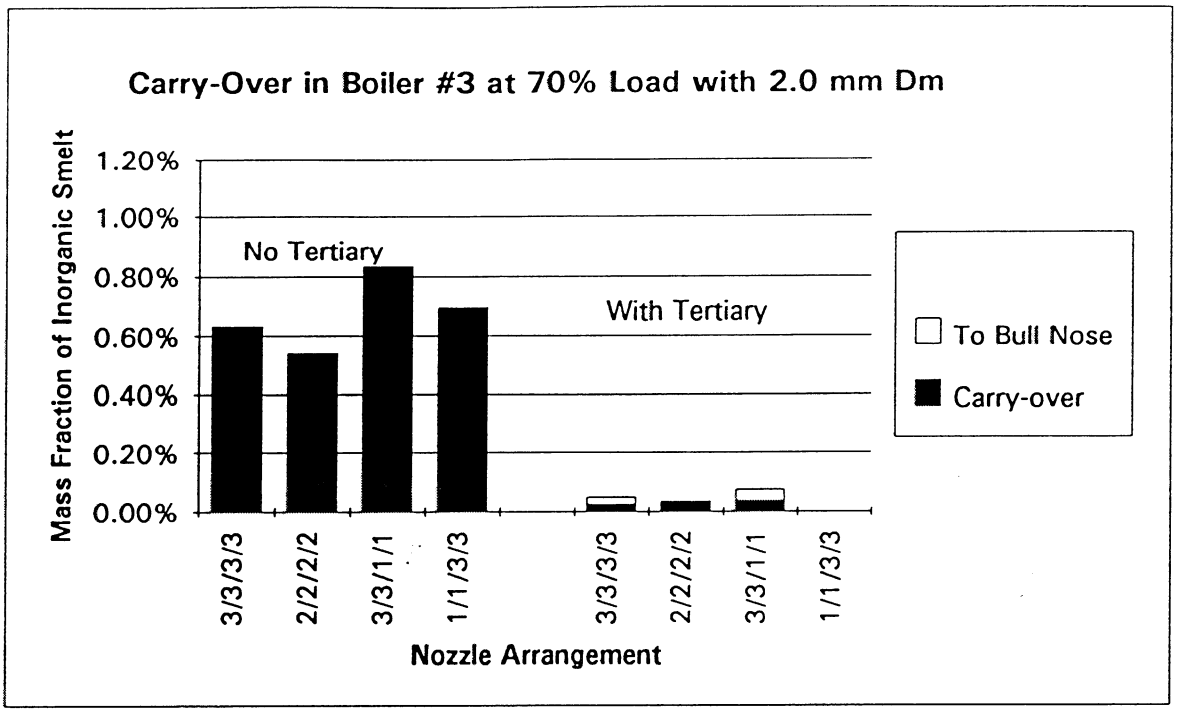

Figure 13 Carryover at 70% of Load (Dm = 2.0 mm)

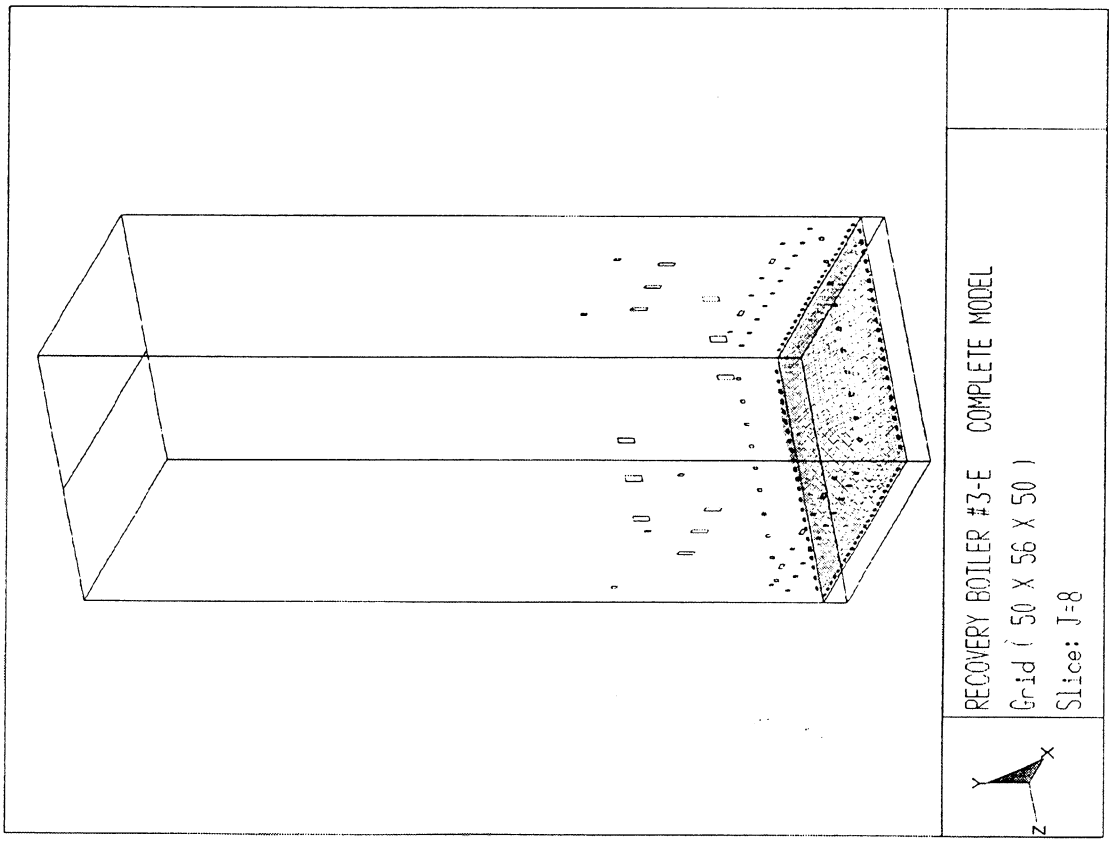

Figure 14 RB #3-E - Non-isothermal Grid

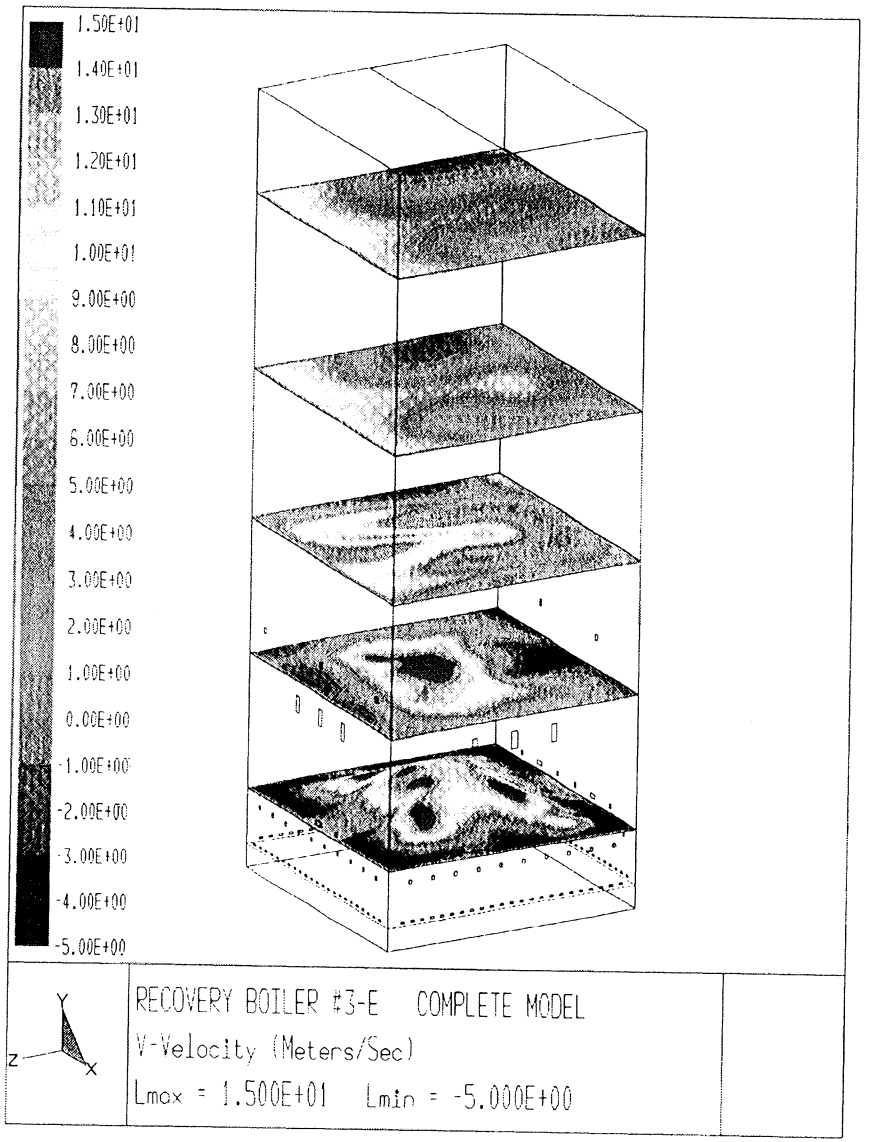

Figure 15 RB #3-E - Flow Field

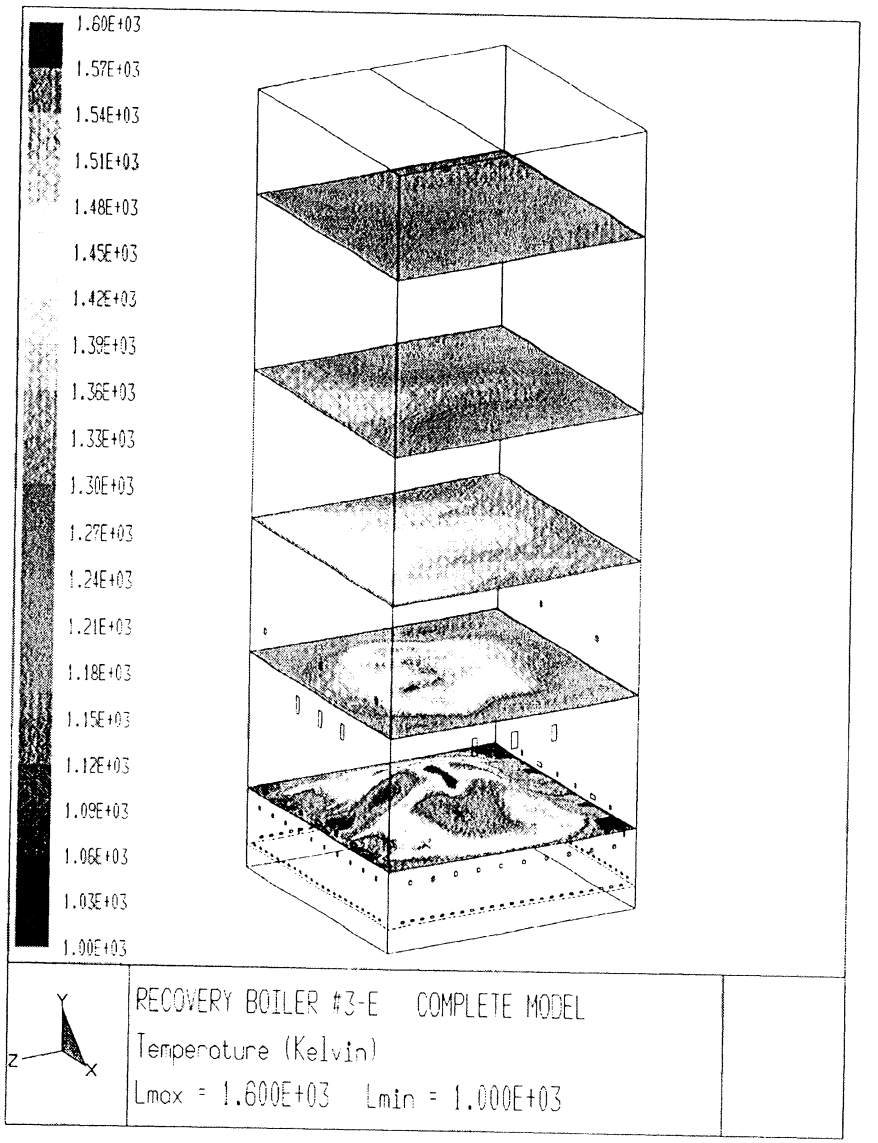

Figure 16 RB#3-E - Temperature

KRAFT RECOVERY FURNACE -

NO_X REACTIONS

THE EVOLUTION OF FUEL NITROGEN DURING BLACK LIQUOR PYROLYSIS

Denise Martin
Ph.D. Candidate

Thesis Advisor: Dr. Earl Malcolm

Thesis Committee Members:
Dr. Jeff Empie
Dr. Tom Grace
Dr. Junyong Zhu

A490
Chemical and Biological Sciences Division

Institute of Paper Science and Technology
500 10th Street, N.W.
Atlanta, GA 30318
(404) 853-9500

March 23, 1995

The Evolution of Fuel Nitrogen During Black Liquor Pyrolysis

Introduction

Under current operating conditions in recovery boilers, the fuel NO mechanism is the dominant source of NO_x emissions. Only a 20% conversion of the suspected 0.1% nitrogen in black liquor is necessary to account for the majority of the NO_x that is measured. Conversions of black liquor nitrogen have been measured at 20-80% during various laboratory and commercial tests. Therefore, the potential exists for considerably higher amounts of NO_x emissions to be measured at the stack if the fuel nitrogen conversion increases. The effects of the liquor composition both in terms of the fuel nitrogen and the inorganic components are being investigated to provide a fundamental understanding of the nitrogen release and its ultimate oxidation to NO_x.

Thesis objectives have been revised accounting for recently published work in NO_x formation. The focus had been directed at understanding the effects of operational parameters. The focus is now directed toward understanding the effects of the liquor composition and the liquor nitrogen structure on the release of nitrogen and its conversion to NO.

Previous Results and Discussion

Characterization of five black liquors was completed. All liquors were shown to contain less than 0.1%N. Variations in elemental composition, nitrogen content, and the structure of the nitrogen appeared to be liquor specific. Nitrogen species included nitrates, amino acids which were both straight chain and heterocyclic in nature. The heterocyclic nitrogen species included both five and six membered ring species.

Inert pyrolysis experiments with model systems have shown the inorganic composition to be important with regard to the onset temperature for decomposition and volatiles yield of the fuel nitrogen components. Sulfate and carbonate were significant as well as the sodium content. The initial addition of sodium to the system greatly affected the expected volatiles yield for the model fuel nitrogen compounds and also shifted the expected decomposition into a higher temperature range. These phenomena a most likely explained by a complexation which occurs between the inorganic species and the organic fuel nitrogen model compounds.

Inert pyrolysis of commercial black liquors indicated that the volatile nitrogen is released by ~500 °C. It was observed that approximately 10% was released as fixed nitrogen (the sum of NO and oxidizable intermediates, such as NH_3 and HCN), 50% remained in the char, and therefore, approximately 40% was assumed to be N_2.

Current Results and Discussion

The results of the pyrolysis of the commercial liquors were different from those previously published for similar conditions.[1] The results from this work were combined with those of the publication to explain the data. It was found that a relationship existed between the composition of the liquors for the current data and that published with the amount of nitrogen measured as fixed nitrogen. Regression analysis was used to determine the relationship between the nitrogen content and the nitrogen released as fixed nitrogen. An increase in the nitrogen content of the liquors increased the nitrogen

observed as fixed nitrogen ($R^2 = 0.716$). It was also found that the fixed nitrogen decreased with each of the Na/N, C/N, and O/N ratios. The correlations were found to be $R^2 = 0.77$, 0.75, and 0.65, respectively.

A method was developed for a reliable total nitrogen analysis of black liquors. This method is used in this study instead of the Kjeldahl method because it provides greater precision and sensitivity and is safer and less time consuming. The method is a high temperature, excess oxygen combustion means of converting all fuel nitrogen species to NO. The NO_x is detected via chemiluminescence. This method has been verified to provide equivalent results compared with Kjeldahl.[2,3]

A total nitrogen balance in liquor has shown the nitrogen content of the liquors to be approximately two-thirds organic and one-third inorganic including nitrate and proteinaceous compounds. This result is shown in Figure 1 below.

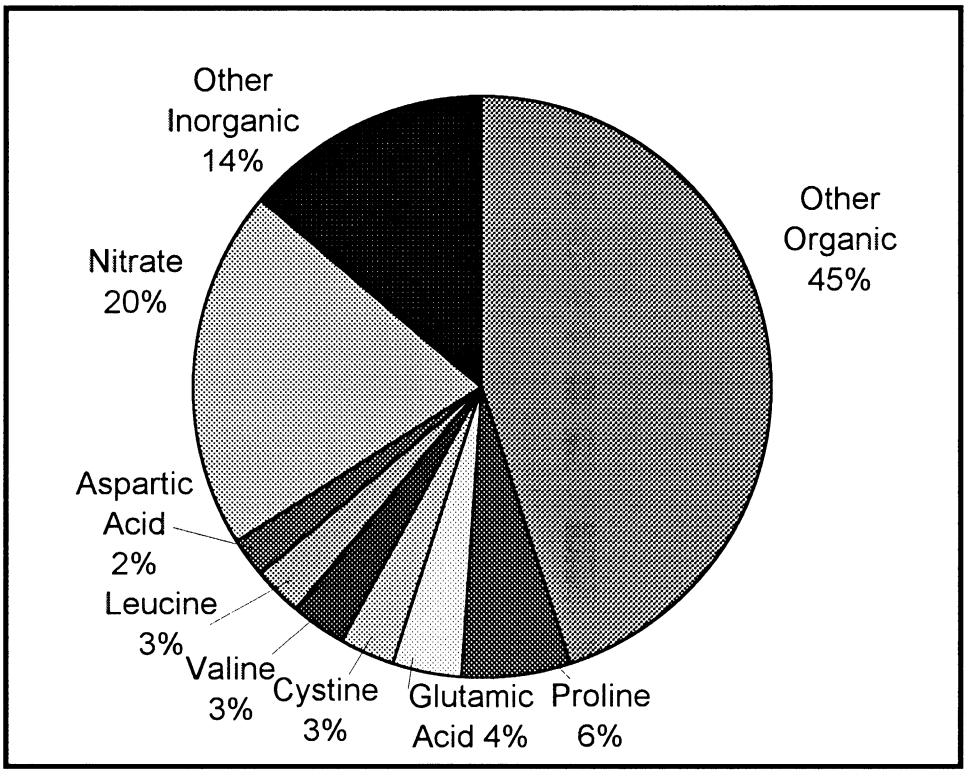

Figure 1. Composition of Southern Pine I black liquor nitrogen.

Tests using model compounds of black liquor nitrogen species indicate that the conversion of the bound nitrogen to NO_x varies greatly. Conversion of nitrate, amine, and heterocyclically bound nitrogen species to NO ranged from 35-90%. The balance of the nitrogen is assumed to be N_2. Exact conversions were dependent on the chemical structure as seen in Figure 2. Thermodynamic and kinetic calculations did not explain the differences observed. Work continues evaluating the nitrogen conversion chemistry for an explanation. All conversion experiments were conducted in an 1100°C, 75% O_2 combustion environment to maximize conversion to NO_x.

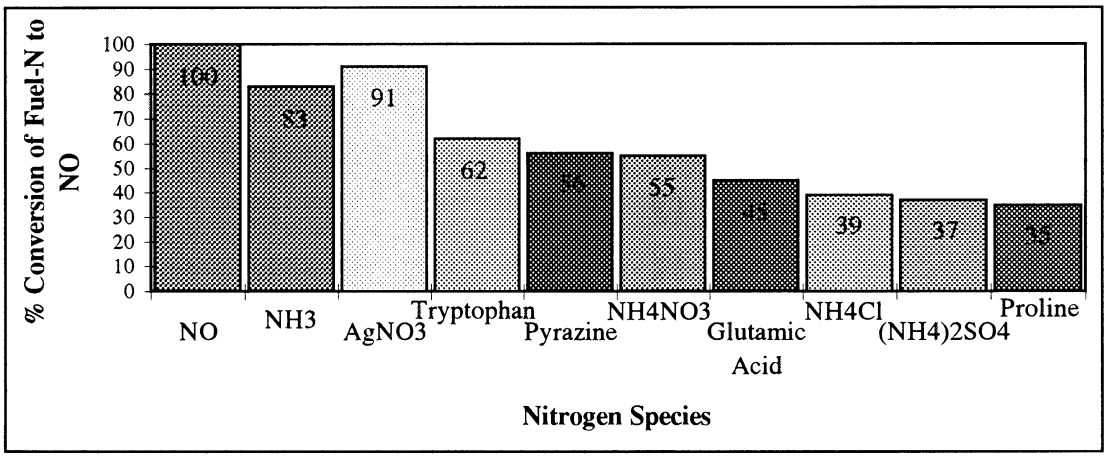

Figure 2. Relative conversion of model fuel nitrogen compounds to NO.

Along with the dependence of the nitrogen structure on the fuel nitrogen conversion to NO_x, the composition of the matrices, i.e. the black liquor, in which the nitrogen is bound also has been shown to be significant. Equivalent amounts of NaOH, Na_2SO_4, and Na_2CO_3 in solution were evaluated for effects on the conversion of the nitrogen NO_x. The conversion of fuel nitrogen to NO_x varied with organic species and organic nitrogen. For example, Na_2SO_4 enhanced the conversion to NO_x of glutamic acid while Na_2CO_3 inhibited the conversion. See Figure 3. Increasing concentrations of Na_2CO_3 enhanced the conversion to NO of NH_4Cl as seen in Figure 4. More work is required to understand the relationship between the inorganic composition and the fuel nitrogen conversion to NO.

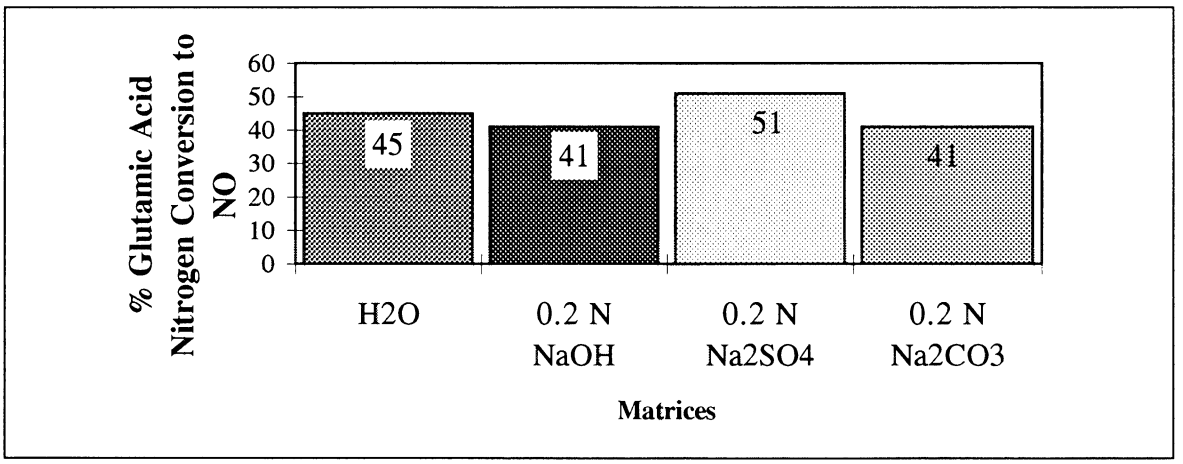

Figure 3. Effect of sodium species in the matrices on the conversion of glutamic acid nitrogen to NO.

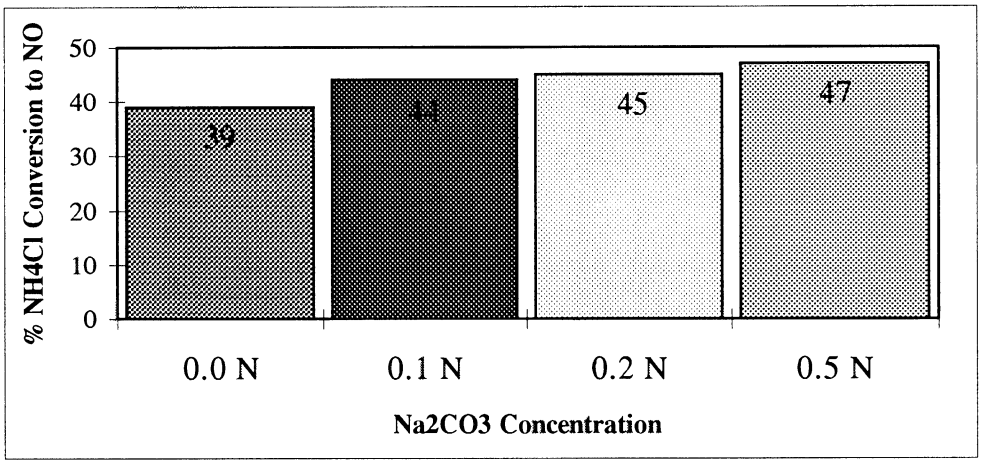

Figure 4. Effect of Na_2CO_3 concentration on the conversion of NH_4Cl nitrogen to NO.

Summary

The basis for any NO_x data is a reliable determination of the nitrogen in the black liquor. One such test method has been developed for the evaluation of total nitrogen in black liquor and its conversion to NO. Black liquor nitrogen is approximately two-thirds organic and one-third inorganic. The conversion of the black liquor nitrogen species to NO is dependent on the chemical structure of the nitrogen and the inorganic nitrogen species and its concentration in the matrices.

Future Work

Future work includes completion of the black liquor composition effects. Specifically, the effect of nitrogen structure during pyrolysis on the release and oxidation of the nitrogen to NO will be evaluated. Also, the effect of the inorganic composition, residual alkali, total sodium, and residual sulfide will be evaluated. Some work evaluating heating rate effects will also be done. The results of these investigations will be applied to Kraft recovery operations to provide alternative NO_x control strategies.

Literature Cited

1. Aho, K.; Hupa, M.; Nikkanen, S. "Release of Nitrogen Compounds During Black Liquor Pyrolysis." Tappi Engineering Conference Proceedings, Orlando, FL, September 1993.

2. Kostantinides, F.N.; Boehm, K.A.; Radmer, W.J.; Storm, M.C.; Adderly, J.T.; Weisdorf, S.A.; Cerra, F.B. "Pyrochemiluminescence™: Real-Time, Cost-Effective Method for Determining Total Urinary Nitrogen in Clinical Nitrogen-Balance Studies." Clinical Chemistry. 34(12):2518-2520 (1988).

3. Jones, B.M.; Daughton, C.G. "Chemiluminescence vs. Kjeldahl Determination of Nitrogen in Oil Shale Retort Waters and Organonitrogen Compounds." Analytical Chemistry 57:2320-2325 (1985).

THE RATE OF DEPLETION OF NO BY REACTION WITH MOLTEN SODIUM SALTS

Laura M. Thompson
Ph.D. Candidate

Advisory Committee:
Dr. Jeff Colwell
Dr. Jeff Empie (Primary Advisor)
Dr. Lucy Sonnenberg

A490
Chemical and Biological Sciences Division

Institute of Paper Science and Technology
500 10th Street, N.W.
Atlanta, GA 30318
(404) 853-9500

March 23, 1995

The Rate of Depletion of NO by Reaction with Molten Sodium Salts

Laura M. Thompson and H. Jeff Empie

Institute of Paper Science and Technology

Atlanta, Georgia

Abstract

Reactions of NO with molten sodium species have been identified as a possible depletion mechanism in a kraft recovery furnace. Experiments have been conducted in which nitric oxide in helium was bubbled through molten sodium carbonate (Na_2CO_3) and mixtures of Na_2CO_3 and sodium sulfide (Na_2S). Results show that the depletion of NO follows a pseudo first order rate expression. The rate of reaction is enhanced by the presence of sodium sulfide. Calculated activation energies are 89.0 and 41.2 kcal/mol for reaction with Na_2CO_3 and Na_2CO_3/Na_2S mixtures, respectively. Analysis of gaseous products indicates that NO is being reduced to nitrogen and oxygen according to the overall stoichiometry:

$$NO \rightarrow \tfrac{1}{2}N_2 + \tfrac{1}{2}O_2 .$$

Introduction

The formation of NO_x in a kraft recovery furnace is believed to occur by way of the fuel NO_x formation mechanism. However, it has been estimated that only ~ 25 % of the nitrogen in black liquor is emitted as NO_x from a typical recovery furnace.[1] Thus the question remains as to the fate of the remaining nitrogen. It is feasible that a portion of the nitrogen does not get oxidized and either remains in the char or is released as a reduced nitrogen species in the flue gas. It is also possible that once NO_x is formed, it reacts with other species present in the furnace and is reduced.

In previous papers we presented the concept that the concentration of nitric oxide could potentially be reduced in a recovery furnace by reacting with molten sodium species.[2,3] Experiments were conducted in which nitric oxide in helium was bubbled through molten sodium carbonate (Na_2CO_3). Results showed that NO was reduced by 10 to 75 % over the temperature range of 860 to 973 °C.[3] The rate of depletion was shown to follow a pseudo first order rate expression as follows:

(Eq. 1)
$$-r_{NO} = -\frac{1}{V_L}\frac{\delta N_{NO}}{\delta t} = \frac{aP_{NO}}{\frac{1}{k_g} + \frac{H_{NO}}{\sqrt{D_{NO/Na}k_1}}}.$$

Upon rearranging terms, equation (1) can be written as:

(Eq. 2)
$$k_1 = \frac{1}{\frac{(a\ell)^2}{\left(-\ln\left(\frac{P_{NO_f}}{P_{NO_i}}\right) - \frac{1}{H_{NO}k_g}\right)^2}} (D_{NO/Na})^{-1} \quad (\sec^{-1}).$$

Constants in equation (2) are calculated from correlations found in the literature. In short, a and t are functions of the gas flow rate. H_{NO}, k_g, and $D_{NO/Na}$ are dependent on temperature. Thus, the pseudo first order rate constant can be found as a function of concentration, flow rate, and temperature. A complete list of equations and notation is included at the end of the paper.

The derivation of equation (1) assumes the reaction to be first order with respect to NO.[4] Data verifying this assumption will be presented here. This paper also presents results of experiments investigating the reaction of NO with mixtures of Na_2CO_3 and sodium sulfide (Na_2S). In addition to the rate data, analysis of the gaseous products has been conducted by on line gas chromatography to determine the products of the reaction.

Experimental Apparatus

A schematic of the experimental apparatus is shown in Figure 1. Helium and a mixed gas of nitric oxide in helium are fed from pressurized gas cylinders. Flow is measured by Hastings-Teledyne™ digntal mass flowmeters and is controlled manually by needle valves. The gas is fed to the reaction chamber (Figure 2) which is described in detail below. Exit gas from the system is analyzed by a chemiluminescent NO_x analyzer (provided by NCASI). A Carle™ Model 8000 Basic Gas Chromatograph equipped with a six-port sampling valve was used for detection of oxygen (O_2) and nitrogen (N_2) in the exit gas. The GC was fitted with a 15 foot x 1/8 inch stainless steel column packed with Carboxen™ 1000. The column and inlet temperatures were held constant at approximately 40°C. Chromatographic grade helium was used as the carrier gas at a flow rate of 28 cc/min. The sample loop in the sampling valve had a volume of 1.0 cc.

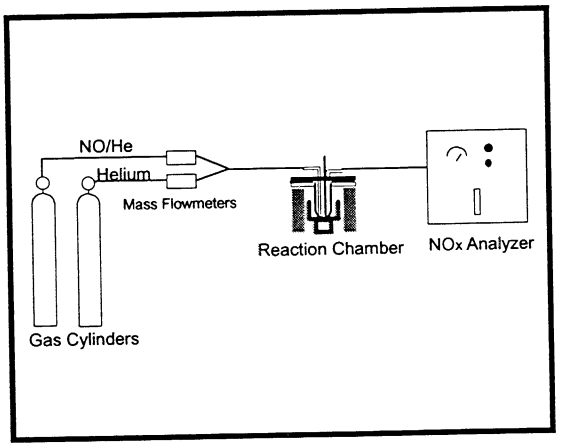

Figure 1: Experimental Apparatus

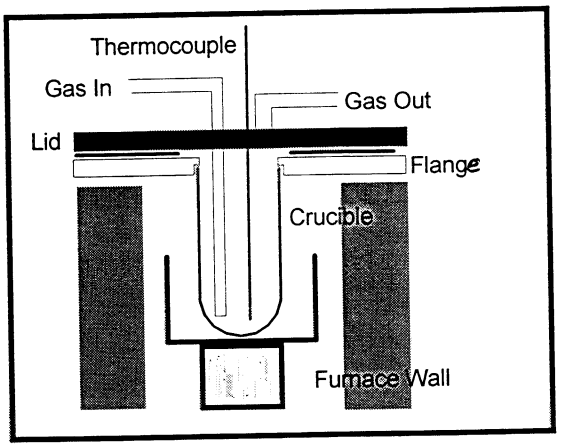

Figure 2: Reaction Chamber

Molten salt is contained in a 4 cm x 10 cm alumina crucible which is cemented to a stainless steel flange. A graphite gasket is placed between the flange and the lid which is held in place by eight bolts to form a gas-tight seal. The reaction vessel is heated by a tube furnace. Gases are bubbled through the salt using a 0.4 cm ID alumina tube. A type-K thermocouple, protected by an alumina well, is used to measure the temperature of the molten salt. The mass flowmeters, thermocouple, and NO_x analyzer are connected to a personal computer for data acquisition. Data are acquired at a rate of 0.5 Hz.

Experimental Conditions

The independent variables for each experiment include: gas flow rate, NO concentration, temperature, and the mass of each salt. The experimental conditions for each run are listed below in Tables 1, 2, and 3. The first set of experiments was conducted to verify the assumption of the first order behavior with respect to the concentration of NO. For the second set of experiments, the exit gases were analyzed by on-line GC. The third set of experiments was conducted to compare the rate of reaction for mixtures of Na_2CO_3/Na_3S with the results for Na_2CO_3 only. On line GC analysis was conducted for all of the experiments with the mixed salts. For experiments where samples were analyzed by GC, three to five replicate samples were analyzed at each set of conditions.

Table 1: Experimental Conditions For Determining Order of Reaction With Respect to [NO]

Experiment	Total Flow Rate (L/min)	$[NO]_{in}$ (ppm in helium)	Temperature (°C)	Mass of Na_2CO_3 (g)	Mass of Na_2S (g)
1	1.3	2700-8400	864-946	35.0	---
2	1.3	2700-8400	868-954	35.0	---
3	1.3	2000-9400	883-890	38.0	2.0
4	1.3	2000-9400	895-912	38.0	2.0

Table 2: Experimental Conditions For Depletion of NO by Na_2CO_3 With Gas Analysis by GC

Experiment	Total Flow Rate (L/min)	$[NO]_{in}$ (ppm in helium)	Temperature (oC)	Mass of Na_2CO_3 (g)	Mass of Na_2S (g)
5	1.1	8400	887-961	30.0	---
6	1.1	8400	897-962	30.0	---
7	1.0	8400	894-966	40.0	---
8	1.0	8400	905-962	40.0	---
9	1.2	8400	910-946	25.0	---
10	1.3	9600	889-951	40.0	---

Table 3: Experimental Conditions For Depletion of NO by Mixtures of Na_2CO_3 and Na_2S With Gas Analysis by GC

Experiment	Total Flow Rate (L/min)	$[NO]_{in}$ (ppm in helium)	Temperature (oC)	Mass of Na_2CO_3 (g)	Mass of Na_2S (g)
11	1.3	9600	887-934	40.0	1.5
12	1.3	9600	860-914	40.0	1.5
13	1.3	9600	878-920	40.0	1.5
14	1.0	9600	878-917	35.0	1.3
15	1.0	9600	879-914	35.0	1.3
16	1.1	9600	882-915	30.0	2.0
17	1.1	9600	864-928	30.0	2.0
18	0.92,1.3	9600	870-916	37.0	3.0

Results

To verify that the depletion of NO is first order with respect to [NO], experiments were conducted in which the inlet concentration was varied between 2000 to 9400 ppm at a constant temperature. This was repeated at several temperatures between 860 to 955 °C for reactions with Na_2CO_3 and a mixture of Na_2CO_3 and Na_2S. The results of these experiments were plotted as conversion *vs.* inlet concentration. The data are shown below in Figures 3 and 4. The percent conversion is defined as:

(Eq. 3) $$X = 100\left(1 - \frac{[NO]_f}{[NO]_i}\right).$$

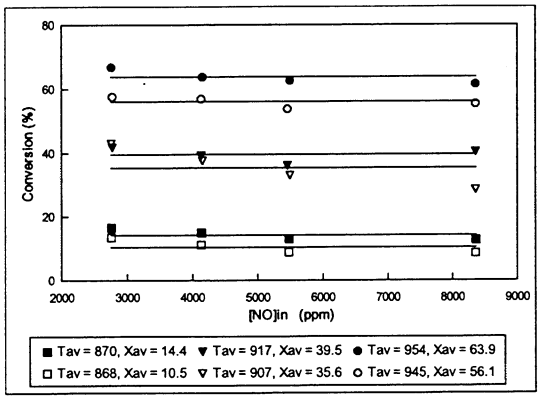

Figure 3: Conversion of NO as a Function of Inlet Concentration for Experiments 1 and 2. Reactant: Na_2CO_3.

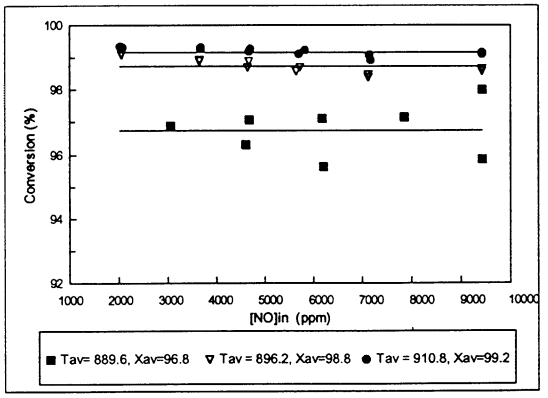

Figure 4: Conversion of NO as a Function of Inlet Concentration for Experiments 3 and 4. Reactant: Na_2CO_3/Na_2S Mixture.

Inspection of Figures 3 and 4 shows constant conversion over the range of inlet concentrations at each temperature. This behavior is indicative of a first order reaction. It should also be noted that much higher conversions are observed for the reactions with the mixed salt.

The gas chromatograph was calibrated using a certified gas mix standard of 5100 ppm O_2 and 5040 ppm N_2 in UHP helium. By mixing the standard with NO in helium, the GC was calibrated at five concentrations between 0 to 5100 ppm O_2, 0 to 5040 ppm N_2 and 0 to 4600 ppm NO. The peak areas for nitrogen were linear with respect to concentration. It was found that the presence of nitric oxide reduces the peak area for oxygen. Therefor, a multiple linear regression for peak area as a function of NO and O_2 concentration was used. Typical results from the regression analyses are as follows:

For Nitrogen: (Eq. 4) Peak Area = 9.40 x $[N_2]$ (R-squared = 0.9753)

For Oxygen: (Eq. 5) Peak Area = 7.05 x $[O_2]$ -2.13 x [NO] (R -squared = 0.9533)

It should be noted that at low peak areas for O_2 and/or high concentrations of NO, the multiple regression model will over predict the O_2 concentration.

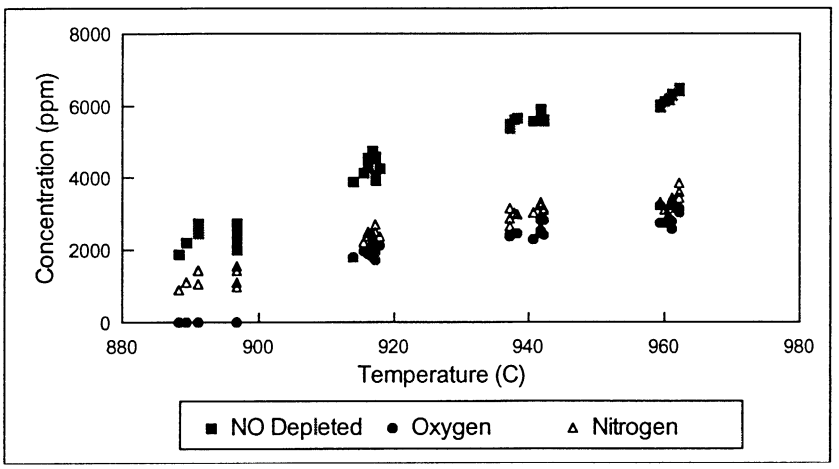

Figure 5: GC Analysis of Exit Gas For Experiments 5 and 6.

Figure 5 shows the amount of NO depleted (NO_{in} - NO_{out}) and the exit gas concentrations for oxygen and nitrogen for experiments 5 and 6. These data show that over the temperature range 890-965 °C, the O_2 and N_2 concentrations are approximately equal to each other and approximately half of the NO concentration that was depleted. This indicates that the NO is being reduced completely to N_2 and O_2 which can be represented by the stoichiometric equation : NO = ½ N_2 + ½ O_2. By assuming this stoichiometry, the percent recovery for each species can be calculated as follows:

(Eq. 6) % Recovery = 100 * 2 * $[O_2$ or $N_2]$ /$[NO]_{depleted}$.

Figures 6 and 7 show the percent recovery of each species for experiments 5 through 10. The data shown in Figures 6 and 7 are summarized in Table 4. The percent recovery is reported as the average for each experiment plus or minus one standard deviation.

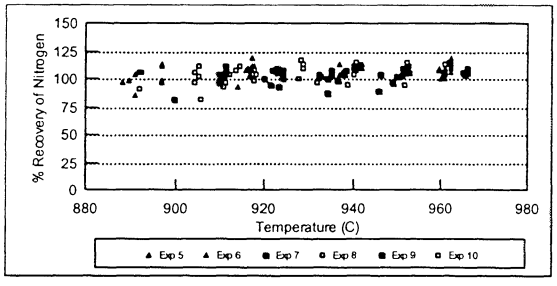

Figure 6: % Recovery of NO as Nitrogen (N_2)

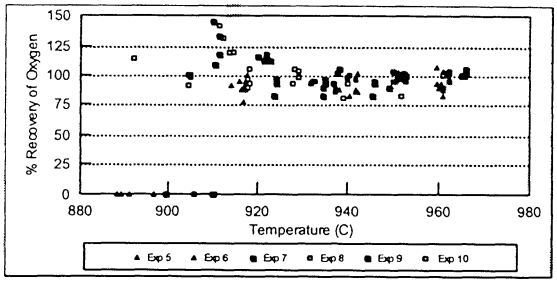

Figure 7: % Recovery of NO as Oxygen (O_2)

Table 4: % Recovery of NO as Nitrogen and Oxygen For Experiments 5 - 10.

Experiment	5	6	7	8	9	10
% Recovery as N_2	103.5 ± 6.3	109.8 ± 5.3	103.9 ± 6.4	107.2 ± 8.5	102.2 ± 6.3	102.7 ± 4.4
% Recovery as O_2	89.8 ± 5.8	92.6 ± 6.4	103.8 ± 7.1	102.0 ± 13.7	99.2 ± 17.0	97.2 ± 5.8

The third set of experiments (11-18) was conducted to determine the rate of depletion of NO by reaction with mixtures of Na_2CO_3 and Na_2S. During these experiments the exit gas was also analyzed by on-line GC. In the presence of sodium sulfide it was not possible to detect any oxygen in the exit gas. It was therefore assumed that the oxygen was reacting with sulfide to form sodium sulfate. By assuming the overall reaction: $4NO + Na_2S \rightarrow Na_2SO_4 + 2N_2$, it is possible to calculate the rate of depletion of Na_2S as a function of the amount of NO depleted. Figure 8 shows the measured values of the NO concentration along with the calculated values for total NO consumed and total Na_2S remaining as a function of time for experiment 15.

Inspection of Figure 8 reveals several interesting points:

- When all of the sodium sulfide has reacted (Na_2S remaining = 0) there is a sudden rise in the concentration of NO. This indicates a shift in the reaction mechanism upon total consumption of Na_2S.
- GC analysis of gas samples analyzed after this point show the presence of oxygen in equal proportion to N_2. This also supports the concept that the sulfide has been oxidized.

- As long as Na_2S is present, the concentration of NO is constant at any given temperature regardless of the concentration of Na_2S. Just before the sulfide is completely consumed, the NO concentration starts to change. This supports the concept that the reaction is pseudo first order as long as there is at least approximately .002 mol of Na_2S in the melt.

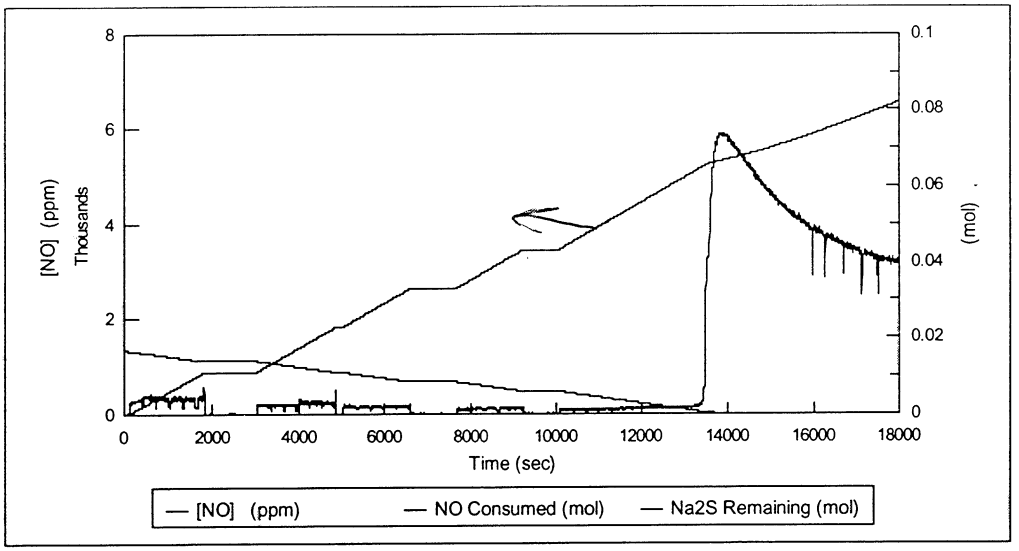

Figure 8: Depletion of NO by Reaction with Molten Na_2CO_3/Na_2S; Experiment 15.

Equation 2 was used to calculate values for k_1 over the temperature range, T= 860 to 934 °C, for experiments 11 through 17. These results were then used to calculate the activation energy (E_a) and the pre-exponential factor (k_o) by plotting $\ln(k_1)$ *vs* 1/T as shown below in Figure 9.

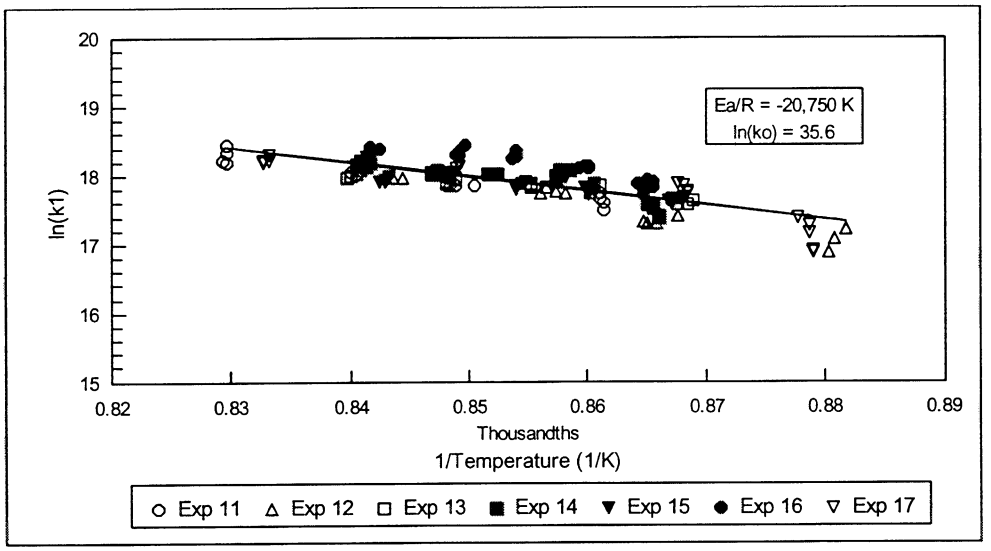

Figure 9: Determination of Activation Energy for Depletion of NO by Na2CO3/Na2S Mixtures. Experiments 11-17.

Based on the results in Figure 9, the slope, $-E_a/R$, and intercept, $\ln(k_o)$, were found to be -20,750 ± 2457 K and 35.63 ± 0.37, respectively. These results are reported at a confidence level of 95 %. Thus, the pseudo first order rate constant, k_1, may be written as: $k_1 = 2.98 \times 10^{15}\, e^{-20{,}750/T}\ (s^{-1})$.

With values for the rate constant it becomes possible to predict the exit gas concentration as:

(Eq. 7) $[NO]_f = [NO]_i \times \exp\left(-\left(\frac{at}{\frac{1}{H_{NO}k_g} + \frac{1}{\sqrt{D_{NO/Na}k_1}}}\right)\right)$. This expression was used to compare predicted values for NO concentration with the measured values. Results of this comparison are shown in Figures 10A-D for experiments 13,14,17 and 18.

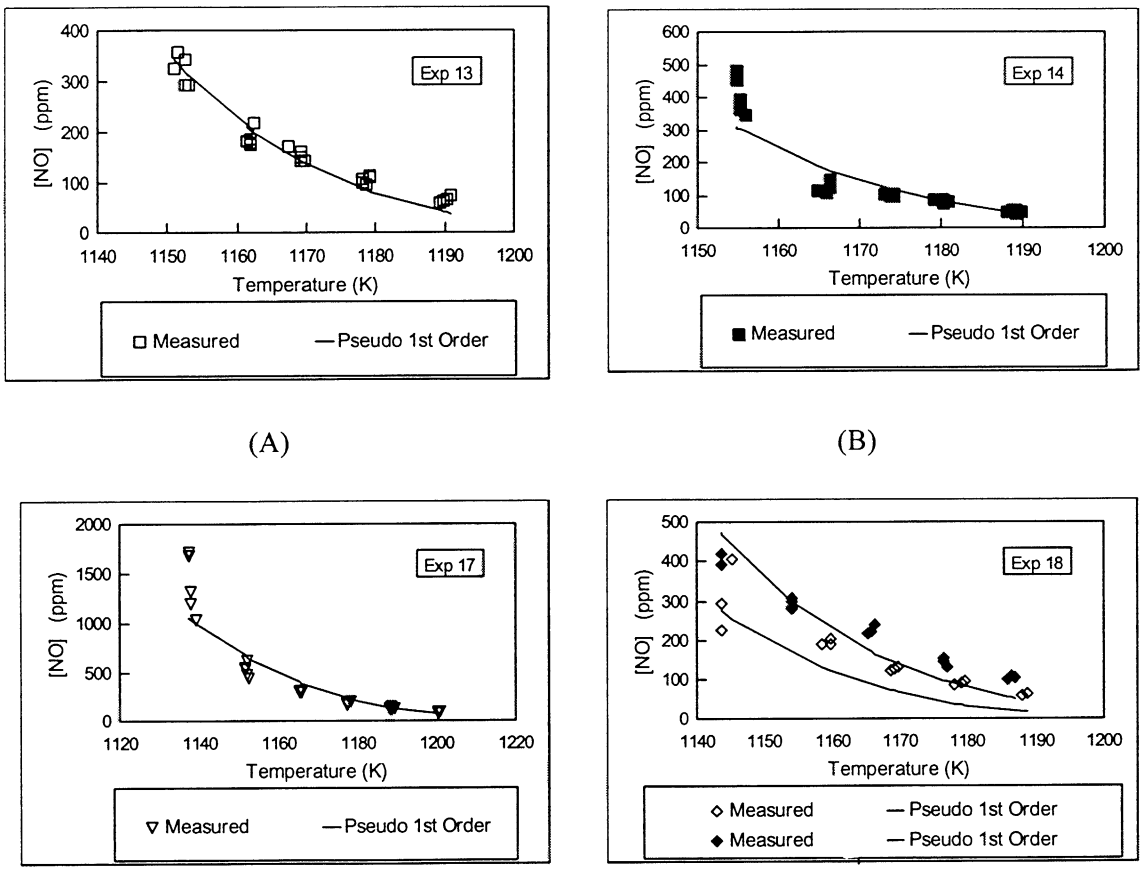

Figure 10: Comparison Of Predicted And Measured Values For Concentration Of Nitric Oxide In Exit Gas; Experiments 13,14,17 And 18. $[NO]_{in}$ = 9600 ppm for each Experiment.

Inspection of Figure 10 shows excellent agreement between the experimental and predicted values for the concentration of NO in the exit gas over a wide range of experimental conditions.

Discussion/Conclusions

The rate of depletion of nitric oxide by reaction with molten Na_2CO_3 and Na_2CO_3/Na_2S has been shown to follow a pseudo-first order rate expression. A comparison of the two systems is summarized in table 5 below.

Table 5: A Comparison of Kinetic Parameters for the Depletion of NO by Reaction with Na_2CO_3 and Na_2CO_3/Na_2S Mixtures.

Reactant	Temperature Range (°C)	% Conversion of NO	E_a/R (°K)	k_1 at T = 900 °C (s^{-1})
Na_2CO_3	860-973	10-75	44,780	8.14×10^5
Na_2CO_3/Na_2S	860-934	90-99.9	20,750	6.19×10^7

The results shown in Table 5 show the depletion of NO to be greatly enhanced by the presence of Na_2S.

It is not clear at this point what the mechanism for the reaction is, however analysis of the exit gas shows that all of the NO that is depleted can be detected as O_2 and N_2. It is feasible that a nitrite or nitrate intermediate is formed which then thermally decomposes to nitrogen and oxygen. In the presence of sulfide, the oxygen is consumed forming sodium sulfate. Because the rate is independent of the concentration of Na_2S, this does not affect the rate of reaction until nearly all of the sulfide has been oxidized.

These reaction data, coupled with aerosol (fume) formation modeling, should be able to predice the amount of depletion that occurs in the upper region of a recovery furnace. However, it should be noted that it is not known what affect other gases (e.g. H_2O, O_2, CO, CO_2, SO_x) may have on the rate of depletion of NO.

Acknowledgments

Portions of this work were used by L.M.T. as partial fulfillment of the requirements for the Ph.D. degree at the Institute of Paper Science and Technology.

EQUATIONS

(Eq. 8)[5] $a = \frac{6\varepsilon}{d_b}$

(Eq. 9)[6] $\varepsilon = 0.5\left(\frac{U_{br}}{\sqrt{gR_c}}\right)^{0.4}\left(\frac{U_{gs}}{U_{br}}\right)^{0.8}$

(Eq. 10)[7] $d_b = \left[\left(\frac{\alpha\gamma D_t}{\Delta\rho g}\right)^2 + 9.5\left(\frac{V_R^2 D_t}{g}\right)^{0.867}\right]^{\frac{1}{6}}$

(Eq. 11)[8] $D_{NO/He} = \frac{10^{-4}\left(1.084-0.249\sqrt{1/M_{NO}+1/M_{He}}\right)T^{1.5}\sqrt{1/M_{NO}+1/M_{He}}}{P_t(r_{NO/He})^2 f\left(\frac{kT}{\varepsilon_{AB}}\right)}$

(Eq. 12)[9] $D_{NO/Na} = \frac{\left(117.3\times10^{-18}\right)(\varphi M_{Na})^{0.5}T}{\mu\upsilon^{0.6}}$

(Eq. 13)[10] $k_g = \frac{D_{NO/He}P_t}{RTzP_{He,m}}$

(Eq. 14)[11] $k_L = 0.42\left(\frac{D_{NO/Na}}{d_b}\right)\left(\frac{d_b^3 g\rho^2}{\mu^2}\right)^{\frac{1}{3}}\left(\frac{\mu}{\rho D_{NO/Na}}\right)^{0.5}$

(Eq. 15)[12] $K_H = \frac{\exp\left(\frac{-4\Pi Nr^2\gamma}{8.314T}\right)}{82.06T}$

Physical properties of molten sodium carbonate can be calculated as a function of temperature according to the following:

(Eq. 16)[13] $\rho = 2.4797 - 0.4487 * 10^{-3}\ T\ (g/cm^3)$

(Eq. 17)[13] $\mu = 3.832 * 10^{-5} \exp(13215/T)$ (cp)

(Eq. 18)[14] $\gamma = (254.8 - 0.0502\ t)/1000$ (N/m), t = temperature (°C)

Notation

a = interfacial area per unit volume (cm^2/cm^3)
A = solute gas
[A*] = interfacial concentration of A (mol/cm^3)
B = non-volatile reactant
[B_o] = concentration of B in the bulk (mol/cm^3)
C_{Na2CO3} = concentration of molten Na_2CO_3 (mol/cm^3)
C_{NO} = concentration of NO in liquid film (mol/cm^3)
d_b = bubble diameter (cm)
$D_{NO/He}$ = diffusivity of NO in Helium (m^2/s)
$D_{NO/Na}$ = diffusivity of NO in Na_2CO_3 (m^2/s)
D_t = outside diameter of purge tube (m)
Ea = activation energy (J/mol)
f (kT/ε_{AB}) = collision function (= 0.31) (Treybal[10], p. 32)
g = gravitational constant = (9.81 m/s)
H_{NO} = phase distribution coefficient (atm cm^3/mol)

k = second order rate constant (mol/cm^3 s)
k_0 = pre-exponential factor (1/s)
k_1 = pseudo first order rate constant (1/s)
K_H = Henry's Law constant (mol/cm^3 atm)
m = order of reaction with respect to A
m_{Na} = mass of Na_2CO_3 (g)
M_i = molecular weight of species, i
n = order of reaction with respect to B
N = Avogadro's number = (6.022×10^{23})
N_{NO} = moles of NO (mol)
$[NO]_f$ = exit concentration of NO (ppm)
$[NO]_i$ = inlet concentration of NO (ppm)
$P_{He,m}$ = log mean pressure of helium (atm)
P_{NO} = partial pressure of NO (atm)
P_t = total pressure (atm)
r = molecular radius (m)
$-r_{NO}$ = rate of depletion of NO based on volume of liquid (mol/cm^3 s)
$r_{NO/He}$ = molecular separation at collision (nm)
R = universal gas constant = (8.314 m^3 J/mol K)
R_c = radius of column = (0.02 m)
t = time (s)
T = absolute temperature (K)
U_{br} = bubble rise velocity (m/s)
U_{gs} = superficial gas velocity (m/s)
V = flow rate of gas (cm^3/s)
V_g = flow rate of gas (m^3/s)
V_l = volume of molten salt (cm^3)
X = percent conversion of NO
z = film thickness = (10^{-4} m) (estimated)
α = correlation factor (assumed 30)
ε = gas hold up
ϕ = association factor for solvent = 1
ν_{NO} = solute molal volume at boiling point (= 0.0236 m^3/kmol)

References

1. Nichols, K.M., and Lien, S.J.,Formation of Fuel NOx During Black Liquor Combusiton, *Tappi Journal*, 76(3):185(1993).

2. Thompson, L.M., and Empie, H.J., A Proposed Mechanism for the Depletion of NO_x in a Kraft Recovery Furnace, Proceedings of the 1993 TAPPI Environmental Conference, Boston, MA, 643-647(1993).

3. Thompson, L.M., and Empie, H.J., Kinetics of NO Depletion by Reaction with Molten Sodium Carbonate, Proceedings of the 1993 AIChE Annual Meeting, St. Louis, MO, xxx-yyy(1994).

4. Levenspiel, O., Chemical Reaction Engineering, 2nd Edition, Chapter 13: Fluid-Fluid Reactions, John Wiley & Sons, New York, 1972.

5. Treybal, R.E., Mass-Transfer Operations, 3rd Edition, McGraw-Hill Book Company, New York, 1980, p.144.

6. Cheremisinoff, N.P., Encyclopedia of Fluid Mechanics, Volume 3: Gas-Liquid Flows, Gulf Publishing Company, Houston, 1986, p.1199.

7. Cheremisinoff, N.P., Encyclopedia of Fluid Mechanics, Volume 3: Gas-Liquid Flows, Gulf Publishing Company, Houston, 1986, p.228.

8. Treybal, R.E., Mass-Transfer Operations, 3rd Edition, McGraw-Hill Book Company, New York, 1980, p.31.

9. Treybal, R.E., Mass-Transfer Operations, 3rd Edition, McGraw-Hill Book Company, New York, 1980, p.35.

10. Treybal, R.E., Mass-Transfer Operations, 3rd Edition, McGraw-Hill Book Company, New York, 1980, p. 45.

11. Cussler, E.L., Diffusion: Mass Transfer in Fluid Systems, Cambridge University Press, New York, 1984, p.230.

12. Andresen, R.E., J. Electrochemical Society, 328-334(1979).

13. Janz, G.J., Dampier, F.W., Lakshminarayanan, G.R., Lorenz, P.K., and Tomkins, R.P.T., Molten Salts: Volume 1, Electrical Conductance, Density, and Viscosity Data, National Standard Reference Data Series-National Bureau of Standards 15, October, 1968.

14. Janz, G.J., Lakshminarayanan, G.R., Tomkins, R.P.T., and Wong, J., Molten Salts: Volume 2, Section 2: Surface Tension Data, National Standard Reference Data Series-National Bureau of Standards 28, August, 1969.

KRAFT BLACK LIQUOR DELIVERY SYSTEMS
PROJECT 3657-2

ANNUAL PROGRAM REVIEW

March 23, 1995

Jeff Empie
Steve Lien

Institute of Paper Science and Technology
500 10th Street, N.W.
Atlanta, GA 30318
(404) 853-9500

Project Title: KRAFT BLACK LIQUOR DELIVERY SYSTEMS (DOE Funded)
Project No.: 3657-2
Project Staff: Jeff Empie, Steve Lien
FY 94-94 Budget: $38,000

IPST GOAL:

Increase recovery boiler capacity and operating efficiency through improved black liquor spraying technology.

OBJECTIVE:

Develop new and improved black liquor spraying nozzles that give the operator some capability to control droplet size and size distribution.

PRIOR RESULTS:

Early results were obtained on the performance of the three basic types of black liquor spray nozzles: the splashplate, the swirl cone, and the U- and V-jets. From the visual analysis of the video tapes of the spray patterns, it was apparent that the solids concentration of the black liquor had a strong effect on droplet formation. At low solids (50%), the majority of the drops were spherical, but at high solids (70%), most of the images were large, irregularly shaped drops connected to strings and filaments.

Several drop size distribution models were tested to fit the experimental data; the best one continued to be the square root-normal distribution. It was shown that the ratio of the standard deviation to the square root of the mass median diameter has a constant value of 0.2, and therefore only one parameter, the mass median diameter, is necessary to characterize the square root-normal distribution for black liquor sprays.

A test series with the B&W splashplate, CE swirl cone, and SS V-jet nozzles was completed, using a 3x3x3 matrix (solids of 50, 60, and 70%; viscosities of 270, 90, and 30 cP; and nozzle pressures of 15, 30, and 45 psig). Pressure vs. flow rate correlations were derived as a function of Reynolds Number. For the three tests at high viscosity and low pressure, the flow rate was too low to produce sheet breakup.

Data on droplet size distributions from a B&W splashplate nozzle and a CE swirl cone nozzle showed a weak dependence on liquor velocity and fluid physical properties. The ratio of median

velocity and fluid physical properties. The ratio of median droplet diameter to nozzle diameter was related to the product of Reynolds Number and Euler Number, each raised to an experimentally determined non-integral power; similarly, Euler and Schmidt Numbers also correlated well. Both dimensionless correlations were broken down into the product of the individual physical parameters, each raised to an experimentally determined power. It was shown that the parameters which most strongly influenced median drop diameter were nozzle diameter, and liquor density and velocity. At high solids levels, liquor viscosity became important. When droplet diameter was empirically correlated with velocity and temperature raised to appropriate exponents, drop size was shown to decrease as either operating parameter was increased.

A study of the behavior of spray nozzles at liquor temperatures above the atmospheric boiling point was performed. Three different nozzles were tested at temperatures ranging from 200° to 270°F using 65% solids liquor. As temperature was increased, drop diameter gradually decreased until a transition temperature was reached (6°-9°C above the atmospheric boiling point) where the drop size abruptly decreased by about 20%; the normalized standard deviation for the drop size distribution remained unchanged at 0.2. This effect was accompanied by a noticeable change in the physical appearance of the spray. The normally planar spray sheet became oval in cross-section, and, for a splashplate nozzle, the central plane of the sheet came off the plate at a 20 to 40 degree angle, rather than at zero degrees. These phenomena can be attributed to flashing at the nozzle. This effect would result in a several-fold increase in the number of drops being fired into the furnace, increasing burning rates and possibly carryover rates.

Spraying tests on five different black liquors from four kraft mills were conducted to determine the effect of liquor type on droplet size and size distribution. A wide range of spraying conditions was examined with the finding that liquor type was not important at comparable viscosities; mean drop diameter depended primarily on nozzle type and diameter, pressure, temperature, and liquor viscosity.

Measurements were made of the local distribution of liquor flow in the spray pattern as a function of the angle from the sheet centerline. Results for both the splashplate and V-jet nozzles showed the mass flow distribution to be parabolic, with the maximum mass flow being at the centerline and decreasing with increasing angle. Limited analysis of drop size as a function of the angle from the sheet centerline showed no significant difference.

A series of trials was conducted at James River's Camas Mill to study black liquor sprays in a recovery furnace environment. High-speed video images of sprays were taken through a gun port on Camas' No.4 recovery boiler. Three different nozzles were

operated at two levels of liquor flow and fired liquor temperature. Changing one nozzle and/or firing conditions for a short period of time did not produce significant changes in furnace operation as indicated by particulate count or lower furnace temperatures. There was evidence of liquor sheet breakup by perforation, which agrees with the findings of the present study. Differences in sheet breakup between nozzles were seen in the video images; however, it was not possible to detect variation due to firing conditions. The video images were optically too dense to determine droplet size distribution by image analysis.

Alternative commercial nozzles were surveyed, including two-phase, sonic, and rotary atomizers and full-cone nozzles with and without swirl. Most of these strive to give very fine droplets or mists, which are unsuitable for recovery boiler operation. Ultimately, three of these nozzles were tested, and only one, the Delavan Raindrop®, exhibited any noticeable difference in performance. It gave a coarser-than-normal droplet size, but did not result in a different distribution width. None of the alternative commercial nozzles demonstrated any ability to give independent control over drop size distribution.

Development of new nozzle concepts started with modified splashplate nozzles with no moving parts. Making various physical changes to the surface of the splashplate (e.g., grooves, slots) resulted in 25% smaller median drop diameters, with no change in the distribution width. One design, on which small cylindrical pegs were mounted normal to the splashplate surface around its outer periphery, also gave smaller drops, but with a larger normalized standard deviation, characteristic of a bimodal distribution. A different design specifically aimed at generating a bimodal distribution employed two different sized orifices back-to-back using opposite sides of the same splashplate. The two liquor sheets formed tended to interact during break-up, giving larger-than-normal droplets with the usual distribution width. The two orifice conditions tested were not different enough to give component median diameters far enough apart that would yield a recognizable bimodal distribution.

It is apparent that gaining any degree of control over drop size distribution will require some external force, independent of the viscous, momentum, and surface tension forces which fundamentally control the droplet formation process. The concept of vibratory assist should provide an independently controlled means of influencing the sheet formation/break-up process. Application of vibrations normal to the plane of the sheet gave a 15-30% increase in median diameter and distribution width using an air vibrator, but no change in either parameter using a mechanical vibrator.

Two nozzle designs featuring axial vibratory assist were conceptualized, fabricated, and tested with the black liquor

liquor flow by interrupting the flow at frequencies up to 270 Hz. Reliable operating characteristics were demonstrated. Results showed a weak dependence of drop size distribution width on pulsation frequency, with the distribution narrowing slightly as frequency increased. The existence of a harmonic frequency where the distribution width exhibits a local minimum was suspected, but must still be substantiated.

The second design pulsed the flow directly by +/-20% for frequencies up to 150 Hz. No dependence of median drop size or size distribution width was detected. Nozzle operating characteristics were less reliable with this design.

An alternative independent external force that can be applied to spray sheet break-up is an electrostatic one using dielectrophoresis. The non-uniform electric field applied can exert a force on the electrically neutral droplets in a direction normal to the bulk flow direction. This has potential for promoting droplet coalescence, and hence could skew the drop size distribution away from the smaller sizes. The limited data obtained did not substantiate the desired effect.

SUMMARY OF RESULTS SINCE LAST REPORT:

Additional tests have been completed for liquor spraying through a V-jet nozzle featuring axial vibratory assist (interrupted flow mode). The frequency range was extended from 270 Hz up to 450 Hz; liquor solids and temperature (∴ viscosity) were held constant. Interestingly, median drop size increased from 2.2 mm with no pulsation up to a maximum of 3.5 mm at about 230 Hz, then decreased steadily to 2.5 mm at 450 Hz. The shape of the drop diameter vs. frequency curve was nearly sinusoidal, supporting the expectation of harmonic behavior that should be characteristic of a vibratory process. The normalized standard deviation of the drop size distribution did not show any variation with pulsation frequency.

These results were used to calculate the frequency dependence of the mass fraction of drops in a given spray that would be less than 1 mm in diameter. Results show that 4% of the drops would be less than 1mm at zero pulsation and about 1% at the 230 Hz condition. Hence, the fraction of smaller drops in the spray would be reduced by a factor of four using an independently controlled variable - namely pulsation frequency. This may have interesting implications for reducing carryover in recovery boilers. Predictions using the IPST recovery boiler model currently being developed will be generated to confirm or deny this expected result.

PLANNED ACTIVITY THROUGH FY 95:

* Close out present project with final report (DOE contract expired 9/30/94).

* Obtain approval and funding for proposed study to establish feasibility of using effervescent spraying as a way to deliver high solids (>80%) liquor to a recovery boiler without requiring high liquor temperatures.

* Consider new proposal to further develop the potential shown by spraying with axial vibratory assist.

Black Liquor Delivery Systems Final Report

by

Jeff Empie

Steve Lien

ABSTRACT

An improved spray nozzle for black liquor injection into kraft recovery boilers has been sought which is expected to result in obtaining a controlled, well-defined droplet size distribution. An environmentally sound experimental spray facility capable of delivering black liquor at normal firing temperatures has been operated at the Institute of Paper Science and Technology to help achieve that goal. Previous work showed that black liquor sprays have a characteristic size distribution which is determined by the fluid mechanical forces breaking up the spray sheet issuing from the nozzle. Recent work has centered on applying vibratory assist as an independently-controlled force on the sheet break-up process in an attempt to change the drop size distribution. Results are presented which feature vibratory assist applied in the axial direction.

EXECUTIVE SUMMARY

The research work described in this report represents the results of a six-year project designed specifically to develop the optimum black liquor delivery system for the current recovery boiler. Black liquor obtained from normal mill operation was used in this study.

The primary objectives of the research program have been:

* To develop laboratory equipment and methods for quantitatively studying commercial black liquor nozzle designs when spraying kraft liquors at typical operating conditions;

* To quantify droplet size distribution, velocity, and mass distribution for commercial nozzles spraying kraft liquors at typical boiler feed conditions;

* To develop techniques currently envisioned for improving the control of black liquor spray droplet size distribution with commercial nozzles; and

* To extend current liquor spraying technology by testing several fundamentally different, but commercially viable, delivery systems.

Success with this program should yield benefits in increased thermal efficiency and process productivity, as well as have potential for improvements in equipment design and process control. Coupled with the recovery boiler modeling project currently under way at IPST, the potential value of these programs to the industry is approximately $93MM/year for increased thermal efficiency and $240MM/year for increased productivity.

It was apparent from the work on standard commercial nozzles that gaining any degree of control over drop size distribution is going to require some external force, independent of the viscous, momentum, and surface tension forces which naturally control the droplet formation process. The concept of vibratory assist was visualized as a way to provide an independently controlled means of influencing the sheet formation/break-up process. Application of vibrations transverse to the plane of the sheet were ineffective. Vibration in the direction of flow (i.e., axial pulsation) was expected to be more effective for reducing the randomness of the sheet break-up process.

Two nozzle designs featuring axial vibratory assist were conceptualized, fabricated, and tested with the black liquor spray apparatus. The more promising design could pulse the liquor flow by interrupting the flow at frequencies up to 450 Hz. Reliable operating characteristics were demonstrated. Results showed a dependence of median drop size on pulsation frequency, with a maximum occurring in the range of 220-260 Hz; the distribution width did not change. The implication of these results is that operating in the 220-260 Hz range will reduce the fraction of small droplets formed, which should result in reduced entrainment/carryover rates in the recovery boiler without changing any of the normal process operating parameters, such as temperature, solids, or flow rate.

1.0 INTRODUCTION

The most important unit operation employed in the recovery cycle of the kraft pulping process is combustion of black liquor in the recovery boiler. This step is initiated by spraying the concentrated liquor through one of several types of commercial nozzles, the most common being the splashplate, the V-jet, and the swirl cone. Black liquor issues from the nozzle as a thin sheet, which subsequently breaks up into droplets. These droplets then go through the sequential processes of drying, pyrolysis and gasification, combustion, reduction, and smelt coalescence [1]. The rates at which these physical and chemical processes occur are highly dependent upon the size and size distribution of the droplets formed from the spray. The smaller the droplet, the greater the surface area per unit mass of liquor and hence, the greater the rates of heat and mass transfer between the liquor particles and the furnace gases. While this is desirable for increasing recovery boiler capacity, it is offset by higher entrainment and carryover in the upward flowing turbulent gas stream. Inevitably, the result is accelerated fouling of the relatively cool boiler tubes and more rapid plugging of the steam producing section of the boiler.

To achieve increases in both black liquor throughput for recovery boiler-limited mills and recovery boiler energy efficiency, control of not only median droplet size, but also the width of the size distribution must be improved. Existing recovery boiler nozzles have been designed with two primary objectives - deliver production rates of liquor in a drop size range which gives acceptable combustion and reduction rates and efficiencies, and deliver the liquor reliably with minimal nozzle and boiler plugging. Any improvements which provide incremental capacity, while maintaining high efficiencies, will require better control of the size distribution.

Whether or not a narrower distribution should be the goal for an improved black liquor spray technology is still an open question. Too narrow a size distribution might not allow for a proper balance between suspension burning and burning on the char bed. It seems more likely that a drop size distribution having a reduced fraction of the finer sizes would enable increased capacity without increasing carryover, while maintaining high combustion and reduction efficiencies.

The mass flow distribution of liquor within the furnace firing zone is not known and will not be in the near future because of the extreme difficulty of taking measurements in this turbulent, particulate-laden, corrosive, inaccessible, high temperature region. Characterization is best achieved through mathematical modeling using computational fluid dynamics and fundamental kinetic and transport rate data.

The key to successfully modeling the recovery boiler furnace zone is to start with an accurate understanding of black liquor

nozzle performance. Drop size and size distribution data are, of course, paramount. With regard to spatial distribution, it is also important to know not only the total angle of the spray sheet produced initially by given nozzle and liquor flow conditions, but also how the mass flow of black liquor varies with angular position within the sheet.

The ultimate answer will come from diagnostic tests on an operating recovery boiler. Regardless of what results are generated, both calculated and experimental, the bottom line is that some degree of operator control over drop size must be established so that the desired drop size distribution can be delivered to the firing zone of the recovery boiler.

1.1 OBJECTIVE

This research program was initiated as an applied effort to identify the optimum black liquor delivery system for the kraft recovery boiler and to present it to the industry in a timely fashion. Because it is not known what are the preferred spraying conditions for optimum recovery boiler operation, the fundamental objective was to develop ways to control the formation of black liquor droplets such that, once the optimum conditions are actually known, the specified drop size and size distribution can be obtained and the optimum achieved. The recovery boiler modeling program currently under way at IPST may ultimately be the best way to establish what are the preferred operating conditions for optimum operation.

1.2 DELIVERABLES

This research effort has delivered the following:

a) A test facility capable of quantitatively assessing the performance of commercially viable spray systems while processing kraft black liquors at typical furnace feed conditions.

b) The best commercial spray delivery system available with current technology.

c) An appraisal of the technical viability of a fundamentally different black liquor delivery system.

1.3 BENEFITS

Potential benefits from this applied study have been projected in previous reports on this project; they are reproduced verbatim from last year's report in Table 1.1 below [2].

The increased thermal efficiency value for the industry is approximately $93 million/year; the incremental value of a 1% increase in process productivity for the industry is estimated at $240 million/year. These estimates reflect savings increments above the state-ot-the-art recovery boiler technology that is available.

Table 1.1 Benefits from Proposed Research

Goals:
1. Increased thermal efficiency
2. Increased process productivity
3. Improved equipment design potential
4. Improved process control potential

Targets:
1. Increased thermal efficiency

Element	Improvement	Value 10^5 Btu/adtp	Value $/adt
Increased fired per cent solids	70 to 75%	2.3	1.5
Reduced flue gas temperature	350 to 325F	1.2	0.74
Reduced carbon in smelt	1.5 to 1.0%	0.86	0.54
Reduced sootblowing steam	3.0 to 2.5%	0.72	0.45
	(Total)	5.1	3.2

2. Increased process productivity

Incremental production	1%	400

Industry Value:

1. Increased thermal efficiency
   5.1×10^5 Btu/adt x 60×10^6 adt/yr = 3.1×10^{13} Btu/yr
   3.1×10^{13} Btu/yr x $3.00/$10^6$ Btu = $93,000,000/yr

2. Increased process productivity (1%)
   60×10^6 adt/yr x $400/adt x 0.01 = $240,000,000/yr

Thermal efficiency and process productivity goals are not independent. The recovery boiler is often the bottleneck in the entire pulping process. Thermal efficiency is often sacrificed for high productivity. Hence, thermal efficiency and productivity increases may not be realized simultaneously. On the other hand, the recovery boiler is the only pulp mill operation which can often claim that improved unit productivity will result in increased millwide productivity.

The in-place capital investment in recovery boiler technology is so large (>$10 billion) that radical changes, expansions, and replacements will be rare for the foreseeable future. Barring a significant departure from the kraft process in the near term, the industry will be firing black liquor in conventional recovery boilers well beyond the year 2000.

1.4 SUMMARY OF PREVIOUS RESULTS

1.4.1 Experimental

Black liquor was sprayed continuously through commercial nozzles using a heated, recirculating pump-around loop system [2]. The central component of the system was a spray chamber which served the dual purpose of providing a visible spray pattern while containing and storing the liquor inventory. The front and rear walls contained 1.5 m x 1.2 m tempered glass windows to allow back-lighting and video-taping the liquor spray sheet and droplets. The side of the chamber had an opening for the spray nozzle which was oriented to deliver the liquor sheet in a horizontal trajectory parallel to the windows. Images of the black liquor spray pattern and breakup into droplets were obtained using a Xybion ISG-250 high-speed video camera, in combination with a Tracor-Northern TN-8500 image analyzer. Additional details are contained in refs.[2-7].

A two-stage Moyno pump circulated the liquor from the spray chamber through a spiral heat exchanger for temperature control, then through a Brookfield viscometer and back to the chamber. Correlations of liquor solids with viscosity and temperature enabled on-line control of liquor solids. The system had the capacity to deliver up to 150 L/min (as measured by a Foxboro magnetic flowmeter) of liquor to the nozzle at 650 kPa (80 psig). Because of odor control considerations, the spray chamber was operated under a slight negative draft. An ID fan drew air in through eight adjustable dampers, after which this gas flow, plus any volatiles coming from the liquor spray, were pulled through a carbon absorber (provided by Westvaco Corp.) before being exhausted to the atmosphere.

The three nozzles used predominantly in this work were a Babcock & Wilcox (B&W) 12/45 splashplate, a Spraying Systems Co. (SS) 11/65 V-jet, and a Combustion Engineering (CE) swirl cone. Each type is widely used for black liquor spraying (cf. ref.[5] for additional detail). Video recordings of the spray pattern were made at different positions and distances from the nozzle. From the visual analysis of the video tape, it was apparent that the solids concentration of the black liquor had a strong effect on droplet formation. At low solids (50%), the majority of the drops were spherical, but at high solids (70%), most of the images were large, irregularly shaped drops connected to strings and filaments.

Several drop size distribution models were tested to fit the experimental data; the best one was the square root-normal distribution. It was shown that the ratio of the standard deviation to the square root of the mass median diameter had a constant value of 0.2, and therefore only one parameter was necessary to characterize the square root-normal distribution for black liquor.

Samples of sprayed liquor were collected by using two different types of patternators. The first arrangement used a single box with a large 7.6 cm x 7.6 cm opening. This collected samples from the V-jet nozzle at a distance of about 84 cm from the nozzle. A second patternator was constructed for the B&W splashplate nozzle. Nine 2.5 cm x 2.5 cm sampling boxes were arranged on a half-circle frame at 20° intervals. The radial distance from the nozzle to the front edge of each box was fixed at 11.5 cm. The sampling boxes cut the liquor sheet into sections which could be collected simultaneously for a fixed time and accurately weighed to determine the mass flux at the nine different angles (cf.ref.[3] for additional detail).

1.4.2 Mechanism of Droplet Formation

In the black liquor spraying process, the bulk fluid issues from the nozzle orifice and is converted into a fluid sheet, which subsequently breaks up into drops. Both a wave mechanism and a perforation mechanism have been postulated as the first step in the breakup of the sheet [8,9]. These both lead to the formation of cylindrical strands of fluid, which then form droplets according to jet breakup theory. The common denominator of the two mechanisms is that aerodynamic, inertial, viscous, and surface tension forces will be active in the ultimate droplet formation process. The balance of these forces is governed by fluid dynamics, subject to the random disturbances present in all systems. The inevitable result is a characteristic distribution of drop sizes. Spielbauer and Aidun discuss this in greater detail [8,9].

1.4.3 Drop Size Distribution

The range of droplet sizes in most commercial sprays is very broad, with more than two orders of magnitude between the smallest and largest diameter. Mathematical description of droplet sizes in a spray is most often presented in the form of a statistical distribution function. Because for most sprays the droplet diameter was not distributed in the manner of a normal, or Gaussian, curve, several alternative distribution curves were considered. Included were the Log-Normal, Square Root-Normal, Upper Limit Log-Normal, and Rosin-Rammler. For pressure atomizers and two-fluid atomizers, the Square Root-Normal distribution was recommended [10]. Previous research on black liquor sprays was correlated according to the Square Root-Normal distribution [11].

The statistical distribution models listed above were examined in this work, with the Square Root-Normal distribution best fitting the drop size data [3]. Use of the Square Root-Normal distribution allowed each of the experimental size distribution curves to be represented by just two parameters, the median diameter, D_m, and the standard deviation, σ. Because σ

tended to increase as D_m increased, it was useful to define a normalized standard deviation, δ, as $\sigma/\sqrt{D_m}$. This latter parameter was a better measure of the width of the size distribution because it removed the effect of the magnitude of the median diameter.

The data showed that the normalized standard deviation (δ) was essentially constant for a given nozzle. This reduced the Square Root-Normal distribution to a one-parameter model, namely, the median drop diameter.

Examination of the drop size data for all three types of nozzles with several different black liquors over various combinations of solids concentration, temperature, and nozzle pressure gave a δ-value of 0.20 ± 0.03. This relationship is valuable in predicting drop size distribution in that once D_m is known, σ can be calculated, along with the entire distribution.

That δ is invariant may be rationalized through the basic laws of mass and momentum conservation. What is essential to the drop formation process is the balance between viscous, inertial, pressure, and surface tension forces present in the system. These are dependent upon fluid properties, flow velocities, and nozzle design, i.e., the fluid mechanics of the system. There are no independently applied forces to change or upset the naturally occurring balance. This would imply that changes in drop size distribution, both in shape and width, must come from a nozzle design that features some independent external force, such as vibratory assist.

1.4.4 Flow/Pressure Drop Characteristics

Flow rate/pressure drop characteristics for the three nozzle types were correlated from a standard mechanical energy balance using the following equation:

$$\Delta P = C_f(\tfrac{1}{2}\rho_L v_n^2) \qquad (1)$$

where: ΔP = pressure drop (Pa)
ρ_L = liquor density (kg/m^3)
v_n = nozzle velocity (m/s)
C_f = flow coefficient

The flow coefficient is a function of the type of spray nozzle. Pressure drop across the nozzle was assumed to be equal to the gauge pressure at the nozzle inlet because the outlet of the nozzle was at atmospheric pressure. For high temperature operation where the liquor was above the boiling point temperature, it was found that ΔP must be based on the difference between the inlet pressure and the vapor pressure of the black liquor.

The explanation for this is that the minimum pressure in the nozzle occurs near the outlet at the *vena contracta*. The pressure at this point cannot drop below the vapor pressure of the black liquor. The result is that the nozzle exit pressure is maintained at the vapor pressure for temperatures above the boiling point.

A test series with the B&W splashplate, CE swirl cone, and SS V-jet nozzles was completed, using a 3x3x3 matrix (solids of 50, 60, and 70%; viscosities of 270, 90, and 30 cP; and nozzle pressures of 204, 307, and 410 kPa (15, 30, and 45 psig). Pressure vs. flow rate correlations were derived as a function of Reynolds Number. For the three tests at high viscosity and low pressure, the flow rate was too low to produce sheet breakup. Another three tests at 70% solids and low viscosity could not be completed because the heat exchanger did not have the capacity to heat liquor to well over the boiling point (130°C) in a single pass.

For the three splashplate nozzles tested (B&W 12/45, B&W 15/52, and Tampella 18) at various run conditions, C_f was correlated with Reynolds number according to the following equation (r^2= 0.91):

$$C_f = 1.35 + 371\ Re^{-0.9} \qquad (2)$$

For the SS V-jet nozzles (V-11/65, -21/65, -24/65), the corresponding correlation (Reynolds number based on nozzle hydraulic diameter) was:

$$C_f = 1.06 + 66.4/Re \qquad (3)$$

For the CE V-jet nozzle (V-15), the flow coefficients were significantly higher (about 20%) than for the SS V-jets. Therefore, unlike the splashplate correlation, eq.(3) does not apply universally to all V-jet nozzles.

For the CE swirl cone (Sw-12), the flow coefficient was independent of Reynolds number and had an average value of 1.12.

1.4.5 Droplet Diameter

Background

Bennington and Kerekes [12] were the first to report on the size and size distribution of droplets from black liquor nozzles. The orifice diameter for their nozzle was only 0.7mm, and resulting drop sizes were about one-tenth those from typical recovery boiler nozzles. Nonetheless, the distribution of drop

sizes about the median was similar to those found in this study. They noted that the size distribution about the mean was primarily a function of the mechanism for sheet breakup. Spielbauer, et al. [13] noted the same result using more typical black liquor nozzles. Hence, the basic mechanism of sheet breakup appears to be invariant and leads to a characteristic size distribution.

Effect of Spraying Conditions

Drop size measurements were correlated with physical and operating parameters (e.g., viscosity, density, surface tension, temperature, nozzle pressure, and nozzle design) by using appropriate dimensionless groups and the ratio of the median drop diameter to the nozzle diameter. The dimensionless groups chosen were Reynolds number, Euler number, and Schmidt number; Weber number and Ohnesorge number would have been of interest, but because these feature surface tension which could be neither varied nor measured, these groups were not considered. The three dimensionless groups are defined in order below:

$$Re = D_n v_n \rho_L / \mu_L$$

$$Eu = g_c P_w / (v_n^2 \rho_L)$$

$$Sc = \mu_L / (\rho_L D_{WL})$$

where:
D_n = nozzle diameter (m)
v_n = nozzle exit velocity (m/s)
ρ_L = liquor density (kg/m^3)
μ_L = liquor viscosity (kg/m/s)
g_c = gravitational constant
P_w = vapor pressure of water (kg/m/s^2)
D_{WL} = diffusivity of water in liquor (m^2/s)

Each of the dimensionless groups can be related to various physical forces. Reynolds number represents the ratio of inertial to viscous forces; Euler number is the ratio of pressure to inertial forces and would characterize the process of water escaping the liquor sheet in the form of vapor, resulting in the formation of perforations. The Schmidt number relates mass and momentum transfer, characterizing the process of water molecules diffusing through the boundary layer at the gas-liquid interface surrounding the liquor sheet.

Taking two groups at a time and relating them to the droplet/nozzle diameter ratio, two correlations for the swirl cone nozzle emerged with r^2-values above 0.95:

$$D_m/D_n = 0.64(Re)^{-0.14}(Eu)^{0.09} \qquad (4)$$

$$= 0.10(Eu)^{0.16}(Sc)^{0.09} \quad (5)$$

For the V-jet:

$$D_m/D_n = 0.73(Re)^{-0.12}(Eu)^{0.11} \quad (6)$$

$$= 0.14(Re)^{0.17}(Sc)^{0.08} \quad (7)$$

In terms of discrete physical parameters these reduced to:

$$D_m = 1.68(D_n)^{0.86}(v_n)^{-0.32}(\rho_L)^{-0.23}(\mu_L)^{0.14}(P_w)^{0.09} \quad (4a)$$

$$= 0.10(D_n)(v_n)^{-0.32}(\rho_L)^{-0.25}(\mu_L)^{0.09}(P_w)^{0.16}(D_{WL})^{-0.09} \quad (5a)$$

and:

$$D_m = 1.67(D_n)^{0.88}(v_n)^{-0.34}(\rho_L)^{-0.23}(\mu_L)^{0.12}(P_w)^{0.11} \quad (6a)$$

$$= 0.14(D_n)(v_n)_{-0.35}(\rho_L)^{-0.25}(\mu_L)^{0.08}(P_w)^{0.17}(D_{WL})^{-0.08} \quad (7a)$$

where D_m and D_n are in millimeters. If the diffusivity of water in black liquor is estimated from the Wilke-Chang correlation [14], which shows a reciprocal dependence upon viscosity, then equation (5a) gives an effective viscosity exponent of 0.25.

The functional dependencies exhibited in equations (4a), (5a), (6a), and (7a) give interesting interpretations. Droplet diameter decreases as both velocity and density increase. Both are related to the kinetic energy of the liquor issuing from the nozzle, implying the greater the energy that is dissipated, the smaller the drop size. It is interesting to note the relative insensitivity of D_m to liquor physical properties, with the exponents in equations (4a)-(7a) generally in the 0.1 to 0.3 range. The apparent stronger dependence on nozzle diameter is artificial, since nozzle diameter was not varied for these correlations. (Data were obtained for different diameter splashplate nozzles, and these are reported below.)

The only operating parameters that were varied significantly within the data base for the above correlations were velocity and temperature. Hence, a correlation of the diameter ratio in terms of these two parameters was established:

$$D_m/D_n = \kappa \; v_n^{\alpha} \; T^{\beta} \quad (8)$$

where T is in °C and the empirical values for κ, α, and β are given in Table 1.2 [3]. The exponents for velocity are about the same as reported above based on dimensionless groups; the temperature exponents can then be expected to represent the

combined temperature effects embodied in density, viscosity, and vapor pressure. The basic conclusion that drop size decreases weakly as temperature increases is consistent with the limited data of Bennington and Kerekes [12].

Table 1.2 - Constants in Equation (8)

TEST	κ	α	β	r^2
1	1.30	-0.312	-0.194	0.894
2	4.51	-0.426	-0.407	0.820
3	2.61	-0.436	-0.264	0.679
4	0.69	-0.338	-0.092	0.929

Effect of Nozzle diameter

In mill recovery boilers, typical nozzle diameters range from 1 cm up to 3 cm. Since most of the laboratory testing was done with diameters at the low end of this range, it is important to determine how the mean drop size will change with increasing nozzle diameter. Data were obtained for splashplate nozzles of three different diameters (9.5, 11.9, and 18.0 mm) at 84°C and pressures of 238 and 342 kPa (20 and 35 psig) with 56% solids black liquor. Linear regression of the data yielded:

$$D_m = 0.24 * D_n^{0.162} \qquad (9)$$

where D_m and D_n are in centimeters [2]. The relatively low value of the exponent in eq.(9) indicates that drop size is not strongly dependent on nozzle diameter. An increase in nozzle diameter from 1 cm to 3 cm would only increase drop size by a factor of 1.2.

Effect of Black Liquor Type

Black liquor properties vary from mill to mill and from day to day within the same mill, depending upon wood furnish and pulping conditions. These variations can impact recovery boiler operation through changes in the liquor swelling and burning characteristics.

To determine the effect of black liquor variability on drop size, five different mill black liquors were obtained from four different kraft pulp mills. Three were softwood liquors (Georgia), one hardwood (Michigan), and one a 50/50 mixture (Alabama). Each liquor was tested with two different nozzles (CE swirl cone and B&W splashplate), two nozzle pressures (238 and

342 kPa), one solids level (60%), and two viscosities (60 cP and 200 cP).

An analysis of variance (ANOVA) was used to determine significant effects of spraying conditions, including possible interactions. Of the variables studied, nozzle type, nozzle pressure, and liquor viscosity were all statistically significant (99% confidence limit) in their effect on drop size. The change in drop size with liquor type was not statistically significant, even at the 90% confidence limit; neither were any interactions. The most important variable was nozzle type. The effects of viscosity and nozzle pressure mirrored the previous results. In addition, the drop size distribution continued to fit the Square Root-Normal distribution law with a normalized standard deviation of 0.2.

Effect of Temperature

The effect of drop diameter on temperature has been reported above to vary by the -0.1 to -0.4 power. As black liquor temperature was raised continuously, there was a temperature (designated the transition temperature) above which the spray droplet size decreased by more than 20%. At the same time, changes were observed in the shape and direction of the spray pattern. For both the V-jet and splashplate nozzles, the normally flat spray sheet opened up into an oval-shaped cone; also, with the splashplate nozzle, the central plane of the spray sheet moved away from the plane of the splashplate. The angle of this deviation was not measured, but it was estimated to be 20°-40°. These effects were observed to be reversible as temperature was lowered continuously to a value below the transition value.

Both of these changes can be attributed to vaporization of water. The physical effects of flashing can be analyzed by considering the flow of black liquor through the nozzle. Although the specific designs of the nozzles are quite different, they are similar in that the black liquor flows through a restriction before the spray issues from the nozzle. As the liquor flows through the restriction, its velocity increases and its pressure decreases. The pressure at the inlet of the nozzle is higher than the vapor pressure of the liquor and hence single phase flow prevails at this point. As the liquor flows through the nozzle orifice and its pressure decreases, a point is reached where the vapor pressure exceeds the line pressure and vaporization occurs, resulting in a reduced fluid density and an increased velocity.

Since drop size was reported above to decrease as velocity increases, a spray from this two-phase flow emerging from the nozzle above the transition temperature would be expected to have a smaller diameter. The change(s) in shape and/or direction of the spray sheet above the transition temperature with a splashplate nozzle can result from the flashing steam

contributing a component of momentum normal to the plate and, therefore, to the original plane of the spray.

The transition temperature was estimated to be several degrees above the atmospheric boiling point of the liquor and was dependent upon the dissolved solids content of the liquor. In this work, the transition temperatures were observed to be about 5°C above the atmospheric boiling point at 60% solids and about 9°C at 70% solids.

Since the transition temperature (T_{tr}) is the liquor boiling point at some elevated pressure, it should be predictable in the same way that the atmospheric boiling point of black liquor is [7]:

$$T_{tr} - T_{bp} = (K_{tr} - K_{bp})\ S/(100-S) \qquad (10)$$

The value of $K_{tr} - K_{bp}$ was 4°C; typical values of K_{bp} range from 10° to 15°C [15].

Using an average drop size calculated for temperatures above and below the T_{tr}, the ratio of the median diameters above and below the transition temperature was 0.82. Applying this result to recovery boiler operation, a hypothetical 20% decrease in median drop diameter would mean that, for the same liquor mass flow, the number of drops would be doubled and the surface area increased by about 30%.

In addition to measuring the median drop size, the standard deviation of the Square Root-Normal distribution was also calculated for each test. Previous work at temperatures below T_{tr} showed that the normalized standard deviation (δ) was essentially invariant at 0.20 ($\pm$0.03). For temperatures above T_{tr} in this work, the average value for δ was 0.19, signifying essentially no change in δ and leaving the Square Root-Normal distribution model as a one parameter model.

1.4.6 Mass Flow Distribution in Liquor Sheet

The sheets of liquor that issued from splashplate and V-jet nozzles were characterized with respect to distribution of mass flows within the total spray angle (θ), defined as the angle bounded by the left and right outer edges of the spray sheet. A maximum mass flux occurred at the spray centerline which coincides with the nozzle axis. The mass flux exhibited a dependence on angular position (ϕ, defined as the angular position in the spray sheet measured with respect to the centerline of the splashplate), decreasing in magnitude out to the edge of the sheet ($\pm\theta/2$). At the very outer edge was a thick, slow-moving rim; just inside the spray angle the mass flux was larger than expected, while just beyond it the flux was

essentially zero.

The total spray angle increased with operating pressure until it reached a maximum value; above this point the spray angle decreased slightly with increasing pressure. Viscosity had a strong influence on the spray angle, with increasing viscosity causing a reduction in the spray angle. The spray angle for the splashplate was much wider than for the V-jet and approached 180° at high flow rates and low viscosities. The SS V-jet nozzle is classified as a 65° nozzle by the manufacturer, and the measured spray angle values approached this value at high flows and low viscosities.

In order to quantify how the mass flow varied with angular position in the spray sheet, it was necessary to define a mass flow factor (MFF) as the ratio of the measured flow at a given angular position to the average flow over the total spray angle [3,16]. Because each sampling box had a fixed width, the measured mass flow represented an average over the angle, $\Delta\phi$. Hence, the MFF becomes the ratio of the mass flux into the box at angle ($\phi \pm \Delta\phi/2$) to the mass flux averaged over the spray angle, θ.

From visual observations of the liquor sheets, one could see that there was a central core in the angular range from $-15° < \phi < 15°$ having a relatively uniform flow rate. Outside this region, the flow rate dropped off steadily to the outer rim.

A correlation of MFF as a function of angular position (ϕ) was developed for predicting mass flow distribution for a nozzle under specified operating conditions. Although either a linear or a parabolic dependence would have produced a reasonable curve fit of the measured MFF profile, the linear correlation was judged unsuitable because the slope of the "curve" at $\phi = 0$ would have has a discontinuity, whereas the experimental curve was continuous in this region. The parabolic correlation satisfied this criterion at the centerline, and hence it was used to represent the data.

If the MFF is expressed in the form:

$$MFF = P - Q\,\phi^2 \tag{11}$$

the constants P and Q can be approximated, knowing the MFF at $\phi = 0$ and at some other angular position, $\phi(1)$. Hence at $\phi = 0$, $MFF = P$; at $\phi = \phi(1)$, $MFF = MFF(1)$ and $Q = [P - MFF(1)]/\phi(1)^2$. It can be shown further that the model predicts $\theta = (12(P-1)/Q)^{1/2}$ [16]. Modeling the mass flux profile as a parabolic function of angular position, with the maximum flux at the centerline, predicted the mass flux at the sheet centerline to be 1.5 times the average flux for the entire sheet cross-section at the same radial distance from the tip of the nozzle. Model predictions of both the centerline flux and the full spray angle agreed to within 10% of the experimental values for the splashplate nozzle.

These results should provide useful input to mathematical models of the combustion processes occurring in kraft recovery boilers.

1.4.7 Alternative Commercial Nozzles

Commercially available spray nozzles from different commercial applications, ranging from spray coating to aerial application of pesticides for agricultural crops, were evaluated for their use with black liquor. Common commercial nozzle types not presently used with black liquor include: sonically assisted atomizers; two-phase atomizers; rotary disc atomizers; and full-cone nozzles. All but the last one are generally designed to provide fine droplets (under 100 microns) and thus were eliminated from consideration.

The nozzles we chose to test were the Bete Spiral R™, Bete Whirl R™, and Delavan Raindrop R™. All are basically full cone nozzles with design features (internal or external) that give a tangential velocity component to the liquor flow; all are claimed to give coarse, uniform conical sprays.

Comparison tests were run on the three alternative nozzles, along with the standard B&W 12/45 splashplate, CE swirl cone, and SS F-12 V-jet [2]. Operating conditions were 75°C/60% solids (220 cP viscosity) and 89°C/56% solids (70 cP); nozzle pressures of 238 and 342 kPa (20 and 35 psig) were used.

Examination of the median diameters for the four sets of experimental conditions showed that the only nozzle to give a significantly different diameter was the Delavan Raindrop. It gave values 50 - 80% greater than the average of the other five nozzles. All six nozzles fit the square root-normal distribution, and all six gave the usual value for the normalized standard deviation of 0.20 ± 0.02.

Hence, the only alternative commercial nozzle to have shown any promise was the Delavan Raindrop. In this case, the size distribution was essentially shifted to the right, but with the same relative size distribution; the implication is that the fraction of small droplets (i.e.,the ones that tend to be carried over in the recovery furnace) will be lower for the Raindrop, relative to a standard black liquor nozzle operating at the same conditions. Just how the recovery boiler would respond to combustion of a "Raindrop spray" is unknown at this point.

1.4.8 New Nozzle Concepts

A task was undertaken to develop new nozzle concepts in an effort to gain some degree of control over drop size and size distribution. One constraint always kept in view was that any new conceptual nozzle had to be easily implementable and very reliable. This latter limitation recognizes the need for the

recovery boiler to remain on-line around the clock 350 days a year. One approach was to consider physical modifications to an existing splashplate nozzle which would change the nature of the sheet coming off the splashplate to reduce the randomness of the breakup process. A second approach was to employ the principle of vibratory assist and apply it to an existing splashplate or V-jet nozzle.

Modified Splashplate Nozzles

Conceptually, one way to reduce the randomness of the sheet breakup process would be to modify the smooth, flat surface of the splashplate in such a way that the liquor sheet is no longer uniform, but has defined zones of alternating thick and thin cross-section in the flow direction. In this way, the sheet would initially tend to break at the thin spots, which would be governed by how the sheet thickness was perturbed by the surface characteristics of the modified splashplate. Hence, the initial breakup would no longer be random. Of course, subsequent breakup of the resulting individual "jets" into droplets would still be governed by fluid mechanical forces and the randomness that those forces introduce.

Six different modified splashplates were designed, fabricated, and tested in the black liquor spray chamber [2]. All the geometric modifications to the splashplate surface proved ineffective. One which used multiple cylindrical pegs mounted around the splashplate periphery and normal to the splashplate surface gave a 25% reduction in median diameter, with a 0-30% increase in the width of the distribution; both effects are undesirable.

Dual Splashplate Nozzle

It was hypothesized that a bimodal drop size distribution might be attractive in that the smaller size would tend to burn in flight while the larger size would fall to the char bed prior to combustion. An attempt was made to generate a spray with a bimodal size distribution by configuring two splashplates back-to-back, each with its own liquor flow [2]. The liquor feed was divided into two branches, each having a control valve to adjust the flow through its branch. By using different diameter nozzles and different pressure drops in the two branches, two different sheet velocities, and hence two different drop size distributions, were thought to be obtainable. Interaction of the two parallel liquor sheets coming off the splashplates could be varied by providing a spacer between the splashplates. By design, the spacer could not only control the distance between the sheets coming off the plates, but also the angle between the sheets. The sheets could readily be made to converge or diverge, thereby maximizing or minimizing the degree of sheet interaction. Naturally, each branch functioned like a typical splashplate

nozzle, and hence operational reliability of the dual splashplate concept was not a concern.

Results showed that if there was sheet interaction, a larger median drop size resulted in comparison to a single splashplate nozzle; size distribution widths were the same for both cases. If there was little or no sheet interaction, drop size and size distribution were unchanged from the single nozzle case. Under the conditions run, no bimodal drop size distributions were detected.

Vibratory Assist

A number of studies have been carried out regarding the stability of thin liquid sheets moving in a gaseous environment. Inviscid theories of two-dimensional wave growth predict that, in the initial stages of growth, an optimum frequency exists where the growth rate is a maximum. Viscous theory, on the other hand, predicts the absence of a wave of maximum growth rate except at low velocities. Crapper, et al. [17] have claimed that dominant waves seen on a sheet must be of a frequency imposed by some external force. Hence, the role of vibratory assist is to obtain growth rates of low amplitude waves at any distance from the nozzle orifice. Crapper and Dombrowski [18] suggested that drop size may be affected by both nozzle amplitude and frequency. Since these factors may depend upon natural frequencies in the apparatus, drop sizes in industrial settings could well turn out to be different from those given by the same nozzle in the laboratory.

Vibration of the liquor flow can be done either in-line with or normal to the flow. The resulting waves in the liquor sheet issuing from the nozzle should be in the dilational and sinuous modes, shown in Fig.s 2.1 and 2.2, respectively [2]. Conceptually, the dilational mode would be expected to give a narrower drop size distribution, since the breakup of the sheet into ligaments should occur at the points of minimum thickness. These are not randomly placed because of the vibrations imposed on the system. The subsequent breakup of ligaments into drops will still be a random event. On the other hand, the sinuous wave mode maintains a constant sheet thickness, implying that sheet breakup will still be a random phenomenon going to ligaments, which then randomly break up into drops.

The sinuous mode was examined first because it was easier to accomplish experimentally. A splashplate nozzle was vibrated in a direction normal to the plane of the plate by a two-knobbed cam rotating with a motor shaft. Vibrational frequency was varied from 0 to 93 Hz. Splashplate displacements were about 0.1 and 0.2 mm. Using a black liquor flow rate of 12 gpm with liquor viscosities ranging from 75 to 150 cP, no significant changes in median drop size or normalized standard deviation were recorded. We did, however, observe that vibrations caused the liquor sheets to break up sooner than without vibration. The higher

Figure 2.1 VIBRATORY ASSIST

Dilational Wave Generation

- Wave-like Disturbances to Upper and Lower Surfaces of the Sheet Are Out of Phase

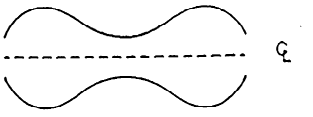

- Vibration in Direction of Liquor Flow (i.e. pulsation of Liquor flow)

Figure 2.2 VIBRATORY ASSIST

Sinuous Wave Generation

- Wave-like Disturbances to Upper and Lower Surfaces of the Sheet Are in Phase

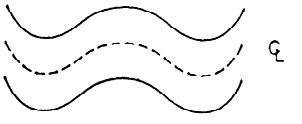

- Vibration in Direction Normal to Plane of the Sheet

vibrational amplitude did form liquor bands whose width decreased with increasing frequency.

An alternative mode of generating transverse waves was examined using an air-driven vibrator. Frequencies up to 130 Hz were tried with the splashplate nozzle operated at the same conditions as for the cam-driven nozzle. Results showed a significant effect on the liquor sheet, the drop size, and size distribution. Bands of liquor formed whose width was inversely proportional to the vibrational frequency. The bands broke into smaller pieces just like sheets formed with no forced vibrations, resulting in a relatively broad range of drop sizes. Relative to the zero vibration case, the median diameter for 70 to 110 Hz on average was 20% higher, and the normalized standard deviation was 24% higher. No trend was observed with increasing frequency. Hence, this did not appear to be a promising route toward obtaining a more controlled drop size distribution.

The dilational wave mode was examined by imposing axial vibrations (i.e., pulses) on the liquor flow. This mode is very difficult to accomplish experimentally, as evidenced by the lack of activity reported in the literature. We conceptualized, designed, built, and tested an apparatus to mechanically pulse the liquor flow to a commercial V-jet nozzle under controlled conditions of vibrational frequency and amplitude [2].

A key feature of the method used to pulse the flow was that the operator could positively control the amplitude and frequency of vibration, not relying on a "spring constant" which most other mechanical vibratory methods do. Also, larger amplitudes could be accomplished than what are normally achieved with traditional acoustic or pneumatic vibrators.

Testing with axial vibratory assist using the pulsed flow mode described above was carried out with 62% solids black liquor flowing through a 3/8-inch V-jet nozzle at 73°C and 8 gpm. Liquor viscosities ranged from about 100 to 160 cP. Frequencies up to 147 Hz were run with a maximum variation in the liquor flow to the nozzle orifice of ±20% of the mean [2].

Compared with the zero vibration case, median drop diameters and normalized standard deviations for the vibratory runs were not significantly different. When the normalized standard deviation (δ) values were correlated linearly with frequency, a small positive coefficient resulted, implying the distribution width increased with frequency. This is counter to the result that was expected. Unfortunately, equipment limitations precluded going to greater frequencies and amplitudes of flow variation with this design.

Dielectrophoresis

An alternative concept which has potential for influencing

drop size distribution in black liquor sprays may use the phenomenon of dielectrophoresis where an electric field is positioned around the spray sheet to alter the direction of flow of the neutral, but polarizable droplets that are formed. By exerting an independently controlled force on the droplets that will be proportional to drop diameter, it may be possible to cause collisions of the smaller drops with larger ones, resulting in coalescence. Electrostatic forces have been used to encourage coalescence in emulsions since the beginning of the twentieth century [19]. Coalescence is known to occur as particles or droplets moving at different velocities collide. Dielectrophoresis enhances this tendency by providing a force of attraction between two polarized droplets.

This concept, if successful, should reduce the fraction of fine droplets and result in a size distribution skewed toward the larger sizes. If a drop size distribution can be achieved having a reduced percentage of the fine fraction, then entrainment/carryover rates in the recovery boiler should be decreased, thereby making room for a capacity increase. Improvements in energy recovery efficiency would also be expected from reduced sootblowing requirements.

Dielectrophoresis is the movement of an uncharged particle in a non-uniform field, by virtue of the dipole induced on the particle by the field [19]. The dielectrophoretic force on a droplet will be proportional to droplet volume, field strength, field gradient, and difference in dielectric constants between the droplet and the gas space through which it is flowing. Typically, field strengths of 10 kV/m are required for dielectrophoretic forces to be significant.

Since the force of an isolated dipole is towards the higher field strength for both polarities of field, both AC and DC fields produce dielectrophoretic motion. In a DC electric field, the dielectrophoretic force is normally much lower than the electrophoretic force, but there is no net electrophoretic motion in an AC field. Hence an AC field can be used to make independent observations of dielectrophoretic effects.

Generation of a non-uniform field can be accomplished by any number of electrode configurations. Of course, parallel plates are excluded because the resulting field is uniform. Our initial choice of electrode configuration which could be mounted in the black liquor spraying apparatus consisted of three rods, contained in each of two parallel planes, spanning the lateral area of the spray sheet and providing a non-uniform field for practically all of the drops that form.

With this geometry, two operating modes were possible. In the first case, the spray was positioned equidistant between the two planes of electrodes. Droplet migration toward both planes was expected, in principle. Only the drops exactly equidistant from the two electrode planes would not experience a non-uniform

field, and hence they would not be subject to the dielectrophoretic force. In the second arrangement, the electrode planes were both on one side of the spray sheet. The electric field lines of force were more non-uniform for all droplets, and hence should have provided a stronger dielectrophoretic force on all drops in the spray.

An exploratory test employing dielectrophoresis was conducted at 38°C using 48% solids black liquor flowing at 12.6 gal/min from a SS 15/65 V-jet nozzle. At these conditions, the liquor viscosity was 130 cP.

The tests were performed both with the spray sheet centered between the two electrode planes and with both electrode sets to one side of the sheet. In both configurations, the closer electrode set was about 9 inches from the center of the spray sheet. Direct current voltages of 3.0 and 5.0 kV were applied between the electrode sets, yielding a maximum field strength of about 10 kV/m.

The voltage limitation in our system was determined by the cutoff current for the power supply. The electrodes were encased in insulating PVC tubing, but this did not prevent current flow for voltages above 5 kV. The key parameter here is the "spark-gap voltage" which, for a given dielectric medium between electrodes of known spacing, is the maximum voltage possible before breakdown occurs. For 5 kV with air as the dielectric, the minimum allowable distance separating the electrodes is 1-2 mm. With black liquor droplets effectively increasing the dielectric constant of the medium between the electrodes, the minimum separation distance is significantly increased. Hence, higher field strengths with this electrode configuration did not appear to be possible.

Drop size determinations using dielectrophoresis conditions showed no significant effect of field strength on drop size or size distribution for field strengths up to 10 kV/m, the maximum field strength allowed before dielectric breakdown occurred. Hence, it did not appear that drop size distribution could be significantly altered by this route.

2.0 RESULTS FROM PAST YEAR

2.1 Axial Vibratory Assist - Interrupted Flow Design

An alternative mode of achieving vibratory assist in the axial direction is to use flow interruptions rather than pulsations. Our initial design reported previously [20] was unreliable mechanically and limited in frequency of pulsation to under 30 Hz. Above this frequency, the rotating tube was subject to binding and seizure. An improved design enabled higher pulsation frequencies with improved operability and reliability. This was accomplished by positioning all holes in both the

rotating and stationary pipes at the same axial position. The rotating cylinder contains two or more holes at a fixed axial position, while the outer pipe section contains two outlets, diametrically opposed at the same axial position. In the first design, the sets of holes were axially displaced.

As with the first design, one outlet on the outer pipe is connected to the nozzle orifice, while the other outlet is connected to a recycle line. Black liquor is fed to the inner cylinder which is rotating at a rate set by a drive motor assembly. Liquor flows out to the nozzle or to the recycle as dictated by whether or not the holes in the rotating inner cylinder line up with a hole in the stationary outer pipe. In general, when liquor flows to the nozzle orifice, it doesn't to the recycle; and vice versa. Leakage through the annular space between the rotating and stationary bodies is minimized by providing a tight clearance between the bodies.

The net effect of this concept is to provide an interrupted flow to the nozzle orifice while not deadheading the black liquor pump. The frequency of interruption is determined by the angular rotation speed provided by the drive assembly. The amplitude of the pulses created in the flow to the nozzle is determined by the relative sizes of the holes and the liquor pressure. Additional pairs of holes could be drilled in the rotating cylinder to increase the frequency of spray interruption.

A Disclosure of Invention has been filed covering a nozzle to give a pulsed black liquor flow by the flow interruption mode described above.

For vibratory assist to work effectively, it must be done at the proper frequency and amplitude of pulsation; otherwise, the natural frequency of the sheet will dominate, giving a normal distribution of drop sizes. An estimate of the required vibrational frequency was calculated from wave theory, assuming that the sheet breaks up into discrete uniform bands with no interactions between adjacent bands [2]. For typical values of the black liquor process parameters, a minimum vibrational frequency of 240 Hz was predicted. There is no easy way to estimate the desired amplitude because it is related to complicated stability theory.

2.2 Axial Vibratory Assist - Interrupted Flow Results

Testing with axial vibratory assist using the interrupted flow mode described above (cf. Fig. 2.3) was carried out with 62% solids black liquor flowing through a 3/8-inch V-jet nozzle at 73°C and 8 gpm. Liquor viscosities ranged from about 100 to 160 cP. The distributor design was machined so that liquor flowed to the nozzle orifice 1/4 of the time (3/4 time going to recycle). The frequency range extended from 0 Hz up to 450 Hz; liquor solids and temperature (∴ viscosity) were held constant.

Figure 2.3 AXIAL VIBRATORY ASSIST

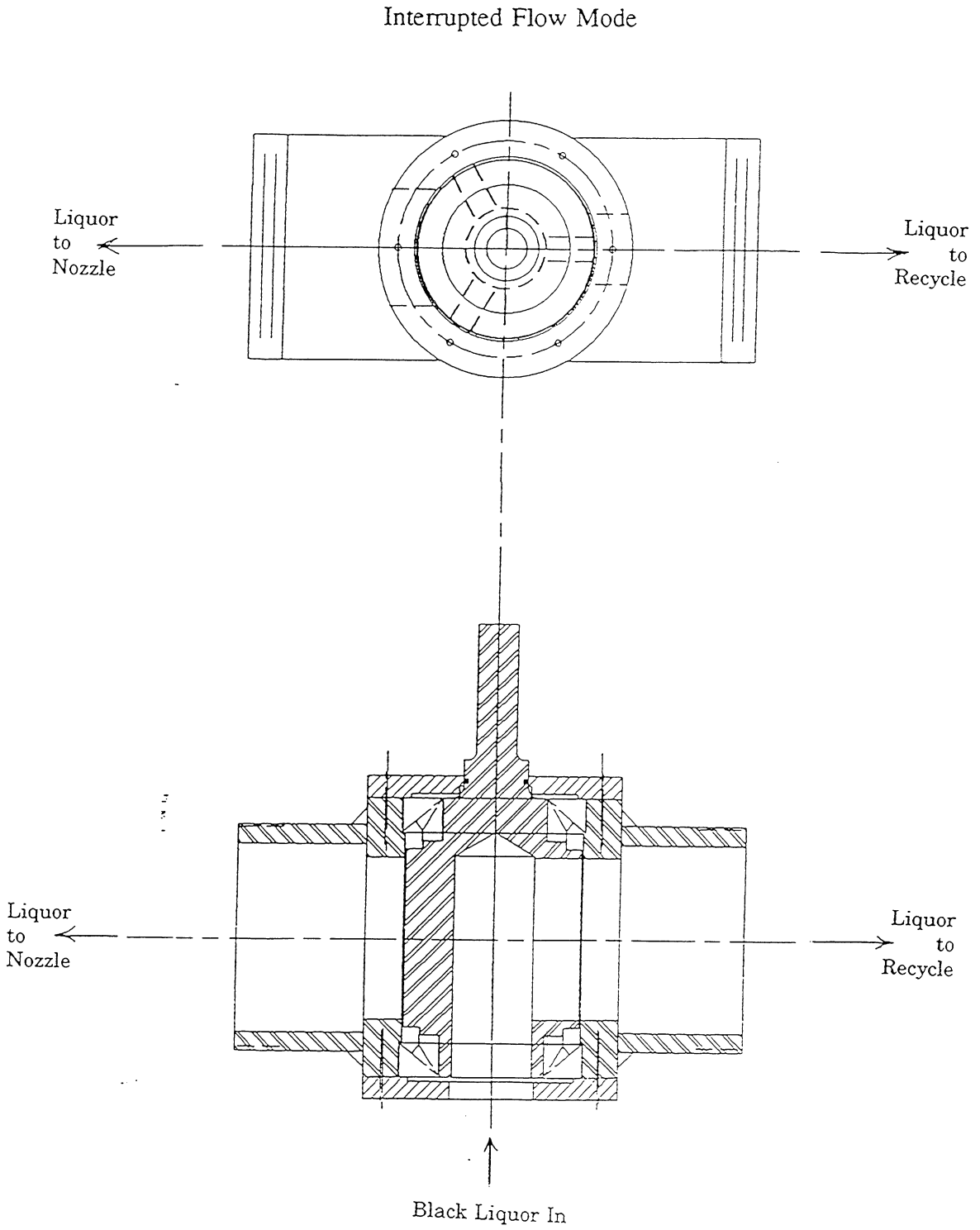

Fig. 2.4 shows the effect of pulsation frequency on median drop size. The filled symbols represent actual data, whereas the unfilled symbols are median diameters calculated for no pulsation from previously reported correlations, at the same respective spraying conditions for each data point. The calculated zero pulsation curve is basically flat. Interestingly, median drop size with pulsation increased from 2.2 mm with no pulsation up to a maximum of 3.5 mm at 220 to 260 Hz, then decreased steadily to 2.5 mm at 450 Hz. The shape of the median drop diameter vs. pulsation frequency curve was nearly sinusoidal, supporting the expectation of harmonic behavior that should be characteristic of a vibratory process (cf. Fig. 2.4). Surprisingly, the normalized standard deviation of the drop size distribution did not show any significant variation with pulsation frequency (cf. Fig 2.5).

Since one of our primary objectives was to be able to spray black liquor into a recovery boiler with minimal droplet entrainment and carryover, it would seem intuitively obvious that the fraction of small drops in a spray should be minimized. Based upon the size distributions measured, we have calculated the fraction of drops in an individual spray at a given frequency that are smaller than 1 mm and 0.5 mm. Plotting the % Less Than 1mm (or 0.5 mm) vs. Pulsation Frequency, the curve goes through a minimum in the frequency range where the maximum median drop sizes occurred (cf. Fig. 2.6).

The important question at this juncture is what do these results mean with regard to optimizing recovery boiler performance? A major operational concern is droplet carry-over, and we haven't demonstrated any ability to narrow the drop size distribution which might result in reducing the fraction of small size droplets, thereby reducing carry-over. But narrowing the drop size distribution is not a necessity.

What we have shown is a way of increasing median drop diameter without changing the size distribution and doing this independent of the normal process operating parameters (e.g., temperature, pressure, % solids); the only quantity we have to change is pulsation frequency.

These results can be used to calculate the frequency dependence of the mass fraction of drops in a given spray that would be less than some small diameter, say 1 mm or 0.5 mm. Fig. 2.7 plots the % Less Than 1 mm (or 0.5 mm) vs. Median Drop Diameter and includes a calculated curve for a normalized standard deviation of 0.19. It graphically shows the benefits of being able to increase median drop diameter by pulsing the liquor flow and obtaining a spray with a reduced fraction of fine droplets. Results show that 4% of the drops would be less than 1 mm at zero pulsation (median drop diameter 2.2 mm) and about 1% at the 230 Hz condition which gave a median drop diameter of 3.5 mm This may have interesting implications for reducing carry-over in recovery boilers; predictions using the IPST recovery boiler model currently being developed will be generated to

Fig 2.4 Drop Diameter vs Frequency - Test 75 and 83

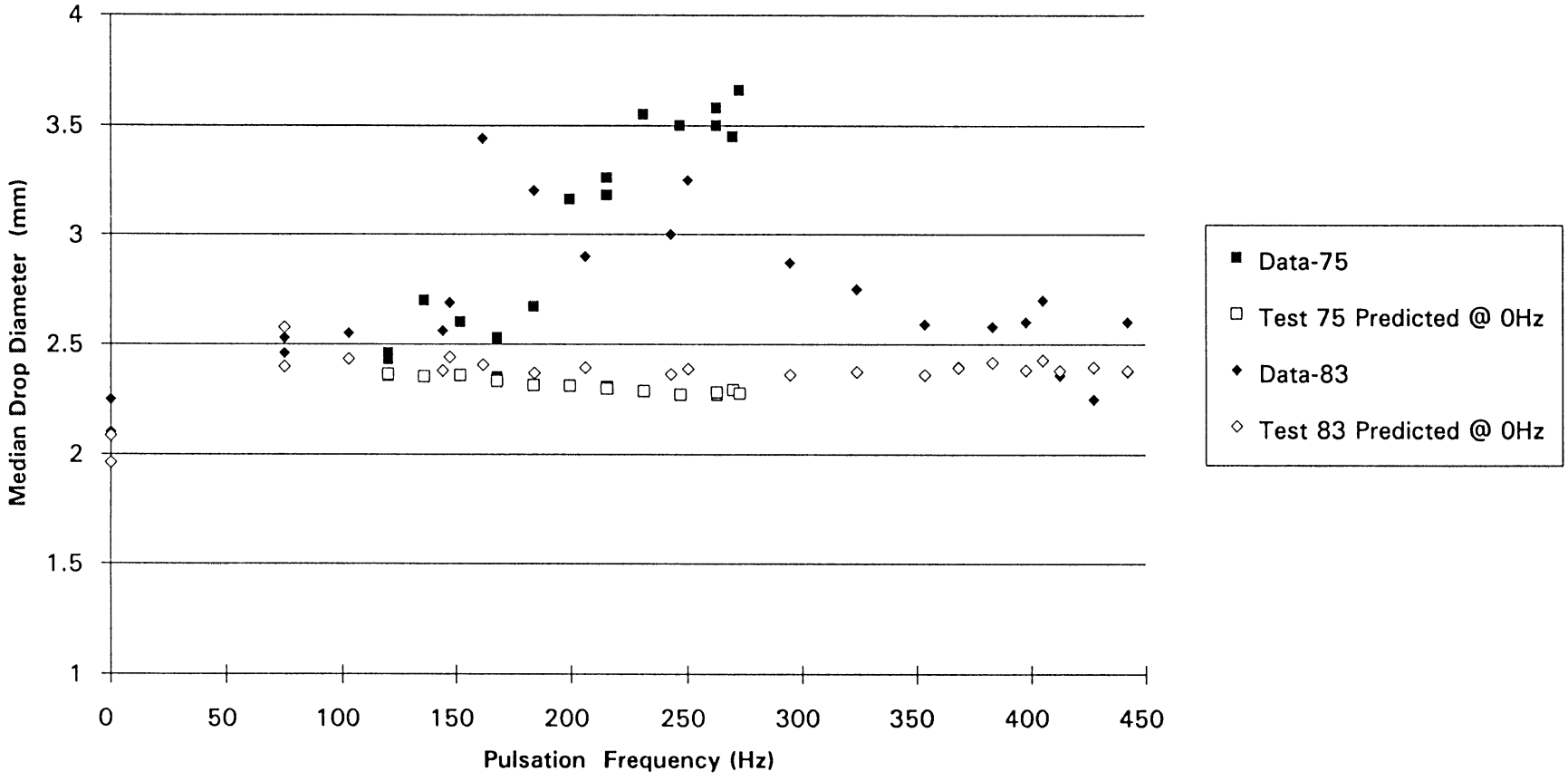

Fig 2.5 Drop Diameter and Normalized Std. Dev. vs Frequency - Test 83

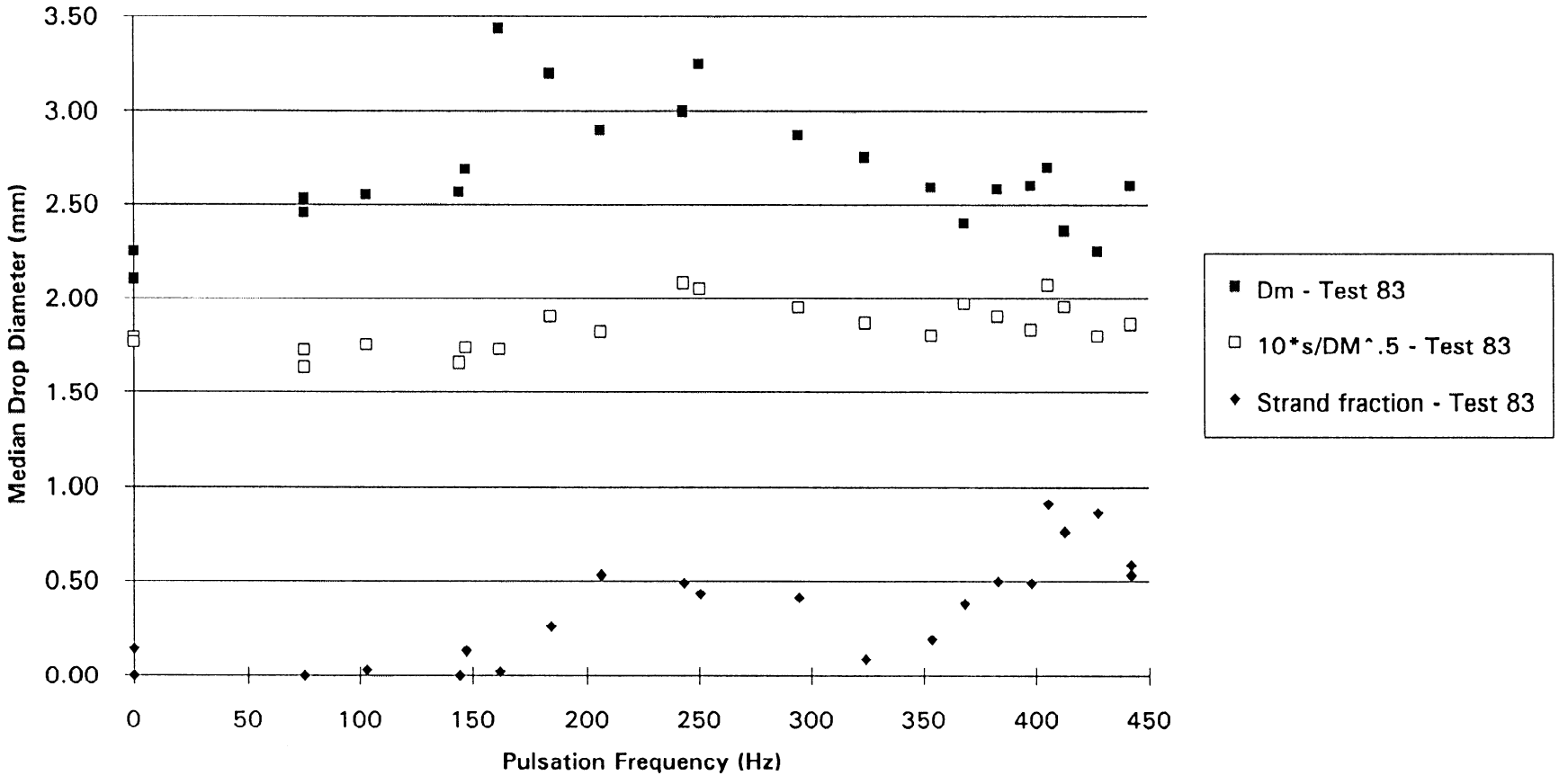

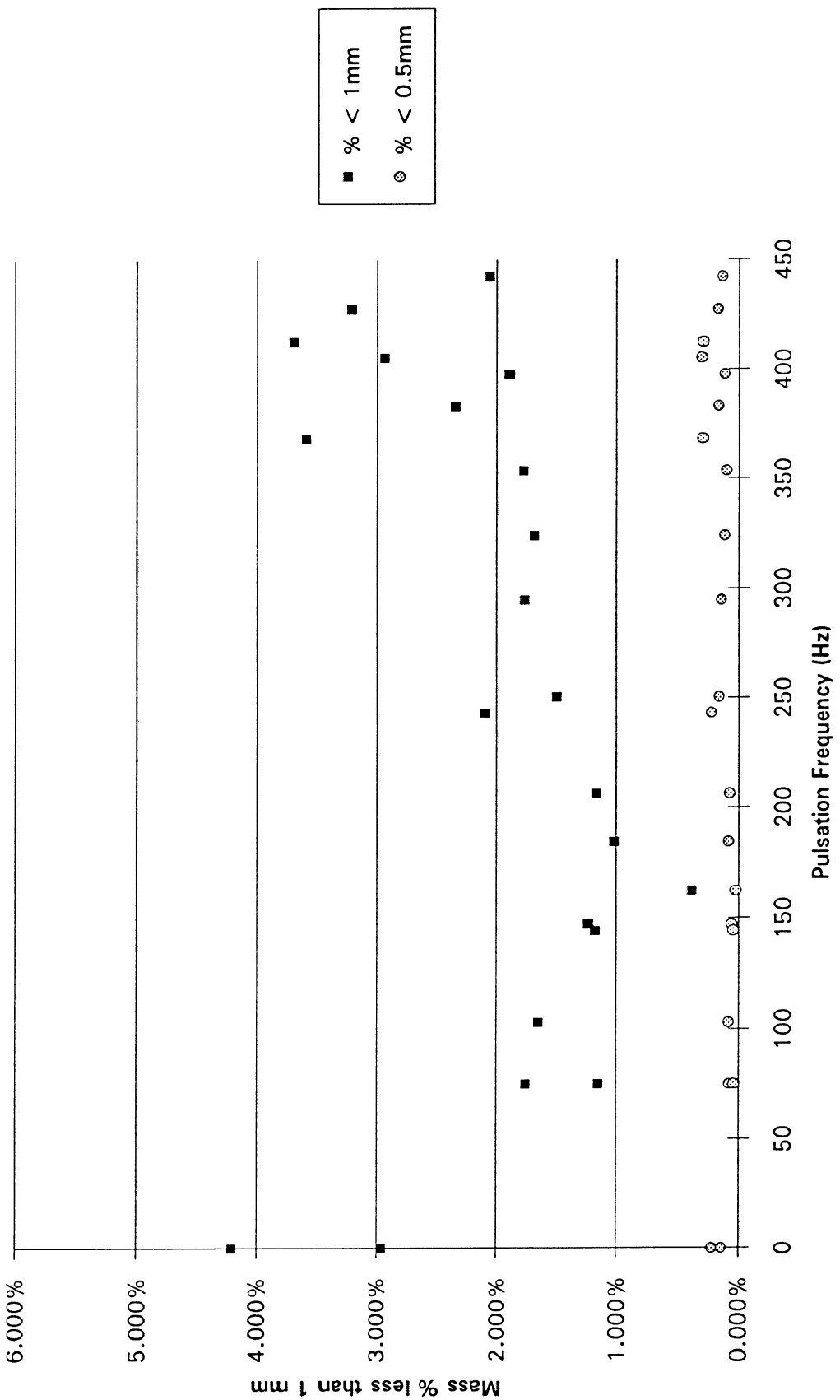

Fig. 2.6 Percent Less Than 1.0 mm vs Frequency - Test 83

Fig. 2.7 Percent Less Than 1.0 mm vs Median Drop Diameter - Test 83

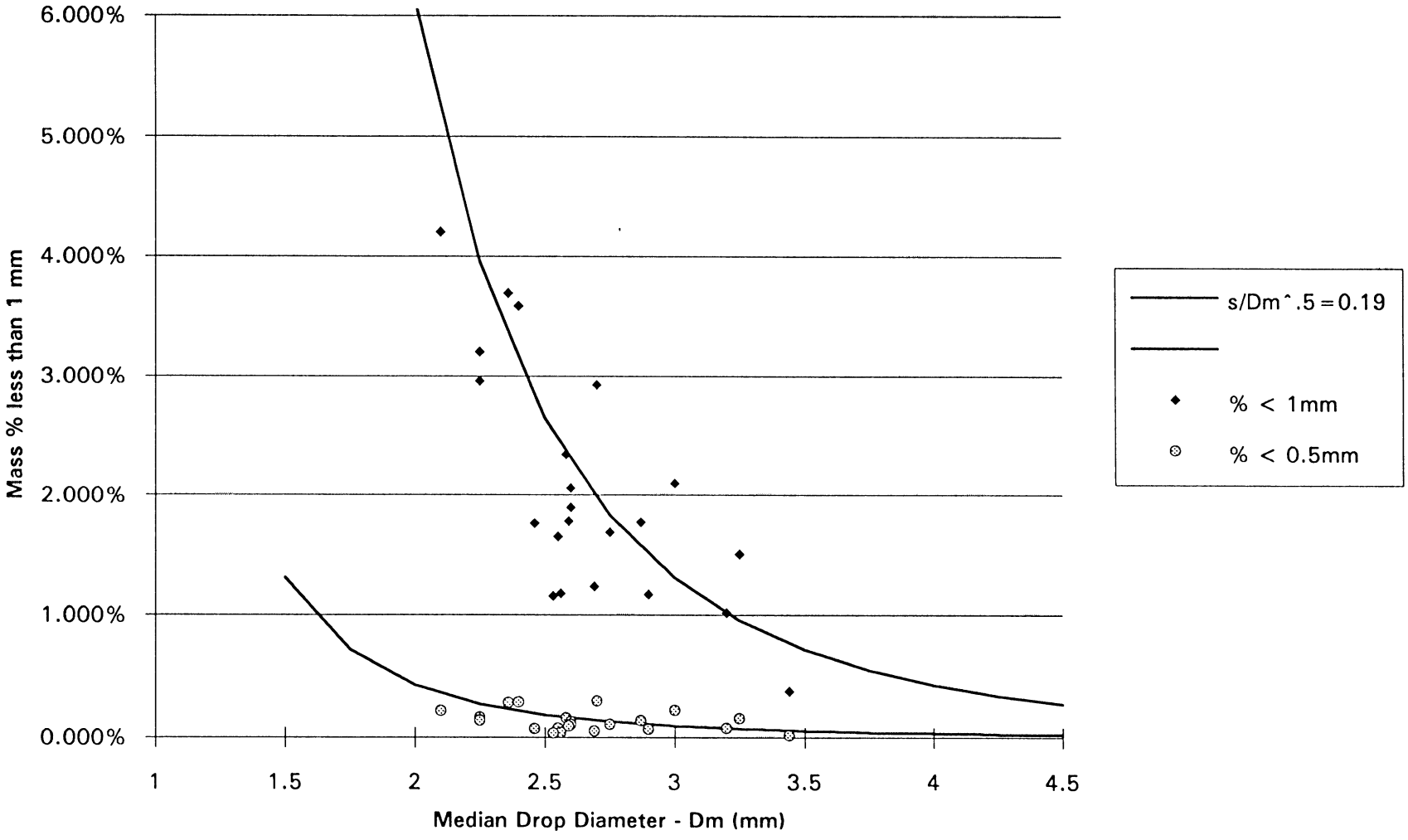

confirm this desired result.

3.0 CONCLUSIONS

1. Gaining independent control over drop size distribution in black liquor sprays from commercial nozzles will require an independently contolled external force, such as vibratory assist.

2. Vibratory assist in the axial direction, as applied to black liquor spraying, was accomplished with two novel nozzle designs. The one achieving a pulsed flow by inducing periodic flow interruptions has shown some promise in changing the mean drop size without changing the normal process operating parameters. There may exist a harmonic frequency where a minimum of small size drops is made.

3. To what extent the drop size distribution should be narrowed or skewed to have a positive impact on recovery boiler performance is not known at this time. An estimate can be obtained by specifying different drop size distributions as input to the recovery boiler model currently being developed by the Institute of Paper Science and Technology and calculating the model predictions.

4. Median droplet size data from a B&W splashplate nozzle and a CE swirl cone nozzle showed a weak dependence on liquor velocity and fluid physical properties. The ratio of median droplet diameter to nozzle diameter was related to the product of Reynolds Number and Euler Number, each raised to an experimentally determined non-integral power; similarly, Euler and Schmidt Numbers also correlated well. Both dimensionless correlations were broken down into a product of the individual physical parameters, each raised to an experimentally determined power. It was shown that the parameters which most strongly influenced mass median drop diameter were nozzle diameter, and liquor density and velocity. At high solids levels, liquor viscosity became important. When droplet diameter was empirically correlated with velocity and temperature raised to appropriate exponents, drop size was shown to decrease as either operating parameter was increased.

5. Several drop size distribution models were tested to fit the experimental data; the best one was the square root-normal distribution. It was shown that the ratio of the standard deviation to the square root of the median diameter has a constant value of 0.2, and therefore only one parameter is necessary to characterize the square root-normal distribution for black liquor sprays.

6. As temperature was increased, drop diameter gradually decreased until a transition temperature was reached (5-9°C above the atmospheric boiling point, depending on % solids) where the drop size abruptly decreased by about 20%; the normalized

standard deviation for the drop size distribution remained unchanged at 0.2. This effect was accompanied by a noticeable change in the physical appearance of the spray. The normally planar spray sheet became oval in cross-section, and, for a splashplate nozzle, the central plane of the sheet came off the plate at a 20 to 40 degree angle, rather than at zero degrees. These phenomena were attributed to flashing at the nozzle.

7. Black liquor spraying characteristics were not sensitive to the type of liquor at the same viscosity. Median diameter was shown to depend most strongly upon nozzle type and pressure, along with liquor viscosity. A weak dependence upon nozzle diameter was also observed.

8. Measurements were made of the local distribution of liquor flow in the spray pattern as a function of the angle from the sheet centerline. Results for both the splashplate and V-jet nozzles showed the mass flow distribution to be parabolic, with the maximum mass flow at the centerline and decreasing with increasing angle. Limited analysis of drop size as a function of the angle from the sheet centerline showed no significant effect.

9. Consideration of alternative commercial nozzles uncovered none which featured improved control over median diameter and width of the diameter distribution. The Delavan Raindrop did give a coarser-than-normal spray, which gives it potential for producing sprays that result in reduced entrainment/carryover rates in recovery boilers.

10. Configuration of a splashplate type nozzle to give two parallel liquor sheets, which subsequently break up into two distinct droplet distributions, gave a larger median drop size than a single splashplate nozzle, if there was sheet interaction. If there was little or no sheet interaction, drop size and size distribution were unchanged from the single nozzle case. Under the conditions run, no bimodal drop size distributions were detected.

11. Geometric modification of the surface of a splashplate nozzle to alter drop size and size distribution at near-normal spraying temperatures proved ineffective. However, using multiple cylindrical pegs mounted normal to the splashplate surface gave a 25% reduction in median diameter, with a 0-30% increase in the width of the distribution. These were attributed to the formation and breakup of multiple jets rather than a sheet of liquor.

4.0 REFERENCES

1. Hupa, M., Solin, P., and Hyoty, P., "Combustion Behavior of Black Liquor Droplets," Proc. Intl. Chem. Recov. Conf. (New Orleans), TAPPI/CPPA, 335-344 (1985).

2. Empie, H.J., Lien, S.J., Rumsey, R.S., and Sachs, D.G., "Kraft Black Liquor Delivery Systems Report No.4," U.S. DOE Contract No. DE-FC02-88CE40839, IPST (Jan. 1993).

3. Empie, H.J., Lien, S.J., Yang, W., Samuels, D.B., and Adams, T.N., "Kraft Black Liquor Delivery Systems Report No.3," U.S. DOE Contract No. DE-FC02-88CE40839, IPST (Dec. 1991).

4. Adams, T.N., Empie, H.J., Lien, S.J., and Spielbauer, T.M., "Kraft Black Liquor Delivery Systems Report No.2," U.S. DOE Contract No. DE-FC02-88CE40839, IPST (Dec. 1990).

5. Adams, T.N., Empie, H.J., Obuskovic, N., and Spielbauer, T.M., "Kraft Black Liquor Delivery Systems Report No. 1," U.S. DOE Contract No. DE-FC02-88CE40839, IPST (Feb. 1990).

6. Empie, H.J., Lien, S.J., Yang, W., and Adams, T.N., "Spraying Characteristics of Commercial Black Liquor Nozzles," Int'l. Chem. Recov. Conf., Seattle, WA (June'92).

7. Empie, H.J., Lien, S.J., and Yang, W., "Effect of Temperature on Black Liquor Droplet Formation from Commercial Black Liquor Nozzles," AIChE Forest Products Symp. Proc.(1992), p.57 (1993).

8. Spielbauer, T.M. and Aidun, C.K., "Mechanisms of Liquid Sheet Breakup and the Resulting Drop Size distributions, Part 1," Tappi J.75(2),136-142 (1992).

9. ibid., "Part 2," Tappi J.75(3),195-200 (1992).

10. Simmons, H.C., "The Correlation od Drop-Size Distributions in Fuel Nozzle Sprays," Trans.ASME, J. Eng. Power, 309-319 (July,1977).

11. Bousfield, D.W., "Research on Droplet Formation for Application to Kraft Black Liquors," Tech. Rept. No.5 (Jan.1990).

12. Bennington, C. and Kerekes, R., "Effect of Temperature on Drop Size of Black Liquor Sprays," Proc. 1985 Int'l Chem. Recov. Conf., TAPPI, Atlanta, GA, 345-354 (1985).

13. Spielbauer, T.M., Adams, T.N., Monacelli, J.E., and Bailey, R.T., "Droplet Size Distribution of Black Liquor Sprays," Int'l Chem. Recov. Conf., TAPPI/CPPA, Ottawa, Can. (1989).

14. Bird, R.B., Stewart, W.E., and Lightfoot, E.N., Transport Phenomena, Wiley & Sons, New York, N.Y. (1960).

15. Green, R.P. and Hough, G., Chemical Recovery in the Alkaline Pulping Processes, p.6, TAPPI Press, Atlanta, GA (1992).

16. Empie, H.J., Lien, S., and Samuels, D.B., "Distribution of Mass Flows in Black Liquor Sprays," AIChE Ann. Mtg., San Francisco, CA (Nov. 1994).

17. Crapper, G.D., Dombrowski, N., and Pyott, G.A.D., Proc. Roy. Soc. London A342, 209-224 (1975).

18. Crapper, G.D. and Dombrowski, N., Int. J. Multiphase Flow 10 (6), 731-736 (1984).

19. Pohl, H.A., Dielectrophoresis, Cambridge Univ. Press (1978), Ch. 4.

20. Empie, H.J., Lien, S.J., Rumsey, R.S., and Sachs, D.G., "Kraft Black Liquor Delivery Systems Report No. 5," U.S. DOE Contract No. DE-FC02-88CE40839, IPST (Jan. 1994)

CLOSED MILL OPERATIONS
PROJECT F017

ANNUAL PROGRAM REVIEW

March 23, 1995

Pat Bryant
Peter Pfromm
Junyong Zhu
Jeff Empie
Terry Adams

Institute of Paper Science and Technology
500 10th Street, N.W.
Atlanta, GA 30318
(404) 853-9500

ANNUAL PROGRAM REVIEW

Project Title: Closed Mill Operations

Project Code: CLDMIL

Project Number: F017

Division: Chemical and Biological Sciences

Project Staff: P.Bryant, JY.Zhu, P.Pfromm, E.Malcolm, T.Adams

FY 94-95 Budget: $487,500

Program Objective:

Develop technology required to move toward closed mill operation.

SUMMARY OF RESULTS:

Previous Results:

This project was initiated in FY '94. A major effort was put into developing proposals to DOE to fund long-term efforts in the closed mill area. Portions of the work proposed to DOE are included in the goals for this project. A summary report on mill closure technologies was initiated to be used in developing project goals in the upcoming year. Work on combustion of nonchlorine bleach plant effluents was resumed under the direction of new faculty in the Recovery Group. Small amounts of external funding have been obtained in support of this activity.

Current Results:

Impact and Control of Non-process Elements (NPE's):

Subtask Objective:

Work began in August 1994 on developing a scientific understanding of the partitioning of NPE's. The research plan includes mill sampling, laboratory experiments, full-mill simulation, predictive model development and model verification.

We are working with three member companies to develop three bleached kraft mill NPE material balances. This work involves sampling and analyzing process streams at each mill for NPE's and developing a full-mill process simulation for each mill. The sampling and full-mill simulation is complete for one mill and analysis of the mill samples is in progress. Work with the other two mills is in the planning stage. This portion of the project is scheduled to be complete by September 1995.

Laboratory experiments have been completed to characterize the behavior of NPE's with three different pulps using different chelants at different pH's. Experiments on the impact of primary and secondary fines on NPE behavior have been completed. Initial experiments exploring the effects of dissolved organics on NPE behavior has been completed. Analysis of samples from these experiments is in progress.

A functional specification has been completed for the development of a NPE equilibrium module (version 1.0) which will run in the WinMAPPS/WinGEMS environment. Programming of the module will be by a third party contractor.

Electro-Membrane Processing:

Subtask Objective:

This is the first report on this new subtask, after the recovery PAC approved the subtask in Fall 1994. A pilot-scale electrodialysis unit was acquired and delivered to IPST in November 1994. Membranes for the separation of chloride from sulfate ions are available in February 1995. The experimental unit will be operational in April, 1995. One Ph.D. student is taking up work in electrodialysis for closed white water systems.

Fundamentals of Dregs Removal:

Based on the recommendation of the Recovery PAC in November, 1994, a proposal was developed for a dregs study. This included the following. A laboratory study starting with a known synthetic smelt composition (including dregs), and adding a fixed amount of specified non-process element chemicals. These will be heated to typical smelt bed temperatures and held in a nitrogen atmosphere for a period of time to allow the chemicals to equilibrate. The cooled reaction products will then be added to hot water to form a synthetic green liquor. The insolubles will be filtered out and washed with hot water. These washed insolubles represent the dregs for the simulated process and will be sampled for chemical analysis. The remainder will be contacted with room temperature water and settling rates determined. Comparisons can then be made with the base conditions of synthetic smelt treated at the same conditions with no NPE's added.

The procedure will be repeated starting with kraft smelt obtained from an operating pulp mill.

Combustion Effects of Filtrate Recycle:

The objective of this subtask is to determine the effects on black liquor combustion that occur as mills increase degree of filtrate recycle and employ newer pulping and bleaching technology.

Limited contract testing has been completed. Proposals for external funding have been prepared.

Current Problems in Mill Closure:

It is important to be aware of actual problems that occur on mill closure. Both literature and direct mill visitation are needed. A report issued to members on status of closed mill technology. A series of mill visits have been initiated to develop a direct, updated knowledge of problems now being encountered as mill increase filtrate recycle and

reduce fresh water usage.

TENTATIVE GOALS FOR 1995-1996:

1. Impact and control of NPE's (Bryant):

   · Develop a scientific understanding of the material balance and the partitioning of non-process elements (NPE) in pulp and paper mill process streams.

   · Provide member companies with mathematical models which predict the behavior of NPE's in pulp and paper mills with different process configurations and operating conditions.

   · Determine the impact of NPE's on mill operations.

   · Initiate development work on NPE control techniques.

2. Electro-membrane Processing (Pfromm):

   · Complete experimental set up for evaluation of membrane separation technologies.

   · Evaluate electrodialysis for removal of chloride from the recovery cycle, and for removal of other inorganic non-process elements from the pulping and bleaching operations. Determine technical and economical feasibility.

3. Fundamentals of Dregs Removal (Empie):

   · Complete experimental set up for laboratory evaluation of dregs separation.

   · Evaluate effects of NPE buildup on dregs separation.

4. Combustion Effects of Filtrate Recycle (Zhu):

   · Develop proposal for work in area.

   · Determine effect of the following on black liquor combustion: extended delignification, oxygen bleaching, ozone bleaching, 100% D_O recycle.

5. Current Problems in Mill Closure (Adams):

   · Write membership report on current mill problems based on direct mill visits.

RECOVERY OPERATIONS IN LOW EFFLUENT MILLS PROJECT F017

SUBTASK: CHLORIDE PURGE FROM KRAFT RECOVERY CYCLE USING ELECTRODIALYSIS

ANNUAL PROGRAM REVIEW

March 23, 1995

Peter Pfromm
Jeff Empie

Institute of Paper Science and Technology
500 10th Street, N.W.
Atlanta, GA 30318
(404) 853-9500

ANNUAL PROGRAM REVIEW

Closed Mill Operations
F017

Subtask: Chloride Purge From Kraft Recovery Cycle Using Electrodialysis

Division: Chemical and Biological Sciences

Project Staff: P.Pfromm, J.Empie

GOAL:

Facilitate mill closure by developing an environmentally acceptable process step for removing chloride from the kraft liquor cycle so that concentration levels in the process streams can be controlled within acceptable limits.

RATIONALE:

Today there is a strong push from the environmental sector to close up our pulp and paper mills, minimizing emissions of liquid, solid, and gaseous pollutants. At the same time, a related problem emerges in the form of non-process elements (NPE's) building up in the liquor streams because opportunities for purge are diminished while input sources remain fixed. Mass balance considerations dictate that concentrations of these unwanted NPE's in process liquor streams must increase.

Serious consequences of increased mill closure are felt throughout the pulping/recovery cycle of both kraft and soda mills. Unwanted silica and alumina compounds, chlorides, and various metal salts cause operating problems in excessive scale formation on metal surfaces, high corrosion rates, and reduced concentrations of active pulping chemicals in the white liquor. The latter factor can lower pulp production rate below nameplate capacity, as well as require more energy to produce a pound of product.

New process technology needs to be developed to address these problems, while maintaining or improving the discharge of unwanted waste materials. The field of electrochemistry has been briefly examined in the past and discarded as unworkable or impractical for recovery and recycle of active pulping chemicals. With the rapid development of membrane technology over the past decade, the field of

electrodialysis has merged the two technologies and shown some unique capabilities to carry out chemical reactions and physical separations not before possible on a commercial scale.

OBJECTIVE:

This project will examine the technical and economic feasibility of applying electrodialysis as a way to purge chloride from the liquor cycle.

APPROACH:

The specific stream to be treated is the electrostatic precipitator (ESP) catch. This particular flow is attractive because the chemical composition is mostly Na_2SO_4, with minor amounts of NaCl and Na_2CO_3. Put in solution, this mixture of chemicals could be treated by electrodialysis using a commercially available anion permeable membrane to separate chloride from the bi-valent sulfate and carbonate. The amount of chloride that is removable is about what is needed to successfully operate a closed mill with acceptable levels of chloride in pulp mill liquor streams.

The other possibility for treatment is the clarified green liquor stream; however, this contains a substantial amount of NaOH also in solution, and the proposed electrodialysis scheme would remove hydroxide anion along with the chloride. This fact, along with the very large flow rate of green liquor that would have to be treated, eliminates this as a possible option.

At some kraft mills, it is common practice to discard some of the ESP catch to purge NaCl from the liquor cycle (or to control sulfidity). In addition to environmental concerns, this method purges sodium from the liquor cycle, increasing make-up chemical costs.

There are several competing purge technologies published in the literature, none of which have been commercial successes. A leaching system was tried by MacMillan Bloedel, but was abandoned because of high maintenance costs brought about by severe corrosion along with other operating problems. White liquor evaporation was practiced in the closed cycle mill at Great Lakes Forest Products Ltd. where again corrosion was significant. The need for exotic metallurgy translated into a high capital cost, contributing to discontinued use of the technology.

Ahlstrom has tried to market a green liquor crystallization process for chloride control, but without success. It too suffers from high capital cost and complex operation. Recently, Champion International has published information on a chloride purge process based on fractional recrystallization of the ESP catch. There is little data on which to evaluate it, but it too appears to be characterized by high capital and cumbersome operation.

BENEFITS:

The results of the proposed work will not only establish technical feasibility, but also generate the necessary technical data to carry out a preliminary cost estimate. This can be compared with the leaching and recrystallization alternatives for the ESP catch already published in the literature.

Longer term, successful development of this technology will insure that mills can operate within the degree of closure mandated by the U.S. Government and satisfy compliance regulations.

TASKS:

1. Technical Feasbility (5/95)

   - Set up laboratory electrodialysis cell and acquire candidate membranes
   - Using purchased chemicals, determine separability of chloride from sulfate and carbonate, all in solution.

2. Performance Characteristics (9/95)

   - Measure the rate and degree of separation of chloride as a function of cell operating parameters, including membrane type, cell spacing, fluid flow rate, voltage supplied, etc.
   - Determine current needs and operating efficiencies.

3. Economic Feasibility (11/95)

   - Complete preliminary cost estimate of ED process for chloride removal from ESP catch
   - Conduct cost comparison with other commercially available systems

4. Proposal for Further Development (12/95)

   - If warranted, write proposal for further development and commercialization of ED process concept.

RECOVERY OPERATIONS IN LOW EFFLUENT MILLS
PROJECT F017

SUBTASK: FUNDAMENTALS OF DREGS REMOVAL

ANNUAL PROGRAM REVIEW

March 23, 1995

Jeff Empie

Institute of Paper Science and Technology
500 10th Street, N.W.
Atlanta, GA 30318
(404) 853-9500

ANNUAL PROGRAM REVIEW

Closed Mill Operations
F017

Subtask: FUNDAMENTALS OF DREGS REMOVAL

Division: Chemical and Biological Sciences

Project Staff: J.Empie

IPST GOAL:

Improve dregs separation from green liquor in support of facilitating closed-mill operations.

OBJECTIVE:

Determine the effect of elevated levels of non-process elements (NPE's) on the composition and settling rate of green liquor dregs.

RATIONALE:

For kraft pulping the elements Na and S are the principal process elements. The non-process elements include Cl, Al, Si, K, Fe, Cu, Mn, Mg, P, and V. These enter the pulping process with the wood, water, other processing chemicals, and make-up chemicals. They can increase in concentration unless purge mechanisms are provided; presently, these purges are mill solid, liquid, and gaseous effluent streams. Tighter "mill closure" implies a reduction in these effluent discharges in order to decrease both water use and the environmental impact of the pulp manufacturing process.

Although the NPE's tend to be present in low levels, they may have a disproportionate effect on the operation of the mill. Some NPE's (viz. Al, Fe, Mg) are sparingly soluble in green liquor, but more soluble in white liquor. If they are not removed with the dregs, they can carry through to the digester and subsequently cause fouling in the evaporators. Aluminum can trigger evaporator scaling when its concentration exceeds 50-100 mg/L in the white liquor. Aluminum can be precipitated from green liquor by the addition of magnesium to form hydrotalcite. Since there is some Mg naturally in the liquor cycle, entering with bleach plant

effluent and make-up lime, some Al is being removed by this mechanism in present mill caustic plants.

Magnesium causes problems when it is allowed to accumulate in the lime mud because it calcines in the lime kiln, consuming fuel. The magnesium hydrates in the slaker, but it has no causticizing power, making it a heat consuming dead load. Magnesium also causes serious problems in the settling and filtration of lime mud. The finely divided particles of magnesium hydroxide in the dregs cause poor settling rates and a tendancy to plug filter cakes. Therefore, it is important to minimize Mg input and control its build-up throughout the caustic plant.

Fe, Cu, and Mn are other trace elements which can cause problems. The only outlet for these elements is the dregs system. Iron build-up is believed to be the cause of dusting from the lime kiln. The concentration of manganese in the lime cycle is quite low because green liquor clarification is effective in removing Mn.

Some NPE's (viz. Si, P) are soluble in green liquor, but less so in white liquor. Hence, if these are not removed from the green liquor, they can accumulate in the lime mud circuit, lowering lime availability and increasing kiln fuel cost. In the presence of lime, phosphorous is precipitated as apatite, $Ca_5OH(PO_4)_3$. In the lime kiln, apatite converts to calcium phosphate, $Ca(PO_4)_2$. Some, but probably not all, of the calcium phosphate converts back to apatite in the causticizing process. P does not precipitate in the green liquor circuit, even when lime is added as a settling or filtration aid. Therefore, its build-up can only be controlled by a purge of lime mud, which is best done at the dregs filter. The recommended bleed is in line with the amount of mud precoat required for optimum operation of the dregs filter.

It is evident that one of the key unit operations in the liquor cycle for controlling NPE build-up is dregs removal. A reduction in the purge rate of green liquor dregs will increase the levels of Mg and Mn in the lime cycle and increase the levels of Al, Fe, and Si in both the liquor and lime cycles. Hence, a detailed study of the effect of increased levels of NPE's on dregs removal, and therefore purge of NPE's, is crucial.

One other NPE that needs to be addressed is chloride. Its removal is difficult because it is soluble and remains with the aqueous liquor streams. Three methods have been practiced commercially in recent years. In the recovery boiler flue gas, SO_2 can react with NaCl, H_2O, and O_2 to form Na_2SO_4 and HCl gas. The HCl can be either scrubbed out of the flue gas by known methods or allowed to escape to the atmosphere. An alternative method for chloride removal is to purge NaCl by leaching precipitator dust. This method has been developed by Champion International, however it appears cumbersome and expensive. Chloride can also be removed by white liquor evaporation-crystallization. This was practiced as part of the closed mill operation at Thunder Bay, Ontario. It has since been discontinued.

PLANNED ACTIVITY THROUGH FY 96:

We propose a laboratory study starting with a known, synthetic smelt composition (including dregs), and adding a fixed amount of specified non-process element chemicals. These will be heated to typical smelt bed temperatures and held in a nitrogen atmosphere for a period of time to allow the chemicals to equilibrate. The cooled reaction products will then be added to hot water to form a synthetic green liquor. The insolubles will be filtered out and washed with hot water.

These washed insolubles represent the dregs for the simulated process and will be sampled for chemical analysis. The remainder will be contacted with room temperature water and settling rates determined. Comparisons can then be made with the base condition of synthetic smelt treated at the same conditions with no NPE's added.

The procedure will then be repeated starting with kraft smelt obtained from an operating pulp mill.

MILESTONES:

1. Base Case (no NPE's added)

A synthetic smelt will be made using purchased chemicals and equilibrated at 850°C under N_2 for 60 minutes. The equilibrated smelt is then cooled, crushed, and dissolved in 90°C water. Filtration at 90°C, followed by washing of the insolubles (dregs) at 75°C, and settling rate determination at 25°C will be carried out. Chemical analyses of the green liquors and dregs will be obtained.

The synthetic smelt will consist of 98% soluble salts (Na_2CO_3, Na_2S, Na_2SO_4, and NaCl) and 2% simulated dregs ($CaCO_3$, Fe_2O_3, $Mg(OH)_2$, MnO_2, SiO_2, Al_2O_3, and C). Relative amounts of chemicals will mirror typical kraft smelts.

2. Non-Process Element Buildup (NPE's added)

The above procedure will be repeated with NPE's added at four different concentration levels to give an indication of solubility effects. The cations to be included are: Al, Si, Fe, Cu, Mn, Mg, K, P, and V. The corresponding anions will include sulfate, carbonate, hydroxide, and oxide.

3. Kraft Smelt

Steps 1 and 2 above will be repeated using actual kraft smelt instead of purchased chemicals.

RECOVERY OPERATIONS IN LOW EFFLUENT MILLS PROJECT F017

SUBTASK: IMPACT ON RECOVERY OF PULPING AND BLEACHING CHANGES TO MEET THE EPA CLUSTER RULE

ANNUAL PROGRAM REVIEW

March 23, 1995

Terry Adams

Institute of Paper Science and Technology
500 10th Street, N.W.
Atlanta, GA 30318
(404) 853-9500

IMPACT ON RECOVERY OF PULPING AND BLEACHING CHANGES TO MEET THE EPA CLUSTER RULE

Terry N. Adams
Professor of Engineering
Institute of Paper Science and Technology
Atlanta GA 30318

ABSTRACT

The purpose of this paper is to estimate the impact of various pulping and bleaching changes on the recovery department. Changes in pulping parameters are shown to have substantial effect on the yield/kappa number relationship, but a rather smaller effect on recovery. Various modifications such as the use of high sulfidities, anthraquinone, and oxygen delignification are shown to impact the heating value and load on recovery by less than 5%. The impact of bleach plant filtrate recycle on chloride concentration in black liquor is also estimated.

INTRODUCTION

Recently the US Environmental Protection Agency proposed new regulations for the effluent and non-combustion-source air emissions from pulp and paper mills (1). These regulations are collectively referred to as the Cluster Rule. They extend previous effluent regulations to include new pollutant categories such as Absorbable Organic Halides (AOX), Chemical Oxygen Demand (COD), effluent color, and a suite of chlorinated organic compounds which can occur in bleach plant discharges. The conventional pollutants, Biological Oxygen Demand (BOD) and Suspended Solids (SS) are also covered by the Cluster Rule. The specific limits on these pollutants will not be finalized until the Cluster Rule is promulgated into law. Whatever the final limits are, they will be strict enough to ensure that changes in every aspect of mill operation will be required to reach compliance. Many of the changes will affect the recovery operation. It is the purpose of this paper to examine the impact of some of these changes on recovery operations.

The pollutant species regulated by the proposed Cluster Rule are all organic materials, AOX, color, COD, BOD, SS and chlorinated organics. Much of the compliance strategy involves routing more organic material through the recovery system for destruction in the recovery boiler rather than allowing them to be discharged with the mill effluent. In mills producing unbleached products, organic material reaches the effluent by means of black liquor spills, open screening operations, wet debarking, and discharges of white water from the pulp or board machine. In addition to these sources, mills producing bleached products also have the discharges from the bleach plant. Bleach plant discharges are a very major portion of organic material in mill effluent, and, for bleaching operations which are not Totally Chlorine Free (TCF), they are the only source of AOX.

It is useful to estimate the additional organic load on the recovery system if all the organic material not found in the pulp were to pass through recovery for destruction. Current pulping practice results in brownstock pulp with a yield of about 47% and a kappa number for softwood of about 30. This kappa number corresponds to a lignin content of about 4.5% on OD pulp, or about 21.1 kg per tonne of OD wood. The organic separated from the wood becomes the organic in black liquor. This is about 530 kg per tonne of OD wood. Comparing these two figures indicates that the additional load on the recovery boiler due to the need to destroy additional organic represents an incremental organic load of about 4%.

The first section of this paper presents the various means of diverting additional organic from the effluent to the recovery operation at various stages of the pulping and bleaching processes. The second section presents a set of simple models for pulping, bleaching, and black liquor heating value which can be used to estimate the impact on recovery operations of various process changes. The final section presents some model results for these impacts.

PULPING AND BLEACHING CHANGES TO REDUCE ORGANIC DISCHARGES

The purpose of Kraft pulping and bleaching is to separate the fiber in the wood (or other feedstock) from the lignin which holds the fibers together. Kraft pulping typically removes about 90% of the lignin, but also removes 50% of the hemicellulose and 20% of the cellulose. Most of this dissolved material ends up in the black liquor.

In the early bleaching stages, the process of lignin removal continues. The later bleaching stages modify the remaining lignin in the pulp to brighten the final product. Bleaching is much more specific in removing lignin and leaving the cellulose and hemicellulose than pulping. Because chlorine compounds have traditionally been used as bleaching agents, the organic materials removed during bleaching have not been routed through the recovery operation, but, rather, have been discharged from the mill.

Many of the schemes for reducing organic discharges from the mill involve recycling bleach plant filtrates back into the pulping and recovery departments. Many schemes retain chlorine compounds as bleaching agents, but significantly reduce the quantity of chlorine used by reducing the lignin content of the pulp entering the bleaching department. Bleach filtrate recycle may also be accomplished through the use of alternative bleaching agents such as oxygen, peroxide, and ozone which are more compatible with recovery.

Pulping Modifications

Conventional Kraft pulping can be carried out to remove a larger portion of the lignin, but this has the very negative economic impact of reducing the yield of pulp. All the modifications to conventional pulping attempt to reduce residual lignin in the pulp while avoiding or reducing yield loss. The three methods for doing this are: 1) adding chemicals such as anthraquinone (AQ) to the cook, 2) modifying the time-temperature profile or the time-chemical charge profile during the cook or, 3) adding a stage after cooking for delignification by reaction with oxygen.

The impact on the pulp yield and residual lignin for two of these, AQ and oxygen delignification, will be discussed below in the model presentation section. The third method is generally referred to as extended or modified cooking. There are equipment and procedures to take advantage of the improvements from this

type of pulping available from each vendor of both batch and continuous digesters. The overall impact of these cooking techniques will be similar to that of conventional cooking followed by oxygen delignification. Because this latter combination has been more thoroughly characterized, it will be investigated below for its impact on recovery.

All pulping and delignification stages are followed by washing stages. Pulp washing separates the organic that has been dissolved during pulping or delignification from the pulp. The final filtrate from these washing operations is the weak black liquor.

Pulp washing is not perfectly efficient at removing black liquor solids from the brownstock pulp. A small residual content of black liquor enters the bleach plant and is mostly removed there. In a mill producing unbleached products, this black liquor may find its way into the paper machine white water. The washing efficiency is often characterized by the sodium or equivalent saltcake (Na_2SO_4) lost with the washed brownstock pulp. This ranges from about 3 to 45 kg saltcake per tonne of pulp. These losses correspond to overall washing efficiency between 95.5% and 99.5%. Considering the estimate in the Introduction of 4% for the potential increase in total organics to recovery, it is clear that changes in washing efficiency of brownstock may be as significant as some of the other changes in pulping operations.

Bleaching Modifications

Pulp bleaching has gone through very rapid change in the past decade and this is certain to continue in the immediate future. The two principle chemicals used in conventional pulp bleaching are chlorine gas (Cl_2) and chlorine dioxide (ClO_2). Traditionally, Cl_2 has been used in the first stage of bleaching primarily for removal of lignin from the pulp. ClO_2 has been used in the later bleaching stages to chemically modify the remaining lignin in the pulp in order to brighten the final product. Using "C" to represent a Cl_2 stage, and "D" to represent a ClO_2 stage, and "E" to represent a caustic extraction stage used to remove dissolved lignin, a very conventional 5-stage bleaching sequence would be CEDED.

Many bleaching schemes have been proposed to replace conventional bleaching sequences. All of these schemes seek to eliminate elemental chlorine (Cl_2). Some schemes seek to eliminate all chlorine. The former is referred to as Elemental Chlorine Free (ECF), while the latter is Totally Chlorine Free (TCF).

Replacing some or all of the Cl_2 in the first bleaching stage with ClO_2 is called "substitution". Because ClO_2 has greater bleaching power than Cl_2 and contains less chlorine, substitution has a dramatic effect on both the total chloride in bleach plant filtrate and on the formation of chlorinated organic compounds. ClO_2 substitution also has impacts on the main function of the bleach plant, delignification and brightening, which are major considerations in its use. Only the aspects of substitution which might directly affect the recovery department will be addressed here. The chloride content of any bleach plant filtrate recycled to recovery would be the most significant impact.

Other bleaching schemes which use chemicals such as oxygen, peroxide, and ozone will not be directly addressed below. The relative magnitude of their impact will be similar to recycling bleach filtrates from ClO_2 bleaching, with the exception of the impact of chloride. The residual lignin content of the pulp entering the bleaching department determines the organic that can be removed during bleaching. The bleaching chemicals and sequence determines how degraded the organic material is, and the content of inorganic accompanying it. In general, chlorine bleaching degrades the lignin less than the oxygen-based compounds, so it represents a larger impact on recovery heat load and, of course, chloride load.

MODEL DESCRIPTION

Black Liquor Heating Value

The black liquor heating value model used here is a very modestly modified version of a robust model proposed by Green and Grace (2). Several models of black liquor heating value are available in the literature (3-4). These models all differ slightly in complexity and specific results. What was sought for the present application was a model which would correctly portray the levels and trends in the black liquor heating value for changes in pulp yield, residual lignin, pulping conditions, and pulp washing efficiency.

The Green and Grace(2) method has been modified here in four ways. The first modification involves the use of a pulping model (discussed below) to relate pulping conditions to pulping results. In the original model, the active alkali-to-wood ratio in the digester could be specified separately from the pulping yield. These two parameters are the most important in determining both the inorganic and the organic content of the black liquor. In practice, they are not independent. The AA-to-wood ratio has a major impact on pulp yield, as will be shown below.

The second modification involves the combination of two classes of black liquor organics into one class. The Green and Grace method recognizes 1) resins and fatty acids (RFA), 2) volatiles, 3) lignin (which is different for hardwood and softwood), 4) organic acids from carbohydrates (OAC), and 5) miscellaneous organic compounds (MOC). Each class of organic material has an assigned heating value. In the current use of the model, the RFA, volatiles, and lignin remain the same, but the OAC and MOC are combined into a category called "carbohydrates" and are given the heating value of the OAC. This change has very little impact on the calculated results. It does remove a category, MOC, which would be difficult to characterize for most woods. This change results in a breakdown of the components of wood into four categories: volatiles, extractives, lignin, and everything else. The breakdown of the components of wood and their assumed heating values are shown in TABLE 1.

TABLE 1 - Components of Wood Found in Black Liquor

	Hard-wood	Soft-wood	Hardwood MJ/kg (Btu/lb)	Softwood MJ/kg (Btu/lb)
Volatiles	1%	1%		
Extractives	3%	3%	37.72 (16,224)	37.72 (16,224)
Lignin	22%	27%	25.12 (10,805)	26.92 (11,578)
"Carbohydrates"	by diff.	by diff.	13.56 (5,832)	13.56 (5,832)

The "carbohydrates" content of black liquor is calculated in a manner similar to the Green and Grace method. The fraction of carbohydrates is 100% less the volatiles, extractives, yield, and the difference between the lignin in the wood and the lignin in the pulp. This breakdown of wood into four categories makes calculation of the hydrogen content of the organic easier, which is useful for the calculation of the Net Heating Value (NHV). The Higher Heating Value (HHV) includes an energy term due to oxidation of reduced sulfur in the black liquor, and a term for condensation of water formed from hydrogen in the black liquor during combustion. Neither of these terms is available during combustion of black liquor in a recovery boiler. The NHV is, therefore, a better measure of the actual heat load on the boiler. The hydrogen content assumed for each component of the black liquor is given in TABLE II.

TABLE II - Hydrogen Content of Wood Components

Component	Hydrogen
Extractives	12%
Lignin	6%
"Carbohydrates"	6.5%

The final modification to the original Green and Grace method is in the calculation of the white liquor density and percent solids. Here, these two are calculated from the specified Total Titratable Alkali (TTA), Active Alkali (AA), and sulfidity.

Pulping Model

The pulping model used here is one reported in a thesis by Saffran(6). The same model is reported incorrectly in reference (7). The values for all the coefficients used in the present work are given in the appendix to this paper. This model is based on multiple linear regression of the results of 115 pulping experiments. These experiments used southern yellow pine chips in laboratory batch pulping experiments covering the range of the parameters shown in TABLE III.

TABLE III- Parameter Range in Experiments Used as the Basis of the Pulping Model (6)

Parameter	Range
AQ	0-0.5% on wood
Effective alkali	14-23%
Sulfidity	11-55%
Liquor to wood ratio	2.4-6.8
Temperature	157-187°C (315-369°F)
H-factor	1100-3700

This model (6) has the advantages of algebraic correlations, which include all the important pulping variables, as well as the effects of anthraquinone on pulping. The trends predicted by this model compare favorably to those reported for other models (8, 9, 10) though exact comparison is not possible due to differences in wood species used as the basis for the model development. The specific results of the present work are restricted to batch digestion and southern yellow pine, though the general levels and trends reported here probably apply more widely.

The pulping model predicts five results for any given set of pulping conditions: 1) the total yield, 2) the screened yield, 3) the pulp kappa number, 4) the unbleached pulp viscosity and, 5) the residual effective alkali. Only the total yield and the kappa number are used in the present work. The actual yield of pulp going to the bleach plant is the screened yield. However, for the range of conditions used here, the screened yield and the total yield are almost identical.

The kappa number is a measure of the amount of lignin that remains in the pulp after pulping and washing. The relationship between kappa number and residual lignin is:

*Residual lignin = kappa number*0.15% on OD pulp* (1)

This means that for a conventional cook of a softwood to a kappa number of 30, the residual lignin in the pulp is 4.5% or 45 kg lignin/tonne pulp. For a hardwood cook, the typical kappa number is 20, making the residual lignin 30 kg/tonne. In both cases, the yield would be between 44% and 49% of the dry wood.

Yield and kappa number are the two key parameters in pulping as far as recovery and bleaching operations are concerned. The pulp quality, as measured by other properties such as pulp viscosity, is of major concern to the overall economic viability of the mill. Yield, however, is the key parameter determining the quality of organic matter in the black liquor, and kappa number determines the amount of lignin that must be removed or brightened in the bleach plant. A plot of yield versus kappa number of the pulp gives an easy comparison of the impact of different pulping variables, and the impact of some alternative schemes. The pulping model was used to generate the graphs in Figure 1. Shown in this figure is the yield/kappa number relationship obtained by varying one of the four variables at a time: sulfidity, H-factor, AA-to-wood, and AQ. The central value and the variable ranges are given in TABLE IV.

TABLE IV - Central Value and Range for the Four Pulping Variables in Figure 1.

Parameter	Low	Central	High
AQ	0%	0%	0.2%
AA/wood	12%	18%	24%
Sulfidity	20%	30%	40%
H-factor	800	1800	2400

The H-factor is a pulping variable which gives an integrated value of the time-temperature profile during cooking which reflects the kinetics of the pulping reactions.

Figure 1 shows the typical trade-off of yield and kappa number for sulfidity, H-factor, AQ, and AA-to-wood. The kappa number of the pulp leaving the pulping department can be lowered, but at the expense of the pulp yield. These plots are for a softwood (southern yellow pine) so the typical result might be something like the central values shown here, a yield of 47% for a kappa number of 30. For the AA-to-wood and H-factor curves, the yield drops to about 44% when a kappa number target of 20 is used. Only 1.5% additional lignin is removed, but the yield dropped by 3%. The curve for varying sulfidity is considerably flatter, and therefore better, than for the other two pulping variables, but very high sulfidities (above 35%) are required to obtain these results. The results with AQ are even better, but the cost and diminishing returns on the use of AQ have, so far, limited its use in North America. When reviewing these results, keep in mind that the

pulping experiments can be run at the conditions stated, and the yield and kappa number will be as shown, but not all of these conditions would produce high quality pulp, either for bleaching or ultimately for sale as a product.

O_2 Delignification Model

The chemical reactions in conventional pulping are not very lignin-specific. Continued pulping to lower kappa number with conventional pulping does not produce a quality product. One alternative is to continue delignification by reacting the washed pulp with oxygen in a separate stage. This process of oxygen delignification is well established technology (11). Within the range of normal practice, oxygen is very specific to lignin removal in either of two basic configurations: medium consistency or high consistence. Delignification by 50% can be achieved with little loss in pulp yield other than lignin loss. The reaction is carried out under alkaline condition using either caustic or oxidized white liquor. For the present work, oxidized white liquor is assumed. It was further assumed that 0.12% of both oxygen and caustic are consumed for each point reduction in pulp kappa number (11,12). The mass and species balance around the oxygen delignification process would be quite simple if it were not for the fact that oxygen reacts with lignin and reduces its heating value.

In the oxygen delignification model used here, the percent reduction in pulp kappa number is specified, so the caustic and oxygen consumption is known (0.12%*kappa number) and the lignin removed is also known (from the definition of kappa number, lignin = 0.15%*kappa number). The chemical oxygen demand (in combustion parlance, the stoichiometric oxygen-to-fuel ratio) is close to 1.5 kg O_2 per kg of lignin. This means that kappa number*0.15%*1.5 or kappa number*0.225% of oxygen would be required to completely oxidize the lignin removed during oxygen delignification. The value 0.12%*kappa number of oxygen supplied represents about 53% of the total COD. The heating value of the organic removed during oxygen delignification has been reduced in the model by this amount from the initial lignin heating value shown above in TABLE I. This allows both the quantity of material removed during O_2 delignification and the total heating value of this material to be calculated even though the organic/inorganic composition is not well known.

Figure 2 shows the result of using oxygen delignification on the pulp produced from the central point conditions shown in TABLE IV and Figure 1. For reference, the plot obtained with varying AA-to-wood ratio is also shown. Oxygen delignification produces a much flatter, and therefore better, trade-off of yield and kappa number than the harsher conditions of increased AA-to-wood. In addition, practical experience shows that delignification by 50% is currently possible with very modest impact on pulp quality. Many schemes to take advantage of this technology have been put forward (11,13).

Bleaching Model

Because the emphasis of the present work is on the impact on recovery operations rather than pulp quality, a very simple bleaching model is adequate. This model assumes that bleach plant filtrate recycle to recovery would consist of all remaining lignin in the pulp after post-oxygen washing, all chlorine added in the first bleaching stage, and all caustic used in the first extraction stage. This model ignores all chlorine compounds added to the later bleaching stages, and any additional caustic in later extraction stages. It does, however, account for all organic material that could be dissolved during bleaching.

The amount of chemical applied to the first bleaching stage is usually specified in terms of the Kappa Factor (KF) or Active

Figure 1—Impact of pulping variables on the yield and kappa number relationship.

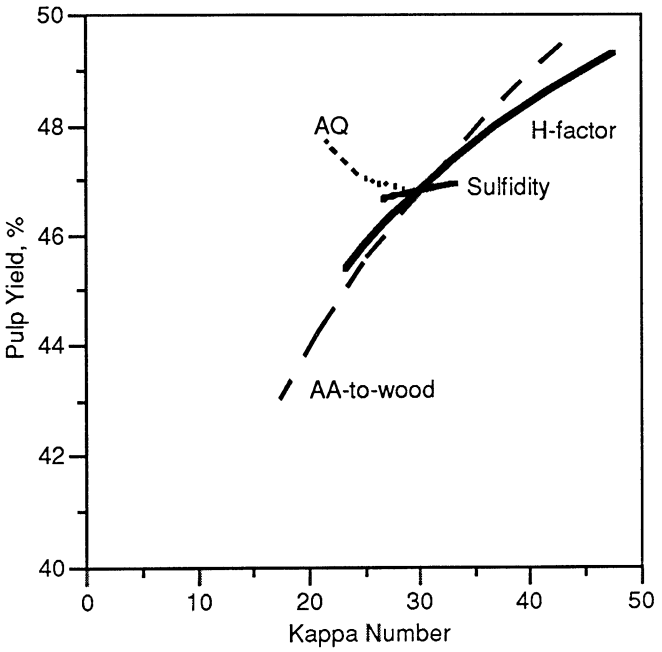

Figure 2—Impact of oxygen delignification on the yield and kappa number relationship.

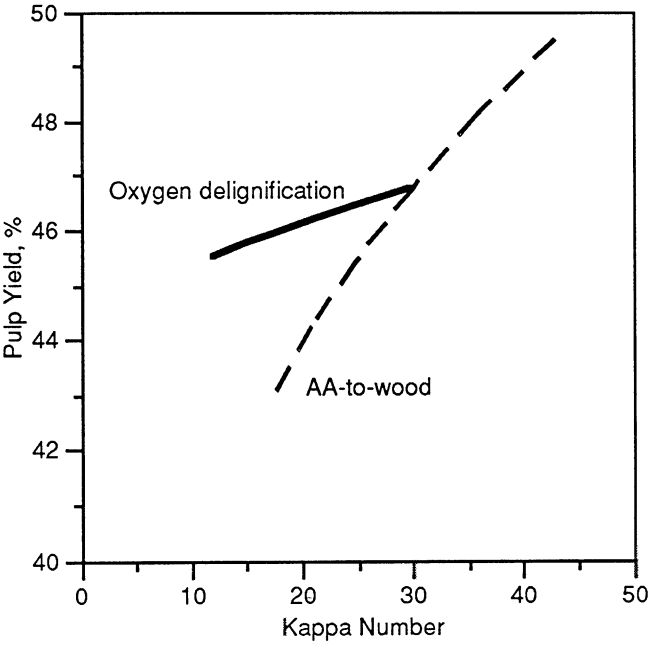

Chlorine Multiple. This is the amount of equivalent chlorine applied per unit of kappa number in the unbleached pulp. A typical value of the kappa factor would be 0.2% on pulp. This kappa factor means that for a pulp kappa number of 30, about 6% Cl_2 on pulp or 60 kg Cl_2 per tonne of pulp would be charged in the first stage. About 10% of this would form AOX in the bleach plant discharge, or 6 kg/tonne pulp (14). This is quite a high value compared to the proposed Cluster Rule limit for AOX of 0.156 kg/tonne in the effluent. Clearly much lower unbleached kappa numbers and kappa factors would be needed to reduce AOX to the proposed levels.

Fortunately, chlorine dioxide has proven to be a good substitute for chlorine. The equivalent bleaching power of ClO_2 is 2.63 times that of Cl_2 , and the chlorine in ClO_2 is only 52.6%. This means that the same bleaching potential can be obtained from ClO_2 with only 20% of the atomic chlorine. The percent ClO_2 substitution is based on equivalent bleaching power so:

$$Equivalent\ chlorine = (kappa\ number)*(kappa\ factor) \quad (2)$$

$$Equivalent\ chlorine = Cl_2 + 2.63*ClO_2 \quad (3)$$

$$Substitution = \frac{2.63 * ClO_2}{Cl_2 + 2.63 * ClO_2} \quad (4)$$

The atomic chlorine in the bleach plant discharge from the first stage is:

$$Atomic\ chlorine = Cl_2 + 0.526*ClO_2 \quad (5)$$

where both Cl_2 and ClO_2 are in kg per tonne of pulp.

MODEL RESULTS

The models of pulping, O_2 delignification, bleaching, and black liquor heating value have been combined and exercised over a range of conditions. The purpose of this effort is to assess the impact on recovery operations of conventional pulping, pulping modifications, and bleach plant filtrate recycle.

Figure 3 shows the impact of white liquor sulfidity on total black liquor solids to recovery. It also shows the HHV and NHV of the black liquor for conventional pulping condition without O_2 delignification or bleach plant filtrate recycle. Higher sulfidity increases both the black liquor solids to the boiler per tonne of pulp and the HHV. However, the NHV is nearly unaffected by the sulfidity level. From the midpoint value of 30% sulfidity, the flow of black liquor solids changes by only $\pm$ 0.3 %, the HHV by $\pm$2.4%, and the NHV by only $\pm$ 0.2 %. This result is not surprising considering the pulping results shown in Figure 1. The change in pulp yield with increased sulfidity is less than the loss of lignin from the brownstock pulp. For the range of sulfidities from 20% to 40%, the predicted kappa number decreases from 33 to 27, a drop of 0.9% in residual lignin. For the same range, the yield decreases by only 0.4%, indicating that more cellulose remains in the pulp at higher sulfidities.

The change in black liquor solids per tonne of pulp along with HHV and NHV is shown in Figure 4 as a function of AA-to- wood ratio. Here, both the HHV and NHV decrease while the black liquor solids per tonne of pulp increases, all due to the increased inorganic load at higher AA-to-wood ratios. The actual heat load

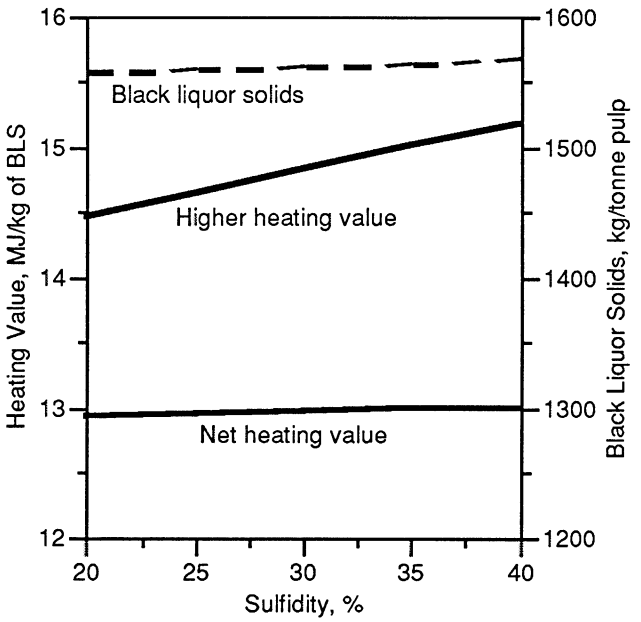

Figure 3—Impact of sulfidity on black liquor heating value and solids to recovery.

on the boiler is the product of the black liquor solids per tonne times the NHV. This increases by 13% as AA-to-wood is increased from 15% to 20%, mostly due to a predicted decrease in yield from 48.2% to 45%. This increase is also partly due to a decrease in pulp kappa number from 34.9 to 22.3. Both decreased yield and decreased kappa number send more organics to recovery.

Figure 5 shows the impact of anthraquinone used in pulping on recovery operation. The HHV and NHV of the black liquor are almost unchanged, but the BL solids per tonne decreases by 2.5%. Figure 1 shows the reasons for this. With AQ addition, the yield goes up while the kappa number goes down. This means that less cellulose and hemicellulose are removed while more lignin is removed. The net quantity of organic material in the black liquor is less, but the carbohydrates with lower heating values are replaced with lignin fragments with greater heating value. The overall result is very little impact on HHV and NHV. The total heat load on the recovery boiler decreases by 1.7% with addition 0.2% AQ on wood according to the model.

Figure 6 shows the impact of adding an O_2 delignification stage after conventional pulping to a 30 kappa number. Figure 6 also gives an indication of the impact of pulp washing changes. The first two points on the black liquor solids curve at 0% kappa number reduction with O_2 delignification are for two different levels of washing. The lower point is for washing to a saltcake loss of 20 kg/tonne of unbleached pulp. The upper one is for 2 kg saltcake loss per tonne of unbleached pulp. This change would be due solely to adding an additional washing stage after normal brownstock washing. The remaining part of this curve shows changes due to oxygen delignification. More inorganic and organic material goes into the black liquor. However, because the organic is partially oxidized during O_2 delignification, the heating value of the additional organic is low. Looking only at the O_2 stage, the increase in black liquor solids is 4%, while the com-

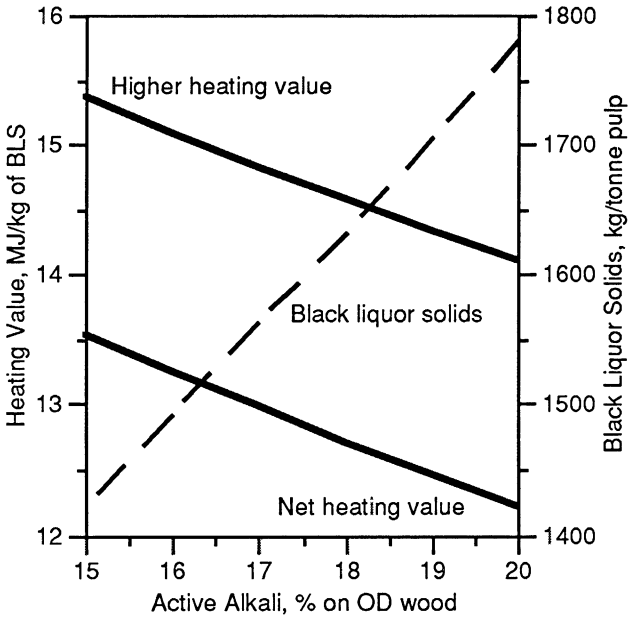

Figure 4—Impact of active alkali charge on black liquor heating value and solids to recovery.

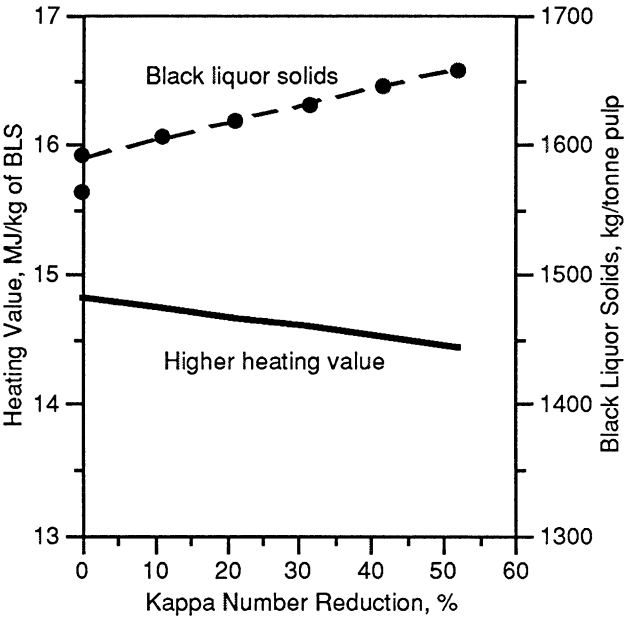

Figure 6—Impact of oxygen delignification on black liquor heating value and solids to recovery.

bined black liquor heating value decreases by 2.6%. Note that for the washing conditions selected, the change in solids due to washing is 1.8%, almost the same magnitude as O_2 delignification.

Figure 7 shows one aspect of recycling bleach plant filtrate to the recovery department. This effect would be the same whether the recycle of filtrate were by means of countercurrent brownstock washing or direct recycle of concentrated bleach filtrate to weak black liquor. Recycling would bring organics, inorganics, and particularly chlorine into the black liquor. Starting with a conventional cook to kappa number 30, followed by O_2 delignification to kappa number of 15, the additional heat load brought back to recovery by bleach plant recycle would be about 2.8%. The increased black liquor solids per tonne would be about 4.4%. Figure 7 addresses the issue of increased chloride level in the black liquor. Decreased kappa factor and increased ClO_2 substitution both help reduce this load, but it is still very high. For the incoming kappa number of 15, a kappa factor of 0.2%, and 100% substitution, about 6 kg Cl/tonne is brought into recovery.

Figure 5—Impact of anthraquinone on black liquor heating value and solids to recovery.

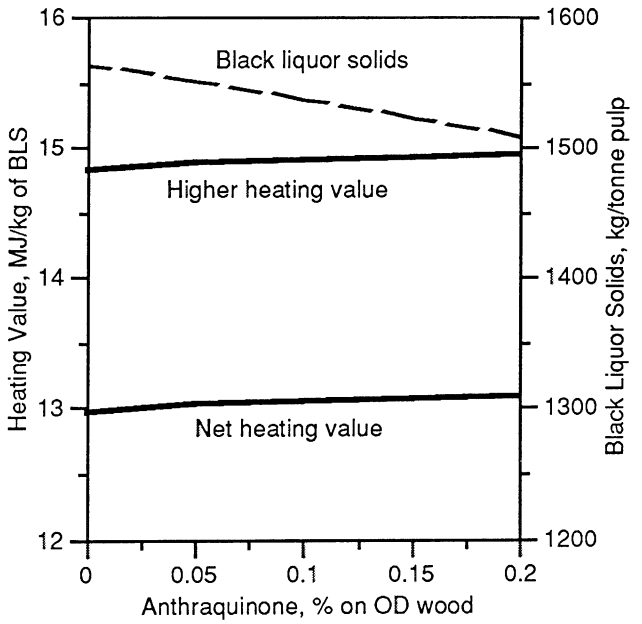

Purging some of the increased chloride load with recovery boiler precipitator dust is possible. However, assuming the typical conditions listed in TABLE V for the recovery boiler, only about 2.5 kg Cl/tonne could be purged in this way. Comparing this to the potential input of Cl from bleach filtrate recycle shows that lower inlet kappa numbers and lower kappa factors would be required to make the Cl input small enough to be purged with precipitator dust.

TABLE V - Parameters in Calculation of Cl Removal from Precipitator Dust.

PARAMETER	TYPICAL	RANGE
Black liquor solids	1600 kg/odt pulp	1400-1800
Sodium in BLS	19%	18-20
Na volatilized to fume/dust in RB	10% of Na in BLS	8-12
Total Na makeup to mill	10 kg/odt pulp	5-20
Cl/Na in BLS	3%	1-35
HCl loss	5% of Cl in BLS	0-25
Cl in BLS	0.6% of BLS	0.2-7
Cl/Na enrichment in fume/dust	2.5 x Cl/Na in BLS	2-3

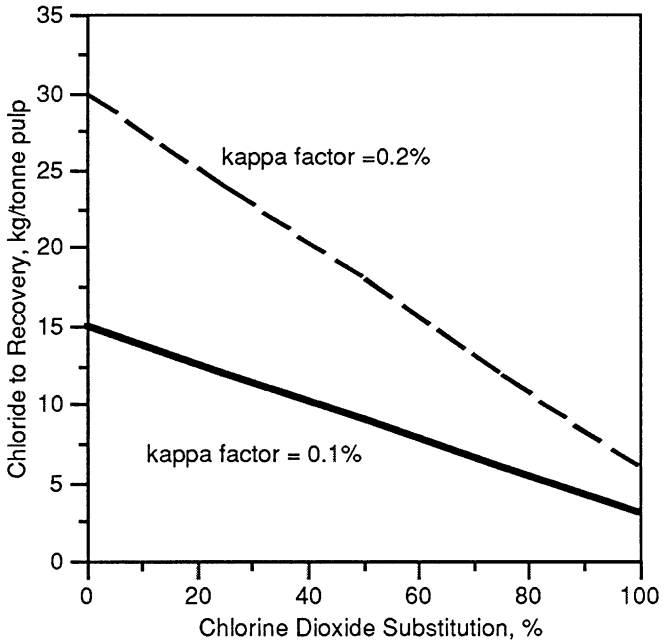

Figure 7—Impact of ClO_2 substitution on chloride to recovery with bleach plant filtrate recycle.

CONCLUSIONS

Models for pulping, oxygen delignification, bleaching, and black liquor heating value, have been brought together to investigate the impact on recovery of various operating strategies. The main focus of the work is on those operating strategies adopted to reduce the discharge of organic materials with the mill effluent. Two of the models used, pulping and black liquor heating value, were taken from the literature with only minor modification. The other two models are fairly simple material and species balances. All the models were selected or developed specifically to address issues of recovery impact, so they have limited value in assessing other aspects of modified operating strategies.

The overall conclusion from this work is that the changes in both heating value and black liquor solids flow per tonne of pulp are relatively modest for the strategies investigated. The strategies were conventional pulping changes, oxygen delignification (with changes in pulp washing efficiency), and bleach plant filtrate recycle. The impact on recovery of any single change is less than 5%. This is in the range of incremental recovery capacity. Where this is definitely not the case is the increase in chloride input with recycle of the filtrate from the first two stages of bleaching. Recycle of this material could increase chloride input to recovery by a factor of 8, even with a kappa number of 15 entering bleaching, and 100% substitution of ClO_2 for Cl_2.

REFERENCES

1. Environmental Protection Agency, 40 CFR parts 63 and 430, Effluent Limitations Guidelines, proposed rule, Federal Register 58 (241), Dec. 17, 1993.
2. GREEN, R. P. AND GRACE, T. M., "A Method for Calculating the Composition and Heating Value of Black Liquors from Kraft and Polysulfide Pulping," *Tappi J.*, 67 (6): 94 (June 1984).
3. ANNERGREN, G. E., HAGLUND, A., AND RYDHOLM, S. A., "On the Composition and Fuel value of Black Liquor," *Svensk Papperstid*, 71: 497 (1968).
4. GULLICHSEN, J., "Heat Values of Pulping Spent Liquors," Sym. on Rec. of Pulping Chems., IUPAC-EUCEPA, Helsinki, Finland: 211 (1968).
5. MCDONALD, K. L., "Calorific Value of Spent Liquors by Carbon Analysis," *Tappi J.*, 60 (12): 107 (1977).
6. SAFFRAN, K. E., "The Development of a Simulation-Optimization Program for the Pulp and Paper Industry," Ph.D. thesis, IPC, Appleton, WI, (1984).
7. "Alkaline Pulping," Pulp and Paper Manufacture, Vol. 5, M. J. Kocurek editor, TPAAI/CPPA Joint Textbook Committee of the Paper Industry: 71 (1989).
8. HATTON, J. V., "Development of Yield Prediction Equations in Kraft Pulping," *Tappi J.*, 56 (7): 97 (1973).
9. TASMAN, J. E., in ref. 7 above., p 71.
10. AGARWAL, N. AND GUSTAFSON, R., "On the Modelling of Kraft Pulping," TAPPI Pulping Conf., 1073 (1993).
11. TAPPI Intl. Oxygen Delignification Conf., San Diego, CA, (June 1987).
12. MCDONOUGH, T. J., "Oxygen Delignification," TAPPI *Bleach Plant Operations Shortcourse*, (1992).
13. SAMUELSON, O. AND OJTEG, U., "NO_2 Treatment of Pulp Followed by Oxygen Bleaching," *Tappi J.*, 73 (2): 141 (1990).
14. MCDONOUGH, T. J. AND COURCHENE, C. E., "Regression Models to Predict Levels of AOX Generation," IPST, (June 1993).

APPENDIX
PULPING EQUATIONS USED IN MODEL(6)

Pulping Variables	Typical Values
AQ = anthraquinone, % on od wood	0.1%
TEMP = temperature, °C	170°C
EA = effective alkali, %	15%
SULF = sulfidity, %	30%
LW = liquor-to-wood ratio	4
HF = H-factor	1800

Dummy variables	Typical Values
A = AQ	0.1
As = SQRT(AQ)	0.316
T = TEMP/1000	0.17
E = EA/100	0.15
S = SULF/100	0.3
L = LW/10	0.4
H = HF/10000	0.18

Pulping Equations

$$Log(total\ yield) = \sum_i a_i * x_i$$

$$Log(kappa\ number) = \sum_i b_i * x_i$$

Equation Constants

x_i	a_i	b_i
constant	1.561	1.12
A	0.0502	
As	0.3529	0.273
T	2.02	7.481
E	0.773	–4.572
S	–0.133	–1.348
L	–0.434	2.282
H	0.141	0.2182
As*T	–1.812	–6.588
As*L	–0.136	
T*E	–10.87	
T*L	2.085	
T*H	–3.758	–20.23
E*L	1.046	
S*H	0.3111	
As*E		1.773
As*S		0.9294
As*L		–0.6266
As*H		1.169
S*S		1.059
S*L		–1.578
S*H		2.134
L*H		–4.241
H*H	0.4479	5.574

BLACK LIQUOR GASIFICATION - Hot Gas Clean-up

ANNUAL PROGRAM REVIEW

March 23, 1995

Junyong Zhu

Institute of Paper Science and Technology
500 10th Street, N.W.
Atlanta, GA 30318
(404) 853-9500

ANNUAL PROGRAM REVIEW

Proposed New Project

Title: Black Liquor Gasification

Division: Chemical and Biological Sciences

Project Staff: Junyong Zhu

IPST GOAL:

The goal of the project is to provide a thorough review on the available hot gas clean-up technologies and research needs in hot gas clean-up for integrated black liquor gasification combined cycle applications.

OBJECTIVE:

The objectives of the program are to: (1) describe the problems of hot gas clean-up for integrated black liquor gasification combined cycle applications, (2) provide a thorough review of available technologies for hot gas clean-up and future research needs, (3) give hot-gas clean up technological and economical recommendations for black liquor gasification applications, and (4) provide operational principles of the recommended technologies.

SUMMARY OF RESULTS:

This project is initiated under the recommendation of the Chemical Recovery PAC during the last meeting. It is a new project and started fall, 1994. Due to the nature of the project, it is anticipated that no external funding will be available to this project. No technician and students are working on the project.

The emphasis of the work since the initiation of the project has been the following: understand the hot gas clean-up needs for integrated black liquor gasification combined cycle applications, collect previous work in the literature, and study various available technologies and their applicabilities.

This is a short term project. However, it can provide useful information and guidance to the industry in selecting new technologies for future chemical recovery operations. It will also give the industry a picture of future chemical recovery operation processes from a different perspective.

STATUS REPORT

Hot Gas Clean-Up for Black Liquor Gasification:

A Brief Review of Available Technologies

JunYong Zhu
Institute of Paper Science and Technology
500 10th Street, NW
Atlanta, GA 30318

Introduction

This status report contains three parts: Background, hot gas clean-up, and hot gas clean-up Technologies. The final report which is due at the next PAC meeting will contain the recommended technologies for hot gas clean-up for integrated black liquor gasification combined cycle, economical analysis of the recommended technologies, future research needs in the subject, and new research proposals on the subject.

Background

Electric power production from black liquor with the integrated gasification combined cycle (IGCC) has attracted great interest recently in the pulp and paper industry due to its high energy efficiency. The IGCC process is based on black liquor gasification technology, the product fuel gas is combusted in a gas turbine to generate power. With an IGCC process, the power to steam ratio could be improved by a factor of 2.5 over the steam cycle cogeneration which is currently used in the industry (Fogelholm and McKeough, 1991). Currently, black liquor gasification technology can be divided into two major categories: partial spray combustion technology (Bostrom and Hillstrom, 1992; Stigsson, 1994) and fluidized bed combustion (Durai-Swami et al., 1989; Salmenoja et al., 1993). No matter how the two technologies are going to emerge in the near future, hot gas clean-up will be an essential factor to the success of black liquor gasification with Integrated Gasification Combined Cycle (IGCC). Therefore, understanding the problems in hot gas clean-up and available technologies is important for the pulp and paper industry to make full use of available resources.

This study presents a brief review on the following issues associated with hot gas clean-up for black liquor gasification: (1) What are the problems of hot gas utilization from black liquor gasification? (2) What are the available technologies for dealing with these problems? How do they work? and What are the costs? and (3) What are the future research needs in hot gas clean-up for black liquor gasification?

Hot Gas Clean-Up

Black liquor gasification is a partial oxidation process. The product gas contains these major species: N_2, H_2, CO, CO_2, H_2S, CH_4, and some minor species, such as NH_3, HCN, and vaporized sodium and potassium salts. It also contains entrained particulate, such as fume particles (alkali salts) formed by condensation, char particles, and aerosols. Both CO_2 and H_2S are considered as acid gases because they can form acid when dissolved in water. For integrated gasification combined cycle application, high content of CO_2 lows the heating value of the fuel gas. H_2S is potentially harmful to the environment and turbomachinery through catalyst poisoning and corrosion, respectively. The particulate can be deposited to turbine blades causing corrosion and reducing turbine efficiency. In particular, the alkali salts can accelerate hot corrosion when reacting with other species and worsen deposition through acting as a cement under high turbine temperatures for deposited particles. Thermodynamic calculation (Salmenoja, et al., 1993) and pilot scale testing (Stigsson, 1994) indicated that most of the sulphur was converted into H_2S except the small quantities of sulphate and sulphur bonded in the carbon residue during a black liquor gasification process. H_2S concentration in black liquor gasification product gas is about 1000 ppm and CO_2 concentration is about 10 -15 % by volume when a gasifier is operated at 850 ^{o}C (Salmenoja, et al., 1993). H_2S concentration can increase up to 0.7% when the gasifier temperature is reduced to 700^{o}C. Depending on the fume particle sizes and gasifier operating conditions, the percentage entrainment of alkali salts can vary. In order to use the fuel gas produced from black liquor gasification in gas turbines, the contents of undesirable species and particulate should be below those of gas turbine manufacture recommended values. Table I lists turbine manufacture recommended allowable alkali and sulphur contents of gaseous turbine fuels (Becker and Murphy, 1976; Case, et al., 1978; Keairns, et al, 1975). These data were specified for other fuels such as gas yielded from coal gasification. The actual allowable alkali and sulphur contents in fuel gases produced by black

liquor gasification is a subject needs to be studied. The common acid gas clean-up targets for coal gasification are CO_2 concentration of 500 ppm and H2S concentration of 0.01 ppm.

Table I Recommended allowable alkali and sulphur contents of gaseous turbine fuels

Turbine Manufacture	Turbine Inlet Temperature (K)	Alkali Metals ppm (wt)		Sulphur
		Na + K	Ca	
United Aircraft	1323 - 1383	0.2-0.6	0.1	0.18 mol %
Pratt and Witney[a]		0.1	0.01	0.18 mol % 0.25% H_2S
Westinghouse	1353	0.07[b], 0.15[c]	1.4[b]	0.28% (wt)
General Electric	1323-1383	0.1	0.23[b]	1 ppm

Notes: *(a) aircraft-derived turbine using gaseous fuel*
(b) based on liquid fuel specifications
(c) coal-derived hot gas

The hot fuel gas produced by black liquor gasification needs to be purified in order to meet requirements of the gas turbine integrated gasification combined cycle (IGCC). Therefore, the two major tasks for hot gas clean-up are to:

(1). Remove H_2S and reduce CO_2 concentration. Because a typical heating value of fuel gas produced by black liquor gasification is around 15 MJ/kg (Stigsson, 1994), above the minimum value required for gas turbine cogeneration and because a typical H_2S -to - CO_2ratio in black liquor gasification product gas is around 1:15, H_2S removal selectivity is desirable to leave as much as possible of the CO_2 in the parent gas as any CO_2 removed increases the cost of gas treating operation by increasing the solvent circulation.

(2). Remove particulate to reduce deposition on turbine blades and the alkali contents in the fuel gas to prevent erosion and corrosion of turbomachinery.

Hot Gas Clean-Up Technologies

1. ACID GAS REMOVAL

The most commonly used approach for acid gas removal in gas clean-up is absorption, either physical absorption or absorption into a solution of a chemical base. Table II lists commercial use of different types of solvent acid gas removal processes (Astarita et al., 1983).

Based on the number of installations, the most widely used chemical solvents are aqueous alkanolamines and promoted hot potassium carbonate processes. Only a limited number of commercial installations are physical solvent process.

Table II Commercial Use of Different Types of Solvent Gas Treating Processes

Solvent and Process	Number of Installations by 1982
Aqueous Alkanolamine: MEA, DEA, DGA, DIPA, MDEA	>1000
Promoted Hot Potassium Carbonate (Benfield): Organic, Inorganic Promoters	>740
Organic Solvent - Alkanolamine: Sulfolane/DIPA, MeOH/MEA/DEA	>130
Aqueous Oxidative Alkaline Solutions (Streford):	~100
Aqueous Solution of Potassium Salt of Amino Acids	~100
Physical (Organic) Solvents: Propylene Carbonate, Polyethylene Glycol Dialkyl Ether, etc.	~70
Flue Gas Desulfurization: Lime/Limestone Slurries in Water, Sodium Sulfite	~200

The principle difference between physical and chemical solvents is that the capacity of a physical absorption process is proportional to acid gas partial pressure in feed gas, while the capacity of a chemical absorption process is not so sensitive to acid gas partial pressure. Therefore, a physical absorption process is favored when acid gas partial pressure is high. Otherwise, it requires many stages and tall tower to remove acid gas completely, which will increase the capital investment. A typical acid gas partial pressure of 300 psia is recommended for gas clean-up in coal gasification plants (Astarita et al., 1983).

Alkanolamines based processes were developed by Bottoms (1930). Since then, many members of the alkanolamine family were introduced into the market, such as monoethanolamine (MEA), diethanolamine (DEA), methydiethanolamine (MDEA), and Diglycolamine (DGA). As a result, sufficient data are now available to enable design engineers

to choose the most suitable compound for each particular requirement (Kohl and Riesenfeld, 1985). Leibush and Shneerson (1946; 1950) studied alkanolamine absorption characteristics and found that increase the acid gas content or decrease liquid flow rate will decrease the absorption coefficient for CO_2 and H_2S. They also found that increase solution temperature will reduce the H_2S absorption coefficient, preventing the process to be operated under high temperature for effective H_2S removal. With MDEA solution, the alkanolamine process is capable of selective absorption of H_2S (Pearce, 1978; Sigmund et al., 1981; Dibble, 1983). Although alkanolamine processes have been widely used for the simultaneous removal of CO_2 and H_2S in high pressure natural gas. Economical evaluation indicate that conventional amine solution are not competitive for hot gas clean-up applications as shown in Figures 1 and 2.

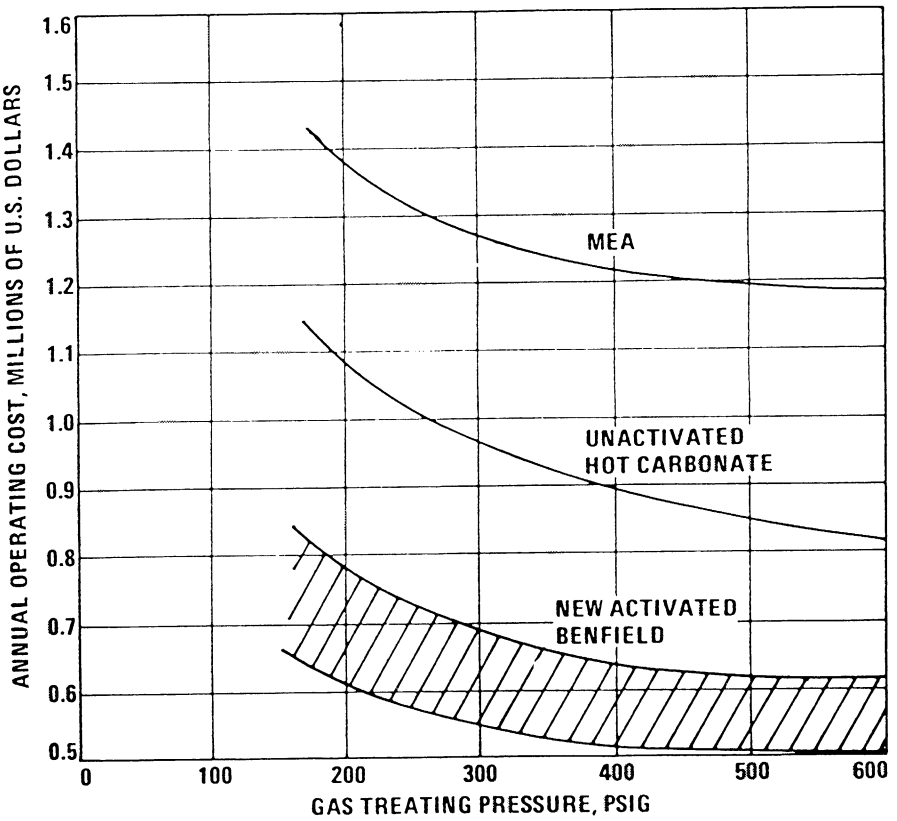

Figure 1. Comparison of operating costs for CO_2 removal by MEA, hot carbonate, and new activated hot carbonate process. Basis: gas flow - 5MMSCF/h; CO_2 in - 20%; CO_2 out - 0.1%; heat - $0.5/MMBtu; power - $0.008/kWh; cooling water - $0.015/kgal; 330 operating days/yr.

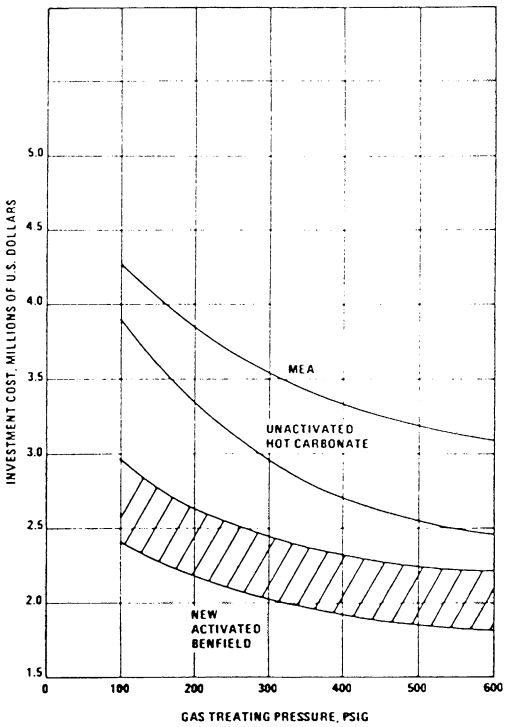

Figure 2. Comparison of capital investment for CO_2 removal by MEA, hot carbonate, and new activated hot carbonate process. Basis same as Figure 1.

A typical example of aqueous oxidative alkaline absorption process is the Stretford process. It was intended to remove H_2S from coal gas when it was developed jointly by North West Gas and the Clayton Aniline Company. However, the process proved to be equally suitable for desulfurization of a variety of the gas streams with very high remove efficiency. As originally conceived and described by Nicklin and Brunner (1961), the process utilized an aqueous solution containing sodium carbonate and bicarbonate in the proportion of 1:3 and sodium salt of anthraquinone dissulfonic acid (ADA). Although the process was tested successfully in commercial installations, it was found that a maximum allowed sulfide loading is only 40 ppm to avoid the formation of thiosufate due to the process dependency of dissolved oxygen for the conversion of hydrosulfide ion to elemental sulfur. This 40 ppm sulfide loading limitation makes the operation economically impossible because a large liquid circulation rate

and considerable power consumption are required. With the addition of sodium vanadate (Wilson and Newell, 1984a), sulfide loading of 500 ppm to 1000 ppm are allowed at present, which greatly improved the economic fate of the process. The major drawback preventing the Stretford process being applied to gas stream clean-up is the contamination of the system by bacterial growth. The problem has been studied in a great depth by the British Gas Corp. (Wilson and Newell, 1984b). Expensive chemicals are needed to combat the problem, which makes the process economically not attractive. The stretford process can not be used for the removal of CO_2, therefore, it is not recommended for hot gas clean-up applications. Rather it should be used for clean up of regeneration off-gas for high purity.

The hot potassium carbonate absorption process, also called the Benfield process uses activated, inhibited hot potassium carbonate (HPC) solutions to scrub CO_2, H_2S and other acid gas components (Bartoo, 1984). The original hot potassium carbonate process was developed at the U.S. Bureau of Mines by Benson, Field, and co-workers in the 1950s (Benson, et al., 1954; 1956; Benson Field, 1959). The process is capable of simultaneously remove CO_2 and H_2S with high H_2S removal selectivity. The process can be operated at a relatively high temperature of 220 ^{o}C, which eliminates the requirement of steam to heat the solution to stripping temperature and therefore the heat exchange equipment between the absorber and stripper. In addition, the high temperature also increases the solubility of potassium bicarbonate, thus permitting operation with highly concentrated solution to achieve high clean-up efficiency and reduce pumping energy requirement. From economics point of view, the hot potassium carbonate process is the most economic process to achieve high CO_2 and H_2S clean-up as shown in Figures 1 and 2. Although the process was originally thought to be the most economical for bulk removal of CO_2, recently developments have shown that the process has high H_2S removal selectivity (Yih and Lai, 1987; Bartoo, 1984). The process is also capable to treating feed gases with a wide H_2S and CO_2 ratio range of from 1:20 to 1:1. Typical clean efficiencies for various H_2S/CO_2 ratios are shown in Figure 3 (Field et al., 1960).

In summary, whether from the number of commercial installations, the economics, or the process characteristics for CO_2 and H_2S removal as shown in Table III, the Benfield process has many advantages for clean-up of black liquor gasified hot gas among absorption processes. Therefore, the Benfield process is recommended for the removal of H_2S and CO_2 in black liquor gasification product gas. When high purity is required, a two stage process can be adopted.

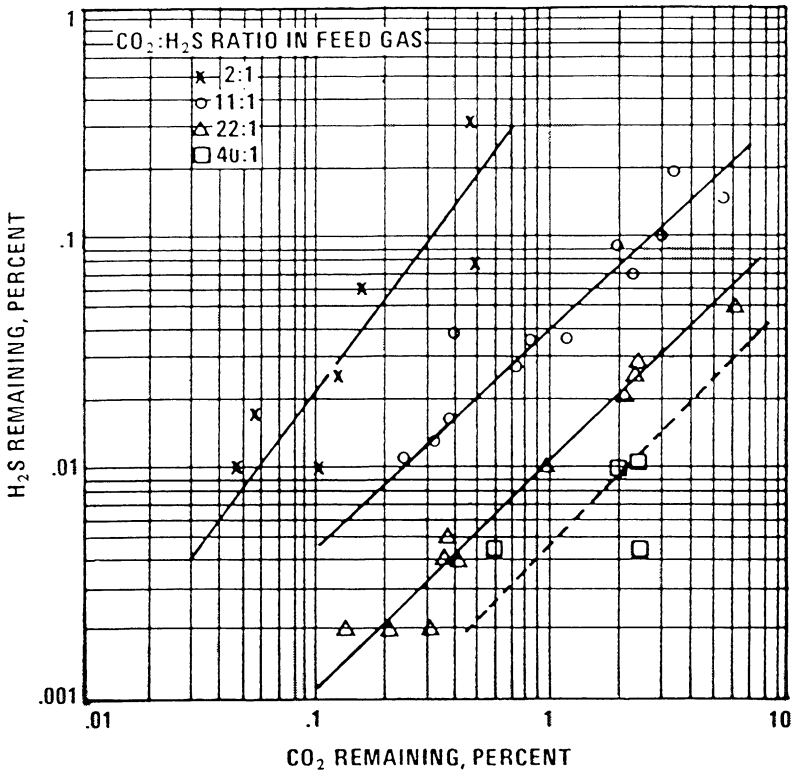

Figure 3. Relationship of H_2S and CO_2 in treated gas with a Benfield process

Table III Characteristics of Gas Treating Processes

Characteristics	MEA	DEA	DGA	Physical Solvent	Potassium Carbonate
Typical H_2S Content in Product Gas (gr/100 scf)	0.1-0.25	0.25-0.5	0.25	0.25	1.0 (single Stage)
Chemical Degradation under COS, CS_2, CO_2	Yes	Some	Yes	No	No
COS Removed	Partial	Partial	Most	Yes	Yes
CS_2 Removed	Yes	Yes	Yes	Yes	Yes
Mercaptans Removed	Partial	Partial	Most	Yes	Some
Selective H_2S Removed	No	No	No	Some	Yes

1.1 The history and the Chemistry of the Benfield Process

Since the early work of Benson et al. (1954, 1956), many researcher made contributions to understand and improve the Benfield process. Tosh et al. (1959a; 1959b) provided equilibrium data for CO_2 and H_2S over hot K_2CO_3 solutions. Kohl and Riesenfeld (1979) and Astarita et al. (1983) summarized the process description and operating conditions in texts. Many improvement and innovations have been made (Bartoo, 1984) by flow-sheet modification such as stream splitting and multistage arrangement, addition of inorganic or organic promoters to promote the absorption rate, and using heat recovery system with thermo-compressors to save energy in steam generation. Simulation and modeling of pilot plant performance for CO_2 and H_2S removal using the Benfield process have been conducted (Joshi et al., 1981; Suenson, 1985; Marini et al., 1985). Yih and Lai (1987) studied the effect of process operating parameters on individual gas removal efficiency in a pilot scale packed absorber-stripper for simultaneous removal of CO_2 and H_2S. Their study provided some guidance for optimizing the process operations. Currently, the process is licensed by Union Carbide Corp. and has gained broad acceptance for acid gas removal. More than 700 units have been installed throughout the world. The process is not one process but a family of related processes, each tailored to meet the specific requirements of an industry.

The chemistry of the process is very simple. The reaction between CO_2 and carbonate was believed to be composed of two steps.

$$K_2CO_3 + H_2O \Leftrightarrow KHCO_3 + KOH$$
$$CO_2 + KOH \Leftrightarrow KHCO_3$$

The overall reaction is,

$$K_2CO_3 + CO_2 + H_2O \Leftrightarrow 2KHCO_3 + Heat \qquad (1)$$

Reaction step 2 is the rate-determining and the kinetics of the reaction has been determined as the second order.

The reaction between H_2S and carbonate is a proton transfer reaction and can be treated as instantaneous:

$$H_2S \Leftrightarrow HS^- + H^+$$
$$K_2CO_3 + HS^- + H^+ \Leftrightarrow KHCO_3 + KHS + Heat$$

The overall reaction is

$$K_2CO_3 + H_2S \Leftrightarrow KHCO_3 + KHS + Heat \quad (2)$$

From the chemistry point of view, the Benfield process has several unique characteristics for practical applications.

1. The regeneration of potassium carbonate is obtained using the reversable nature of reaction (1) and (2). Because the heat of reaction of (1) and (2) are less than half of those comparable alkanolamine processes, less heat is required for the regeneration of hot potassium carbonate.

2. The chemical reactions are specific for CO_2 and H_2S, thus the process inherently gives a clean separation of the acid gas from other feed components in most industrial gas streams.

3. As a chemical absorption process, the rate of absorption increases with the increase of acid gas pressure until it reaches the equilibrium conditions for the chemical reaction.

4. Valuable gases such as hydrogen and hydrocarbons are insoluble in the hot potassium carbonate solutions, there is no loss of these components as compared to physical solvents, important to black liquor gasification product gas clean-up.

5. The process is also capable of absorbing some minor sulphur species present in the black liquor gasification product gas, such as COS.

1.2 Description of a Benfield Plant

A basic Benfield process consists of a absorber for acid gas removal and a regenerator for hot potassium carbonate recovery. As discussed early, because the process can be conducted at relatively high temperature of 200 °C, refrigeration is not required for the absorber. The only energy supplies will be the heating energy for the regenerator and pumping energy for the chemical solutions. Figure 4 shows a schematic of a single stage Benfield process. Conventional packed or trayed towers for countercurrent contact gas and chemical solution arrangements are often employed in the absorber. Hot potassium carbonate is supplied at the top of the absorber from the regenerator. Feed gas is introduced at the bottom of the absorber. The acid gases are absorbed by the hot potassium carbonate solution in the absorber according the reactions of (1) and (2). The feed gas leaving the absorber is therefore purified. The reaction product of rich solution of potassium hydrocarbon $KHCO_3$ is pumped back to the regenerator from the bottom of the absorber. Heat is supplied to the regenerator to achieve high potassium carbonate recovery. The acid gases of CO_2 and H_2S are recovered in the

regenerator according to the reversal reactions of (1) and (2) and then separated from the exhauster. The absorbing pressure and temperature can vary depending on the specific operation requirements. Multi-stage or split-stream methods have been used for high purity and high efficiency acid gas removal as shown in Figure 5. Many improvements have been made since the initial operation of the Benfield process. Corrosion inhibitors are added in operations. To reduce the heating energy of the regenerator, an inorganic activator system has been developed to achieve major reductions in the required heat consumption of the regenerator.

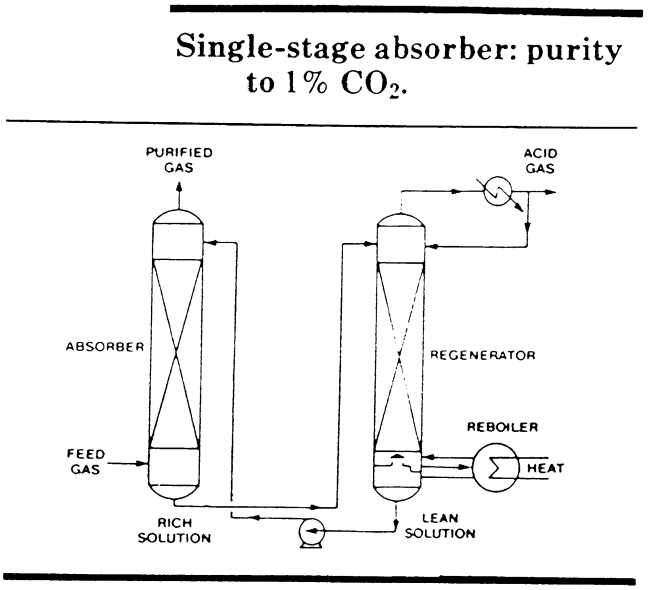

Figure 4. Schematic of a single stage Benfield process

1.3 The Economics of the Benfield Process

In this section, we discuss the costs of a Benfield process with breakdown to heating and pumping energy. We will also compare the costs of various Benfield process designs.

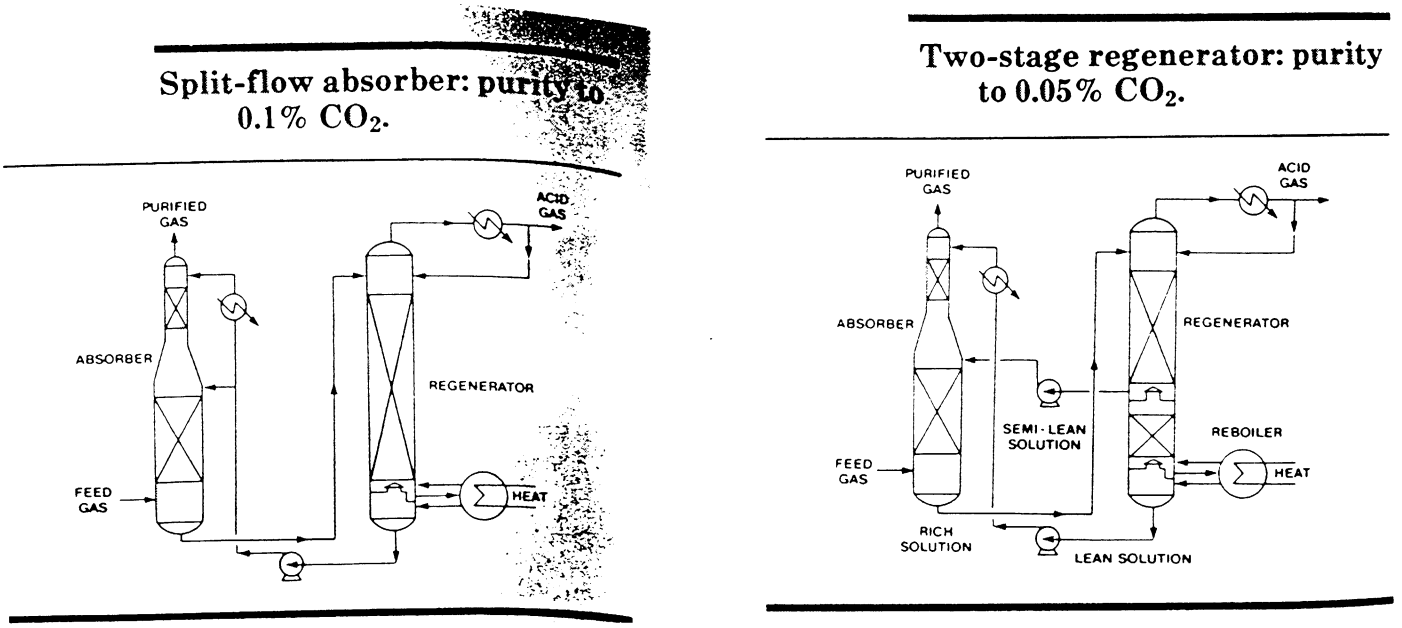

Figure 5. Schematic of a two-stage (a) and a split stream (b) Benfield process

2. PARTICULATE REMOVAL

Removal of particulate is an very important part in hot-gas clean-up process. A black liquor gasification product gas stream can contain particles from entrained dried black liquor ,char, and a large amount of fume (alkali salts) particles. These particles can have a size range of submicron to about 100 micron. Fume particles are formed by condensation and their initial particle sizes are usually below 1 micron which makes available particulate removal technologies, such as cyclones, electrostatic precipitators, ceramic filters etc. insufficient even with many years of research and development. In this section, we will discuss some of the particulate removal technologies and new technologies for separation of submicron particles.

Future Research Needs

Future research needs for black liquor gasification hot gas clean-up mainly lies in new methods and technologies for fine fume particle removal in the product gas.

References

Astarita, G., Savage, D.W., and Bisio, A., (1983), *Gas Treating with Chemical Solvent,* John Wiley and Sons, N.Y.,

Bartoo, R.K., (1984), Removing Acid Gas by the Benfield Process, *Chem. Eng. Prog.,* **80,** p 35

Becker, D.F. and Murphy, B.N., (1976), Gilbert Associates Inc. Report for ERDA, No. FE/1236-15

Benson, H.E., Field, J.H., and Jimeson, R.M., (1954), CO2 Absorption Employing Hot Potassium Carbonate Solutions", *Chem. Eng. Prog.,* **50,** p 356

Benson, H.E., Field, J.H., and Haynes, W.P., (1954), Improved Process for CO2 Absorption Uses Hot Carbonate Solutions, *Chem. Eng. Prog.,* **52,** p433

Benson, H.E. and Field, J.H., (1959), Method of Separating CO2 and H2S from Gas Mixtures, *U.S. Patent* 2,866,405

Case, et al., (1978), *Morgantown Energy Research Center Report,* No. MERC/SP-78/2

Bostrom, G. and Hillstrom, R., (1992), Status Report from the Chemrec Recovery Booster at Frovofors, *Proc. of the 1992 Int. Chemical Recovery Conference*, p13

Bottoms, R.R., (1930), US Patent 1,783,901

Dibble, J.H., (1983), UCARSOL Solvents for Acid Gas Removal. Presented at Petroenergy'83. Houston, TX, Sep. 14.

Durai-Swami, K., Warren, D.W., and Mansour, M. N., (1989), Pulpse-Enhanced Indirect Gasification for Black Liquor Recovery, *Proc. of the 1989 Int. Chemical Recovery Conf.,* p217

Field, J.H., Johnson, E.G., Benson, H.E., and Tosh, J.S., (1960), *Bureau of Mines Report of Investigation 5660*

Fogelholm, C-J and McKeough, P., (1991), Black Liquor as a Fuel Gas for Combined Cycles, *Proc. 5th Symp. on Gas Turbines in Cogeneration, Repowering and Peak Load Generation,* Budapest, Hungary

Joshi, S.V., Astarita, G., and Savage, D.W., (1981), Prediction of Pilot Plant Performance for a Chemical Gas Ansorption Process, *AIChE Symp. Ser.,* No 211, **77,** p 63

Keairns, D.L., et al., (1975), Westinghouse Electric Corp Report to EPA, No. EPA-650/2-75-027-C

Kohl, A.L. and Riesenfeld, F.C., (1979), *Gas Purification*, 3rd Ed., Gulf Publishing Co., Houston, TX

Marini, L., Clement, K., Georgakis, C., and Suenson, M.M., (1985), Experimental and Theoretical Investigation of an Absorber-Stripper Pilot Plant under Nonequilibrium Conditions, *Ind. Eng. Chem. Fundam.* **24,** p 296

Nicklin, T. and Brunner, E., (1961), *Inst. Gas Engrs.* (British), Pub. 593

Salmenoja, K., Janka, K., Kymalainen, M., and Hyoty, P., (1993), Development of Black Liquor Gasification, *Proc. of the1993 TAPPI Engineering Conference,* p969

Shneerson, A.L. and Leibush, A.G., (1946), *J. Appl. Chem.* (USSR), 19, p869

Sigmund, P.W., Butwell, K.F., and Wussler, A.J., (1981), *Hydrocarbon Preocessing,* **60**(5), p118

Leibush, A.G. and Shneerson, A.L., (1950), *J. Appl. Chem.* (USSR), 23, p1253

Pearce, R.L., (1978), Hydrogen Sulfide Removal with Methydiethanolamine. Presented at the 57th Annual GPA Convention, New Orleans, LA, Mar. 20-22

Stigsson, L. L., (1994), Pressurized Black Liquor Gasification: Advanced Technology for Electric Power Production and Recovery of Pulping and Bleaching Chemicals, *Proc. of the 1994 Pulping Conference,* p331

Suenson, M.M., Georgakis, C., and Evans, L.B., (1985), Steady State and Dynamic Modeling of a Gas Absorber-Stripper System, *Ind. Eng. Chem. Fundam.* **24,** p 288

Tosh, J.S., Field, J.H., Benson, H.E., and Haynes, W.P., (1959a), Equilibrium Study of the System Potassium Carbonate, Potassium Bicarbonate, Carbon Dioxide, and Water, *Bureau of Mines Report of Investigation 5484*

Tosh, J.S., Field, J.H., Benson, H.E., and Anderson, R.B., (1959b), Equilibrium Sulfide and Carbon Dioxide over Solution of Potassium Carbonate, *Bureau of Mines Report of Investigation 5622*

Wilson, B.M. and Newell, R.D., (1984a), H_2S Removal by Stretford Process, *Chem. Eng. Prog.,* **80,** p40

Wilson, B.M. and Newell, R.D., (1984b), H_2S Removal by the Stretford Process - Further Development by the British Gas Corporation. Presented at the National AIChE meeting, Atlanta, GA, Mar 13

Yih, Siu-Ming and Lai, Hung-Cherh, (1987), Simultaneous Absroption of Carbon Dioxide and Hydrogen Sulfide in Hot Carbonate Solutions in a Packed Absorber-Stripper Unit, *Chem. Eng. Comm.,* **51,** p277